Molecular Mechanisms Regulating Mycorrhizal Associations in Woody Plants

By

Kevin Richard Cope

A dissertation submitted in partial fulfillment of

the requirements for the degree of

Doctor of Philosophy

(Cellular and Molecular Biology)

at the

UNIVERSITY OF WISCONSIN–MADISON

2018

Date of final oral examination: 09/14/2018

The dissertation is approved by the following members of the Final Oral Committee:
Jean-Michel Ané, Professor, Bacteriology, and Agronomy
Richard Lindroth, Professor, Entomology
Nancy Keller, Professor, Bacteriology, and Medical Microbiology and Immunology
Patrick Krysan, Professor, Horticulture
Mehdi Kabbage, Assistant Professor, Plant Pathology

Abstract

The application of fertilizers in agronomic systems is necessary to meet the nutrient demands of crop production. However, this practice often results in the pollution of the environment. More sustainable practices are needed to prevent the continued degradation of natural systems. In nature, the roots of plants have forged alliances with beneficial microbes in the soil to help alleviate nutrient deficiencies. Understanding how symbiotic plant-microbe interactions form is crucial for developing more sustainable agronomic practices that limit our dependence on fertilizers and minimize negative impacts of crop production on the environment.

Mycorrhizal fungi are one class of filamentous microorganisms that form a mutualistic association with the roots of most land plant species. They provide the roots of their host plants with increased access to limited mineral nutrients in the soil in exchange for carbon derived from photosynthesis. Two major types of mycorrhizal associations include arbuscular mycorrhizal (AM) and ectomycorrhizal (ECM). The molecular mechanisms regulating how both types of mycorrhizal associations form has been a major research topic for decades, although more attention has been given to AM fungi. As a result, an entire molecular signaling pathway has been identified that is necessary for the development of the AM symbiosis. It is known as the "common symbiosis pathway" (CSP) because it is also required for both the rhizobia–legume and actinorhizal symbioses.

The CSP is activated by lipochitooligosaccharides (LCOs), which are symbiotic signaling molecules that are also produced by rhizobia. At the core of the CSP are three genes: *CASTOR*, *POLLUX*, and *CCaMK*. CASTOR and POLLUX regulate a cellular phenomenon known as nuclear calcium spiking which is then decoded by CCaMK leading to changes in gene expression necessary for the development of both the AM and rhizobia–legume symbioses.

Ectomycorrhizal symbioses are one of the most widespread associations between roots of woody plants and soil fungi in forest ecosystems. These associations contribute significantly to the sustainability and sustainagility of these ecosystems through nutrient cycling and carbon sequestration. Unfortunately, the molecular mechanisms controlling the mutual recognition between both partners are still poorly understood. Given the role of the CSP in diverse symbiotic associations, we hypothesized that the CSP might also play a role in ECM associations.

Genomic data suggests that ECM fungi possess all of the genetic components necessary for the biosynthesis of LCOs. Furthermore, the genomes of some ECM-host plants possess all of the genes associated with the CSP (e.g., *Populus*). Using mass spectrometry, we showed that multiple ECM fungi produce an array of LCOs and demonstrated that they can trigger both root hair branching in legumes and, most importantly, calcium spiking in the ECM-host plant *Populus*. For one ECM fungal species, *Laccaria bicolor*, we demonstrated that calcium spiking in *Populus* occurred in a *CASTOR/POLLUX*-dependent manner. Purified non-sulfated LCOs enhanced lateral root development in *Populus* in a *CCaMK*-dependent manner and sulfated LCOs enhanced the colonization of *Populus* by *L. bicolor*. The colonization of *Populus* roots by *L. bicolor* was reduced in both *CASTOR*/*POLLUX* and *CCaMK* RNA interference lines and the expression of a mycorrhiza-induced phosphate transporter, *PT12*, was reduced in the *CCaMK*-RNA interference line compared to wild-type. Altogether, our work demonstrates that *L. bicolor* uses the CSP for full establishment of its mutualistic association with *Populus*.

Future work should focus on determining if the CSP is required for the establishment of other ECM associations using stable gene knock-outs. Furthermore, the role of nutrient transporters in the maintenance of ECM associations should be evaluated. Investigating these areas of research will allow for better utilization of ECM associations in the sustainable production of woody plants and/or management of forest ecosystems.

Acknowledgements

I would first like to thank my wife, Melanie, for the unending support that she provided as I pursued my Ph.D. She has been the ideal companion as I have traversed the roller coaster experience of graduate school. Thank you for your love, support, and patience all along the way, particularly when I unavoidably had to work overtime at home, often into the late hours of the night. You are the reason I was able to reach this lifetime goal, and without you by my side, I never could have succeeded. I look forward to our future together as we unitedly raise our family and hope that one day you will finally understand the purpose of my research.

I also thank my parents, Val and Marilyn Cope, who raised me in a way that allowed me to explore my curiosity and pursue lofty goals that pushed me to my limits. The two of you provided the launch pad from which I was able to take-off and experience opportunities that I never thought possible. No one could ask for more supportive and dedicated parents than you. Thank you for always cheering me on and giving me the tools and skills necessary to succeed.

Thank you to my advisor, Dr. Jean-Michel Ané, who took a risk by allowing me to join his lab as a direct-admit student—I hope I lived up to your expectations and sincerely thank you for more than living up to mine. Most of all, I appreciate your willingness to allow me to develop myself professionally in so many ways. Your mentorship has been vital in helping me become an independent scientist, and I look forward to maintaining our professional relationship as we collaborate on future research projects.

I sincerely thank the many members of the Ané lab from over the past five years. In particular, I thank the following post-docs: Dr. Muthusubramanian Venkateshwaran for spear-heading my project before I arrived, Dr. Dhileepkumar Jayaraman for his wise counsel at each stage of the graduate experience, Dr. Matthew Crook for frequent non-scientific but stimulating conversations, and Dr. Kevin Garcia for training and guidance all along the way. I also thank our

excellent lab technician Junko Maeda for the unending help she provided. I thank all of the fellow graduate students who jointly traversed the gauntlet with me, including: (Dr.) David Marburger, Shane Bernard, Marian Lund, Michelle Keller-Pearson, Tony Bortolazzo, and Zak Keyser.

Finally, I thank all of the undergraduate students who assisted me in completing more experiments, both failed and successful, than I ever could have done on my own, including: Edward Steigerwald, Jonathan Setzke, Emmeline Fung, Tristan Wang, Kimberly Schnell, Nathaniel Schleif, Angad Dhariwal, Mark Horton, Kenneth Jackson, Marissa Cortopassi, Sara Degrave, Chester Zara, Amber Chasteen, Ian Midgordin, Jack Kwan, and Emily Halter-Lindquist.

I appreciate the constructive criticism and guidance of all of my committee members, including: Drs. Patrick Krysan, Nancy Keller, Richard Lindroth, and Mehdi Kabbage. I also thank our collaborators, Drs. Guillaume Bécard, Steve Strauss, Jessy Labbé and their associates for the complementary work they contributed to this joint project.

I am grateful to the Cellular & Molecular Biology program for allowing its students to primarily focus their time and energy on research. I appreciate the program chair, Dr. David Wasserman, for his advice and support, particularly as I applied for both post-doctoral fellowship and positions. I also thank Lauren Weitkamp and Sarah Bierke for keeping me on track as I worked towards graduation.

In conclusion, I thank the plant science graduate students that I associated with from multiple departments and programs, particularly those that I served with on the Plant Sciences Graduate Student Council. All of you turned the campus into an inclusive environment that helped me feel both wanted and needed. I will cherish the memories I made with each of you and look forward to crossing paths with many of you in the future. I hope that all of you find success and enjoyment in your future careers, whatever they may be.

Table of Contents

Chapter 1: Introduction

1.1 Plant Nutrition

As photosynthetic organisms, plants are able to harness the energy provided by sunlight to convert carbon dioxide (CO_2) from the atmosphere and water (H_2O) from the soil into simple sugars ($C_nH_{2n}O_n$) and oxygen (O_2). In this way, plants acquire three of the 17 elements that are essential for plants to complete their entire life cycle, including carbon (C), hydrogen (H), and oxygen (O). The remaining 14 elements are typically derived from the soil and include both macronutrients and micronutrients. Macronutrients are elements that are required in high quantities (e.g., >1 g per kg of plant tissue) and include: nitrogen, phosphorus, potassium, calcium, sulfur, and magnesium. Micronutrients are elements that are required in low quantities (e.g., <1 g per kg of plant tissue) and include: iron, boron, chlorine, manganese, zinc, copper, molybdenum, and nickel (Marschner, 2012).

When plants deplete the stock of mineral nutrients in the soil substrate where their roots reside, they experience nutrient deficiencies which ultimately inhibit their growth or prevent proper development. When this occurs in agronomic systems, the application of fertilizers is a necessary practice to achieve maximum crop production. However, concentrated fertilizers are rarely entirely assimilated by the crops on which they are applied, and as a result, they almost always pollute the environment (Chien et al., 2009). Fortunately, long before humans began cultivating plants, nutrient deficiency was a problem that, in many cases, plants solved on their own by forging alliances with microorganisms that specialize in nutrient acquisition (Martin et al., 2017). Mycorrhizal fungi are one major class of microorganisms that most plants associate with and understanding how they do so is of paramount importance as more sustainable crop production systems are developed.

1.2 Mycorrhizal Fungi

Mycorrhizal fungi are filamentous, soil-dwelling microorganisms that form symbiotic associations with the roots of approximately 90% of terrestrial plant species (Bonfante and Genre, 2010; Brundrett and Tedersoo, 2018). Although there are seven classes of mycorrhizal associations, the two most ecologically and economically important are arbuscular mycorrhizal (AM) and ectomycorrhizal (ECM) (Smith and Read, 2008; van der Heijden et al., 2015). The successful colonization of land by plants was perhaps due in large part to AM fungi, which evolved nearly 450 million years ago (Redecker et al., 2000). In the fungal kingdom, AM fungi belong to the phylum Mucoromycota (Spatafora et al., 2016) and are capable of associating with around 72% of land plants, including most crops (Parniske, 2008; Brundrett and Tedersoo, 2018). They are obligate symbionts that depend on their host plant for all of their energy needs (Tisserant et al., 2012). ECM fungi, on the other hand, evolved from brown and white rot fungi at least 130 million years ago (Hibbett et al., 2000; Kohler et al., 2015) and belong to three fungal phyla, including Ascomycota, Basidiomycota, and Mucoromycota (Spatafora et al., 2016). They associate with approximately 2% of land plants, predominately woody plant species, some of which also associate with AM fungi (Garcia et al., 2015; Brundrett and Tedersoo, 2018). In contrast to AM fungi, ECM fungi are facultative symbionts that are capable of living independently as saprotrophs in the soil but cannot sexually reproduce unless they associate with a host plant (Kohler et al., 2015).

In both types of mycorrhizal associations, AM and ECM fungi provide the plant with water and mineral nutrients mined from the soil, especially phosphorus and nitrogen, but also potassium and sulfur (Casieri et al., 2013; Garcia and Zimmermann, 2014; Garcia et al., 2016). In exchange, the plant provides the mycorrhizal fungus with carbon derived from photosynthesis

(Dosskey et al., 1990; Bago et al., 2000). Broadly speaking, AM associations play a major role in improving the phosphorus nutrition of plants while ECM associations contribute more so to nitrogen nutrition (Smith and Read, 2008). While AM and ECM fungi both provided their host plant with increased access to mineral nutrients in the soil, the structures they utilize to exchange them for carbon are very different. AM fungal hyphae invade the plant root and form highly branched hyphal structures called arbuscules inside of cortical cells; ECM fungi form a dense network of hyphae, or Hartig net, on the surface of root epidermal and cortical cells and a hyphal sheath, or mantle, that encases the entire root tip (Bonfante and Genre, 2010; Balestrini and Bonfante, 2014).

1.3 Arbuscular Mycorrhizal Symbioses

The colonization of plants by mycorrhizal fungi is a complicated process that requires coordinated communication between both the host plant and the symbiotic fungus. If both partners successfully communicate with one another, then the mycorrhizal association can be established. Upon establishment, additional communication is necessary to maintain the symbiotic association. Since AM fungi associate with many crops, the molecular mechanisms regulating the establishment and maintenance of AM symbiosis have been researched more extensively than for ECM symbioses (Garcia et al., 2015).

Establishment. Much of the previous research with AM fungi was completed using various species of model legumes. In addition to associating with AM fungi, the roots of legumes are also colonized by rhizobia, a type of bacteria that induce the formation of nodules, or specialized root structures in which the bacteria can fix nitrogen (Ferguson et al., 2010). The rhizobia-legume symbiosis evolved ~100 million years ago by recruiting the molecular

components of the signaling pathway required for AM symbiosis (Werner et al., 2014); as such, this pathway is referred to as the "common symbiosis pathway" (CSP) (Oldroyd, 2013; Venkateshwaran et al., 2013; Martin et al., 2017). Both rhizobia and AM fungi activate the CSP in their host plants using symbiotic signals known as lipochitooligosaccharides (LCOs) (Lerouge et al., 1990; Maillet et al., 2011). AM fungi can also activate the CSP with short-chain chitin oligomers (COs) which are produced by AM fungi in response to Strigolactones, a class of plant hormones (Genre et al., 2013). Collectively, COs and LCOs produced by AM fungi are referred to as "Myc factors".

Upon their release by AM fungi into the rhizosphere, COs and LCOs are perceived by plants via lysine-motif receptor-like kinases (LysM-RLKs) and a leucine-rich repeat receptor-like kinase (LRR-RLK) co-receptor, termed NORK/DMI2/SymRK (Stracke et al., 2002; Op den Camp et al., 2011; Miyata et al., 2014; Zhang et al., 2015). NORK/DMI2/SymRK interacts with and activates 3-Hydroxy-3-Methylglutaryl Coenzyme-A Reductase1 (HMGR1) leading to the production of mevalonate (Kevei et al., 2007; Venkateshwaran et al., 2015). Through an unknown cascade of events, mevalonate activates a suite of nuclear ion channels including CASTOR, DMI1/POLLUX, and cyclic nucleotide-gated calcium channels which allow for the flow of calcium ions (Ca^{2+}) into the nucleoplasm and around the nucleus (Ané et al., 2004; Charpentier et al., 2008, 2016, Venkateshwaran et al., 2012, 2015). A calcium ATPase, MCA8, then removes Ca^{2+} thus inducing repetitive oscillations in Ca^{2+} concentration within and around the nucleus (Capoen et al., 2011). This phenomenon is commonly referred to as "Ca^{2+} spiking" and is dependent on all of the components described above. COs and LCOs are capable of triggering Ca^{2+} spiking even in the absence of the fungus (Genre et al., 2013; Sun et al., 2015). Repetitive Ca^{2+} spikes in the nucleus lead to the activation of the calcium- and calmodulin-

dependent protein kinase DMI3/CCaMK, which then phosphorylates its primary target, the transcription factor IPD3/CYCLOPS (Lévy et al., 2004; Messinese et al., 2007; Yano et al., 2008; Horváth et al., 2011; Singh and Parniske, 2012). Upon phosphorylation, IPD3/CYCLOPS regulates the expression of multiple transcription factors required for the development of AM symbiosis (MacLean et al., 2017; Luginbuehl and Oldroyd, 2017).

Beyond molecular signaling pathways, additional molecular mechanisms exist in mycorrhizal associations that allow the fungus to suppress the immune response induced by the microbe-associated molecular patterns inherent to fungi (e.g., chitin). During late establishment, the AM fungus *Rhizophagus irregularis* releases SECRETED PROTEIN 7 (SP7). This protein negatively regulates the host plant ethylene-responsive transcription factor (ERF19), which is required for defense signaling (Kloppholz et al., 2011). Suppression of the defense response initially allows AM fungi to penetrate and perpetuate within the plant root; however, following the formation of arbuscules, the fungus must provide some benefit to the host plant in order to persist within the root.

Maintenance. Nutrient exchanges are a crucial factor regulating persistence of AM colonization in the roots of plants (Kiers et al., 2011; Fellbaum et al., 2014). As an example of this, the phosphate transporter MtPT4 in *M. truncatula* is expressed only in plant cells containing arbuscules and is required for persistence of the symbiotic interaction (Javot et al., 2007). MtPT4 functions in the uptake of phosphorous mined from the soil by the fungus and released into the peri-arbuscular space by an unidentified phosphate transporter. In exchange for phosphorous, the plant translocates sugars produced by photosynthesis through sugar transporters into the peri-arbuscular space where it is taken up by the fungal sugar transporter MST2 (Helber et al., 2011;

Casieri et al., 2013). Establishment and maintenance of this bidirectional nutrient exchange constitute the basis for the symbiotic association between AM fungi and plants.

1.4 Ectomycorrhizal Symbioses

Establishment. Similar to AM symbiosis, rhizospheric signaling events do occur that are essential for the development of ECM symbioses (Martin et al., 2001). Plant hormones appear to have a developmental effect. For example, from *Eucalyptus*, the flavonol rutin stimulated hyphal growth while the cytokinin zeatin altered hyphal branch angle in *Pisolithus*, an ECM fungus (Lagrange et al., 2001). However, there appears to be no developmental effect of the plant hormone strigolactone on hyphal branching in multiple ECM fungal species, including *Laccaria bicolor* and *Paxillus involutus* (Steinkellner et al., 2007). Regarding fungal signals, hypaphorine from *Pisolithus tinctorius* inhibited root hair elongation and induced increased cytosolic calcium concentration in *Eucalyptus* (Ditengou et al., 2000; Dauphin et al., 2007). Interestingly, *L. bicolor* stimulates lateral root development in *Populus*, a host plant, and *Arabidopsis*, a non-host plant, by altering auxin transport (Felten et al., 2009, 2010). Despite the progress that has been made in identifying these ECM fungal signals and their effect on the host plant, it is not known if ECM fungi produce COs or LCOs for signaling to the host plant. With the release of the genome for two ECM fungi—*L. bicolor* (Martin et al., 2008) and *Tuber melanosporum* (Martin et al., 2010)—homologs of the LCO biosynthesis genes have been identified (Garcia et al., 2015). This finding suggests that ECM fungi may produce COs/LCOs capable of activating the CSP, but this remains to be tested.

No molecular signaling pathway has been identified that regulates ECM associations; however, due to the availability of the genomes of many plant species that are capable of

associating with ECM fungi, a phylogenetic analysis to search for components of the CSP in genomes or transcriptomes of various woody plant species has been carried out (Garcia et al., 2015). Not surprisingly, plant species, such as *Populus*, that are capable of associating with both AM and ECM fungi contained all of the core components of the CSP. All of the gymnosperms analyzed that are only capable of associating with ECM fungi lacked most or all of the components of the CSP. Although this observation may infer that the CSP is not involved in ECM symbioses, it is not conclusive since no colonization studies have been performed with CSP knock-down or knock-out lines of plants capable of associating with ECM fungi. Furthermore, since ECM associations arose at least 80 times independently in the Basidiomycota clade (Tedersoo and Smith, 2013), it is possible that, similar to the rhizobia-legume symbiosis, parts of the CSP may have been recruited for the establishment of some ECM associations, perhaps including those in *Populus*.

Similar to AM fungi, effectors are also known to play a role in ECM symbioses. For example, expression of *MYCORRHIZA-iNDUCED SMALL SECRETED PROTEIN 7* (*MiSSP7*) in *L. bicolor* is induced by the flavonoids rutin and quercitrin as well as by *Populus* root exudates (host) and *Arabidopsis* (non-host) (Plett and Martin, 2012). In *Populus*, MiSSP7 is imported to the nucleus where it interacts with JASMONATE ZIM-DOMAIN 6 (PtJAZ6) thus blocking its interaction with CORONATINE INSENSITIVE 1 (PtCOI1). PtCOI1 interacts with PtJAZ6 and targets it for degradation in the presence of the plant hormone jasmonic acid. By blocking this JA-induced degradation, MiSSP7 plays a role in suppressing the plant immune response thus facilitating establishment within the plant (Plett et al., 2014a). Other SSPs have been identified in the genomes of *L. bicolor* as well as *Tuber melanosporum* (Martin et al., 2010), *Hebeloma cylindrosporum* (Doré et al., 2015), and multiple other ECM fungal species (Kohler et al., 2015).

Many of these SSPs may be effectors that play a role in suppressing the plant immune response, thus leading to maintenance of the symbiotic interaction.

Maintenance. As in AM fungi, the nutrient exchange is likely required for the maintenance of ECM symbioses. Similar components that are required for nutrient exchange in AM symbioses are also required for ECM symbioses (Casieri et al., 2013; Garcia et al., 2016). Of particular interest are those components that are involved in both; for example, the *Populus* phosphate transporters *PtPT9*, *PtPT10*, and *PtPT12* are up-regulated in AM roots, and both *PtPT9* and *PtPT12* are also up-regulated during ECM associations and phosphorus deficiency (Loth-Pereda et al., 2011). However, it is not known if these phosphate transporters are essential for ECM symbioses, similar to how *MtPT4* is required for AM symbioses (Javot et al., 2007).

1.5 *Populus* as a Model for Studying Mycorrhizal Associations in Woody Plants

The United States depends on fossil fuels for 85% of its total energy needs. This significant dependence results in the addition of 3.2 billion metric tons of CO_2 to the atmosphere annually and is a major contributing factor to global climate change (IPCC, 2014). More sustainable fuel sources must be identified, and atmospheric CO_2 levels need to be reduced in order to mitigate the effects of climate change. Biofuels are an alternative, sustainable energy source and *Populus* is recognized as one of the most important crops for lignocellulosic biofuel production for many reasons (Sannigrahi et al., 2010; Porth and El-Kassaby, 2015). Not only is it fast growing, capable of tremendous biomass production, widely distributed, and genetically diverse, it is also transformable and its genome has been sequenced, thus increasing opportunities for genetic studies and the development of tools for genetic analysis (Brunner et al., 2004; Tuskan et al., 2006).

A contributing factor to the success of *Populus* is its ability to associate with both arbuscular mycorrhizal and ectomycorrhizal fungi. Its association with AM fungi is likely possible because it contains all of the components of the CSP (Delaux et al., 2014; Garcia et al., 2015); however, this remains to be tested. Furthermore, our knowledge of how *Populus* is colonized by ECM fungi is still limited (Martin et al., 2016; Strullu-Derrien et al., 2018). Although many molecular aspects of the association of *Populus* with the ECM fungus *L. bicolor* have been studied relatively extensively (Felten et al., 2009, 2010; Loth-Pereda et al., 2011; Plett et al., 2011; Plett and Martin, 2012; Plett et al., 2014b; Kohler et al., 2015; Vayssières et al., 2015; Pellegrin et al., 2017; Plett et al., 2017), no molecular signaling pathway has been identified to date. Fortunately, as a result of the focus on the *Populus–L. bicolor* association, all the necessary tools are available for interrupting the expression of CSP genes (e.g., *CASTOR*, *POLLUX*, or *CCaMK*) in order to evaluate if they are required for the colonization of *Populus* by *L. bicolor*.

1.6 Justification and Goals

Although much is known about the establishment and maintenance of both AM and ECM fungal associations, many gaps in knowledge still exist. The role of the CSP during AM associations with woody plants has not been demonstrated experimentally. Furthermore, no molecular signaling pathway like the CSP has been identified for ECM associations. Given the role of the CSP in both AM and rhizobia–legume symbioses, it is possible that ECM fungi also use the CSP to colonize woody plants.

In chapter 2, genomic data is provided as evidence that ECM fungi may produce LCOs. This claim is substantiated by additional genomic data in woody plants which shows that the

CSP is present in all angiosperms that associate with ECM fungi. Also, the current molecular mechanisms that regulate the establishment and maintenance of both AM and ECM associations are thoroughly reviewed, and potential experiments for addressing current gaps in knowledge are proposed.

In Chapter 3, experimental approaches are described that allowed for the identification of LCOs in the culture medium of the ECM fungus *L. bicolor*. The first observation of calcium spiking in the woody plant species *Populus* is also described in response to not only AM fungal exudates and purified signaling molecules, but also following exposure to *L. bicolor* hyphae. The enhancement of lateral root development and *L. bicolor* colonization is also demonstrated in response to treatment with LCOs. Finally, *L. bicolor* colonization of *Populus* is shown to be reduced in knock-down lines for multiple CSP genes.

At the end of Chapter 3, additional data is presented which shows that the production of LCOs occurs in other species of ECM fungi and that these species are also capable of triggering calcium spiking. To conclude, the data from Chapters 2 and 3 are discussed in Chapter 4 and the remaining gaps in knowledge are pointed out along with the necessary experiments to address them.

1.7 References

Ané, J.-M. et al. (2004). *Medicago truncatula DMI1* required for bacterial and fungal symbioses in legumes. Science **303**: 1364–1367.

Bago, B., Pfeffer, P.E., and Shachar-Hill, Y. (2000). Carbon metabolism and transport in arbuscular mycorrhizas. Plant Physiol. **124**: 949–958.

Balestrini, R. and Bonfante, P. (2014). Cell wall remodeling in mycorrhizal symbiosis: a way towards biotrophism. Front. Plant Sci. **5**: 237.

Bonfante, P. and Genre, A. (2010). Mechanisms underlying beneficial plant-fungus interactions in mycorrhizal symbiosis. Nat. Commun. **1**: 48.

Brundrett, M.C. and Tedersoo, L. (2018). Evolutionary history of mycorrhizal symbioses and global host plant diversity. New Phytol. https://doi.org/10.1111/nph.14976

Brunner, A.M., Busov, V.B., and Strauss, S.H. (2004). Poplar genome sequence: Functional genomics in an ecologically dominant plant species. Trends Plant Sci. **9**: 49–56.

Capoen, W., Sun, J., Wysham, D., Otegui, M.S., Venkateshwaran, M., Hirsch, S., Miwa, H., Downie, J.A., Morris, R.J., Ané, J.-M., and Oldroyd, G.E.D. (2011). Nuclear membranes control symbiotic calcium signaling of legumes. Proc. Natl. Acad. Sci. U. S. A. **108**: 14348–14353.

Casieri, L. et al. (2013). Biotrophic transportome in mutualistic plant-fungal interactions. Mycorrhiza **23**: 597–625.

Charpentier, M., Bredemeier, R., Wanner, G., Takeda, N., Schleiff, E., and Parniske, M. (2008). *Lotus japonicus* CASTOR and POLLUX are ion channels essential for perinuclear calcium spiking in legume root endosymbiosis. The Plant Cell **20**: 3467–3479.

Charpentier, M., Sun, J., Vaz Martins, T., Radhakrishnan, G. V, Findlay, K., Soumpourou, E., Thouin, J., Véry, A.-A., Sanders, D., Morris, R.J., and Oldroyd, G.E.D. (2016). Nuclear-localized cyclic nucleotide-gated channels mediate symbiotic calcium oscillations. Science **352**: 1102–5.

Chien, S.H., Prochnow, L.I., and Cantarella, H. (2009). Chapter 8: Recent developments of fertilizer production and use to improve nutrient efficiency and minimize environmental impacts. Adv. Agron. **102**: 267–322.

Dauphin, a, Gérard, J., Lapeyrie, F., and Legué, V. (2007). Fungal hypaphorine reduces growth and induces cytosolic calcium increase in root hairs of Eucalyptus globulus. Protoplasma **231**: 83–8.

Delaux, P.M., Varala, K., Edger, P.P., Coruzzi, G.M., Pires, J.C., and Ané, J.M. (2014). Comparative phylogenomics uncovers the impact of symbiotic associations on host genome evolution. PLoS Genet. **10**: e1004487.

Ditengou, F. a, Béguiristain, T., and Lapeyrie, F. (2000). Root hair elongation is inhibited by hypaphorine, the indole alkaloid from the ectomycorrhizal fungus *Pisolithus tinctorius*, and restored by indole-3-acetic acid. Planta **211**: 722–728.

Doré, J. et al. (2015). Comparative genomics, proteomics and transcriptomics give new insight into the exoproteome of the basidiomycete *Hebeloma cylindrosporum* and its involvement in ectomycorrhizal symbiosis. New Phytol. **208:** 1169-1187

DOSSKEY, M.G., LINDERMAN, R.G., and BOERSMA, L. (1990). Carbon–sink stimulation of photosynthesis in Douglas fir seedlings by some ectomycorrhizas. New Phytol. **115**: 269–274.

Fellbaum, C.R., Mensah, J. a., Cloos, A.J., Strahan, G.E., Pfeffer, P.E., Kiers, E.T., and Bücking, H. (2014). Fungal nutrient allocation in common mycorrhizal networks is regulated by the carbon source strength of individual host plants. New Phytol. **203**: 646–656.

Felten, J., Kohler, A., Morin, E., Bhalerao, R.P., Palme, K., Martin, F., Ditengou, F.A., and Legue, V. (2009). The ectomycorrhizal fungus *Laccaria bicolor* stimulates lateral root formation in poplar and *Arabidopsis* through auxin transport and signaling. Plant Physiol. **151**: 1991–2005.

Felten, J., Legué, V., Anicet Ditengou, F., and Ditengou, F.A. (2010). Lateral root stimulation in the early interaction between Arabidopsis thaliana and the ectomycorrhizal fungus *Laccaria bicolor*: Is fungal auxin the trigger? Plant Signal. Behav. **5**: 864–867.

Ferguson, B.J., Indrasumunar, A., Hayashi, S., Lin, M.H., Lin, Y.H., Reid, D.E., and Gresshoff, P.M. (2010). Molecular analysis of legume nodule development and autoregulation. J. Integr. Plant Biol. **52**: 61–76.

Garcia, K., Delaux, P.M., Cope, K.R., An, J., and Ané, J.M. (2015). Molecular signals required for the establishment and maintenance of ectomycorrhizal symbioses. New Phytol. **208**: 79–87.

Garcia, K., Doidy, J., Zimmermann, S.D., Wipf, D., and Courty, P.E. (2016). Take a trip through the plant and fungal transportome of mycorrhiza. Trends Plant Sci. **21**: 937–950.

Garcia, K. and Zimmermann, S.D. (2014). The role of mycorrhizal associations in plant potassium nutrition. Front. Plant Sci. **5**: 1–9.

Genre, A., Chabaud, M., Balzergue, C., Puech-Pagès, V., Novero, M., Rey, T., Fournier, J., Rochange, S., Bécard, G., Bonfante, P., and Barker, D.G. (2013). Short-chain chitin oligomers from arbuscular mycorrhizal fungi trigger nuclear Ca^{2+} spiking in *Medicago truncatula* roots and their production is enhanced by strigolactone. New Phytol. **198**: 190–202.

van der Heijden, M.G.A., Martin, F.M., Selosse, M.-A., and Sanders, I.R. (2015). Mycorrhizal ecology and evolution: the past, the present, and the future. New Phytol. **205**:

1406–1423.

Helber, N., Wippel, K., Sauer, N., Schaarschmidt, S., Hause, B., and Requena, N. (2011). A versatile monosaccharide transporter that operates in the arbuscular mycorrhizal fungus *Glomus* sp is crucial for the symbiotic relationship with plants.The Plant Cell **23**: 3812–3823.

Hibbett, D.S., Gilbert, L.B., and Donoghue, M.J. (2000). Evolutionary instability of ectomycorrhizal symbioses in basidiomycetes. Nature **407**: 506–508.

Horváth, B. et al. (2011). *Medicago truncatula IPD3* is a member of the common symbiotic signaling pathway required for rhizobial and mycorrhizal symbioses. Mol. Plant-Microbe Interact. **24**: 1345–1358.

IPCC (2014). Climate Change 2014: Synthesis Report. Contribution of Working Groups I, II and III to the Fifth Assessment Report of the Intergovernmental Panel on Climate Change.

Javot, H., Penmetsa, R.V., Terzaghi, N., Cook, D.R., and Harrison, M.J. (2007). A *Medicago truncatula* phosphate transporter indispensable for the arbuscular mycorrhizal symbiosis. Proc. Natl. Acad. Sci. **104**: 1720–1725.

Kevei, Z. et al. (2007). 3-Hydroxy-3-methylglutaryl coenzyme A reductase1 Interacts with NORK and is crucial for nodulation in *Medicago truncatula*. The Plant Cell **19**: 3974–3989.

Kiers, E.T. et al. (2011). Reciprocal rewards stabilize cooperation in the mycorrhizal symbiosis. Science **333**: 880–882.

Kloppholz, S., Kuhn, H., and Requena, N. (2011). A secreted fungal effector of *Glomus intraradices* promotes symbiotic biotrophy. Curr. Biol. **21**: 1204–1209.

Kohler, A. et al. (2015). Convergent losses of decay mechanisms and rapid turnover of symbiosis genes in mycorrhizal mutualists. Nature Genetics **47**: 410–415.

Lagrange, H., Jay-Allgmand, C., and Lapeyrie, F. (2001). Rutin, the phenolglycoside from eucalyptus root exudates, stimulates Pisolithus hyphal growth at picomolar concentrations. New Phytol. **149**: 349–355.

Lerouge, P., Roche, P., Faucher, C., Maillet, F., Truchet, G., Promé, J.C., and Dénarié, J. (1990). Symbiotic host-specificity of Rhizobium meliloti is determined by a sulphated and acylated glucosamine oligosaccharide signal. Nature **344**: 781–784.

Lévy, J. et al. (2004). A putative Ca^{2+} and calmodulin-dependent protein kinase required for bacterial and fungal symbioses. Science **303**: 1361–1364.

Loth-Pereda, V., Orsini, E., Courty, P.-E., Lota, F., Kohler, A., Diss, L., Blaudez, D., Chalot, M., Nehls, U., Bucher, M., and Martin, F. (2011). Structure and expression profile of the phosphate Pht1 transporter gene family in mycorrhizal *Populus trichocarpa*. Plant Physiol. **156**: 2141–2154.

Luginbuehl, L.H. and Oldroyd, G.E.D. (2017). Understanding the arbuscule at the heart of endomycorrhizal symbioses in plants. Curr. Biol. **27**: R952–R963.

MacLean, A.M., Bravo, A., and Harrison, M.J. (2017). Plant signaling and metabolic pathways enabling arbuscular mycorrhizal symbiosis. The Plant Cell tpc.00555.

Maillet, F. et al. (2011). Fungal lipochitooligosaccharide symbiotic signals in arbuscular mycorrhiza. Nature **469**: 58–64.

Marschner, P. (2012). Mineral nutrition of higher plants, 3rd ed. P. Marschner, ed (Academic Press).

Martin, F. et al. (2010). Périgord black truffle genome uncovers evolutionary origins and mechanisms of symbiosis. Nature **464**: 1033–1038.

Martin, F. et al. (2008). The genome of *Laccaria bicolor* provides insights into mycorrhizal symbiosis. Nature **452**: 88–92.

Martin, F., Duplessis, S., Ditengou, F., Lagrange, H., Voiblet, C., and Lapeyrie, F. (2001). Developmental cross talking in the ectomycorrhizal symbiosis: Signals and communication genes. New Phytol. **151**: 145–154.

Martin, F., Kohler, A., Murat, C., Veneault-Fourrey, C., and Hibbett, D.S. (2016). Unearthing the roots of ectomycorrhizal symbioses. Nat. Rev. Microbiol. **14**: 760–773.

Martin, F.M., Uroz, S., and Barker, D.G. (2017). Ancestral alliances: Plant mutualistic symbioses with fungi and bacteria. Science **356**: eaad4501.

Messinese, E., Mun, J.-H., Yeun, L.H., Jayaraman, D., Rougé, P., Barre, A., Lougnon, G., Schornack, S., Bono, J.-J., Cook, D.R., and Ané, J.-M. (2007). A novel nuclear protein interacts with the symbiotic DMI3 calcium- and calmodulin-dependent protein kinase of *Medicago truncatula*. Mol. Plant-Microbe Interact. **20**: 912–921.

Miyata, K. et al. (2014). The bifunctional plant receptor, *Os*CERK1, regulates both chitin-triggered immunity and arbuscular mycorrhizal symbiosis in rice. Plant Cell Physiol. **55**: 1864–1872.

Oldroyd, G.E.D. (2013). Speak, friend and enter: signalling systems that promote beneficial symbiotic associations in plants. Nat. Rev. Microbiol. **11**: 252–263.

Op den Camp, R., Streng, A., De Mita, S., Cao, Q., Polone, E., Liu, W., Ammiraju, J.S.S., Kudrna, D., Wing, R., Untergasser, A., Bisseling, T., and Geurts, R. (2011). LysM-type mycorrhizal receptor recruited for rhizobium symbiosis in nonlegume Parasponia. Science **331**: 909–912.

Parniske, M. (2008). Arbuscular mycorrhiza: the mother of plant root endosymbioses. Nat. Rev. Microbiol. **6**: 763–775.

Pellegrin, C., Daguerre, Y., Ruytinx, J., Guinet, F., Kemppainen, M., Plourde, M.B., Hecker, A., Morin, E., Pardo, A.G., Germain, H., Martin, F.M., and Veneault-Fourrey, C. (2017). *Laccaria bicolor* MiSSP8 is a small-secreted protein decisive for the establishment of the ectomycorrhizal symbiosis. bioRxiv: 218131.

Plett, J.M., Yin, H., Mewalal, R., Hu, R., Li, T., Ranjan, P., Jawdy, S., De Paoli, H.C., Butler, G., Burch-Smith, T.M., Guo, H.B, Chen, C.J., Kohler, A., Anderson, I.C., Labbé, J.L., Martin, F., Tuskan, G.A. and Yang, X. (2017). *Populus trichocarpa* encodes small, effector-like secreted proteins that are highly induced during mutualistic symbiosis. Sci. Rep. **7**: 382.

Plett, J.M., Daguerre, Y., Wittulsky, S., Vayssières, A., Deveau, A., Melton, S.J., Kohler, A., Morrell-Falvey, J.L., Brun, A., Veneault-Fourrey, C., and Martin, F. (2014a). Effector MiSSP7 of the mutualistic fungus *Laccaria bicolor* stabilizes the *Populus* JAZ6 protein and represses jasmonic acid (JA) responsive genes. Proc. Natl. Acad. Sci. U. S. A. **111**: 8299–304.

Plett, J.M., Kemppainen, M., Kale, S.D., Kohler, A., Legué, V., Brun, A., Tyler, B.M., Pardo, A.G., and Martin, F. (2011). A secreted effector protein of *Laccaria bicolor* is required for symbiosis development. Curr. Biol. **21**: 1197–1203.

Plett, J.M., Khachane, A., Ouassou, M., Sundberg, B., Kohler, A., and Martin, F. (2014b). Ethylene and jasmonic acid act as negative modulators during mutualistic symbiosis between *Laccaria bicolor* and *Populus* roots. New Phytol. **202**: 270–286.

Plett, J.M. and Martin, F. (2012). Poplar root exudates contain compounds that induce the expression of MiSSP7 in *Laccaria bicolor*. Plant Signal. Behav. **7**: 12–15.

Porth, I. and El-Kassaby, Y.A. (2015). Using *Populus* as a lignocellulosic feedstock for bioethanol. Biotechnol. J. **10**: 510–524.

Redecker, D., Kodner, R., and Graham, L.E. (2000). Glomalean fungi from the Ordovician. Science **289**: 1920–1921.

Sannigrahi, P., Ragauskas, A.J., and Tuskan, G.A. (2010). Poplar as a feedstock for biofuels: A review of compositional characteristics. Biofuels, Bioprod. Biorefining **4**: 209–226.

Singh, S. and Parniske, M. (2012). Activation of calcium- and calmodulin-dependent protein kinase (CCaMK), the central regulator of plant root endosymbiosis. Curr. Opin. Plant Biol. **15**: 444–453.

Smith, S.E. and Read, D. (2008). Mycorrhizal Symbiosis. Mycorrhizal Symbiosis: 611–XVIII.

Spatafora, J.W. et al. (2016). A phylum-level phylogenetic classification of zygomycete fungi based on genome-scale data. Mycologia **108**: 1028–1046.

Steinkellner, S., Lendzemo, V., Langer, I., Schweiger, P., Khaosaad, T., Toussaint, J.P., and Vierheilig, H. (2007). Flavonoids and strigolactones in root exudates as signals in

symbiotic and pathogenic plant-fungus interactions. Molecules **12**: 1290–1306.

Stracke, S., Kistner, C., Yoshida, S., Mulder, L., Sato, S., Kaneko, T., Tabata, S., Sandal, N., Stougaard, J., Szczyglowski, K., and Parniske, M. (2002). A plant receptor-like kinase required for both bacterial and fungal symbiosis. Nature **417**: 959–962.

Strullu-Derrien, C., Selosse, M.A., Kenrick, P., and Martin, F.M. (2018). The origin and evolution of mycorrhizal symbioses: From palaeomycology to phylogenomics. New Phytol.

Sun, J. et al. (2015). Activation of symbiosis signaling by arbuscular mycorrhizal fungi in legumes and rice. The Plant Cell tpc.114.131326.

Tedersoo, L. and Smith, M.E. (2013). Lineages of ectomycorrhizal fungi revisited: Foraging strategies and novel lineages revealed by sequences from belowground. Fungal Biol. Rev. **27**: 83–99.

Tisserant, E. et al. (2012). The transcriptome of the arbuscular mycorrhizal fungus *Glomus intraradices* (DAOM 197198) reveals functional tradeoffs in an obligate symbiont. New Phytol. **193**: 755–769.

Tuskan, G. a et al. (2006). The genome of black cottonwood, *Populus trichocarpa* (Torr. & Gray). Science **313**: 1596–1604.

Vayssières, A., Pěnčík, A., Felten, J., Kohler, A., Ljung, K., Martin, F.M., and Legue, V. (2015). Development of the *Populus-Laccaria bicolor* ectomycorrhiza modifies root auxin metabolism, signalling and response. Plant Physiol.: pp.114.255620.

Venkateshwaran, M., Cosme, a., Han, L., Banba, M., Satyshur, K. a., Schleiff, E., Parniske, M., Imaizumi-Anraku, H., and Ane, J.-M. (2012). The recent evolution of a symbiotic ion channel in the legume family altered in conductance and improved functionality in calcium signaling. The Plant Cell **24**: 2528–2545.

Venkateshwaran, M., Jayaraman, D., Chabaud, M., Genre, A., Balloon, A.J., Maeda, J., Forshey, K., den Os, D., Kwiecien, N.W., Coon, J.J., Barker, D.G., and Ané, J.-M. (2015). A role for the mevalonate pathway in early plant symbiotic signaling. Proc. Natl. Acad. Sci. **112**: 9781–9786.

Venkateshwaran, M., Volkening, J.D., Sussman, M.R., and Ané, J.M. (2013). Symbiosis and the social network of higher plants. Curr. Opin. Plant Biol. **16**: 118–127.

Werner, G.D. a, Cornwell, W.K., Sprent, J.I., Kattge, J., and Kiers, E.T. (2014). A single evolutionary innovation drives the deep evolution of symbiotic N_2-fixation in angiosperms. Nat. Commun. **5**: 4087.

Yano, K. et al. (2008). CYCLOPS, a mediator of symbiotic intracellular accommodation. Proc. Natl. Acad. Sci. U. S. A. **105**: 20540–20545.

Zhang, X., Dong, W., Sun, J., Feng, F., Deng, Y., He, Z., Oldroyd, G.E.D., and Wang, E.

(2015). The receptor kinase CERK1 has dual functions in symbiosis and immunity signalling. Plant J. **81**: 258–267.

Chapter 2: Molecular signals required for the establishment and maintenance of ectomycorrhizal symbioses

This chapter was previously published as:

> Garcia, K., Delaux, P. M., **Cope, K. R.**, & Ané, J. M. (2015). Molecular signals required for the establishment and maintenance of ectomycorrhizal symbioses. New Phytologist, 208(1), 79-87.

Author Affiliation:
Department of Agronomy, University of Wisconsin-Madison, Madison, WI 53706, USA

Contributions:
Kevin Garcia took the lead in writing this review and was the primary contributor for the central section on "Nutrients as regulators of ectomycorrhizal symbiosis". He also prepared Figures 1 and 3 as well as Table 1. Pierre-Marc Delaux and **Kevin R. Cope** contributed equally to the central section on "Signaling events in ECM associations." They also collaborated in preparing Figures 2 and 4.

2.1 Abstract

Ectomycorrhizal symbioses are one of the most widespread associations between roots of woody plants and soil fungi in forest ecosystems. These associations contribute significantly to the sustainability and sustainagility of these ecosystems through nutrient cycling and carbon sequestration. Unfortunately, the molecular mechanisms controlling the mutual recognition between both partners are still poorly understood. Elegant work has demonstrated that effector proteins from ectomycorrhizal and arbuscular mycorrhizal fungi regulate host defenses by manipulating plant hormonal pathways. In parallel, genetic and evolutionary studies in legumes showed that a "common symbiosis pathway" is required for the establishment of the ancient arbuscular mycorrhizal symbiosis and has been recruited for the rhizobia-legume association. Given that genes of this pathway are present in many angiosperm trees that develop ectomycorrhizae, we propose their potential involvement in some but not all ectomycorrhizal associations. The maintenance of a successful long-term relationship seems strongly regulated by resource allocation between symbiotic partners, suggesting that nutrients themselves may serve as signals. This review summarizes our current knowledge on the early and late signal exchanges between woody plants and ectomycorrhizal fungi, and we suggest future directions for decoding the molecular basis of the underground dance between trees and their favorite fungal partners.

2.2 Introduction

Mycorrhizal symbioses are ubiquitous associations occurring between soil fungi and the root system of most terrestrial plants. Although seven types of mycorrhizal associations have been identified, primarily two types, ectomycorrhizal (ECM) and arbuscular mycorrhizal (AM), have been studied extensively due to their ecological and economic importance as well as their phylogenic distribution and the number of plant and fungal species involved (Smith & Read, 2008; van der Heijden *et al.*, 2015). ECM fungi colonize preferentially woody plants whereas AM fungi associate with the vast majority of land plants, including most agricultural crops. The development of mycorrhizal symbioses is controlled by various developmental and environmental factors (Smith & Read, 2008). Although the molecular cross-talk resulting in AM associations is being studied extensively, the mutual recognition events and long-term maintenance factors controlling ECM symbioses remain largely unknown (Venkateshwaran *et al.*, 2013). In ECM and AM associations, both partners benefit from the bidirectional transfer of nutrients. Typically, host plants provide a carbon source and fungi improve the uptake of water, macronutrients (nitrogen, phosphorous and potassium) and micronutrients (Casieri *et al.*, 2013). Recent studies suggest that the control of these nutrient fluxes might play a key regulatory role in the maintenance of AM associations (Carbonnel & Gutjahr, 2014). Here we review advances and gaps in our understanding of regulatory mechanisms controlling the initiation and maintenance of ECM associations. We also propose new hypotheses, including the putative involvement of the common symbiosis pathway in the establishment of some but not all ECM associations as well as the role of nutrient fluxes as signals for the long-term maintenance of these symbiotic associations.

2.3 Signaling Events in Ectomycorrhizal Associations

The response of mycorrhizal fungi to plant root exudates

The first steps in the dance between host plants and mycorrhizal fungi start with the recognition of signal molecules released by both partners. Plants exude many primary and secondary metabolites in the rhizosphere, including sugars, hormones and enzymes that affect the root microbiome. In ECM associations, the effect of these root exudates on the growth of ECM fungi was first described in the 50's (Melin, 1954; Fig. 1a). Later, Fries *et al.* (1987) observed the germination of *Suillus* spp. spores in response to abietic acid present in root exudates of *Pinus sylvestris.* The first report of a plant flavonoid acting as a signal molecule in ECM association was reported in the *Eucalyptus globulus* spp. *bicostata – Pisolithus* spp. interaction (Lagrange *et al.*, 2001). In this study, rutin secreted by the host plant enhances the hyphal growth of two *Pisolithus* strains collected under *Eucalyptus* trees, suggesting a role of flavonoids in ECM symbiosis specificity. Later, rutin was found in the root exudates of many plants and its effect on hyphal growth was described in several pathogenic fungi (Kalinova & Radova, 2009). These results highlight the important role of this plant metabolite in the regulation of the rhizosphere fungal community but also a lack of specificity for symbiotic associations. Kikuchi *et al.* (2007) demonstrated that seven flavonoids found in *Pinus densiflora* root exudates strongly stimulate spore germination of the ECM fungus *Suillus bovinus*. Interestingly, two plant flavonoids trigger the expression of a fungal effector protein in *Laccaria bicolor* (Plett & Martin, 2012; see below). Flavonoids were also shown to stimulate branching, growth and spore production of AM fungi and to increase the colonization levels of AM fungi, but their role remains unclear (reviewed in Abdel-Lateif *et al.*, 2012).

Similarly, the growth stimulation of AM fungi by root exudates has been known for several decades (Mosse & Hepper, 1975). However, the active "branching factors" that trigger

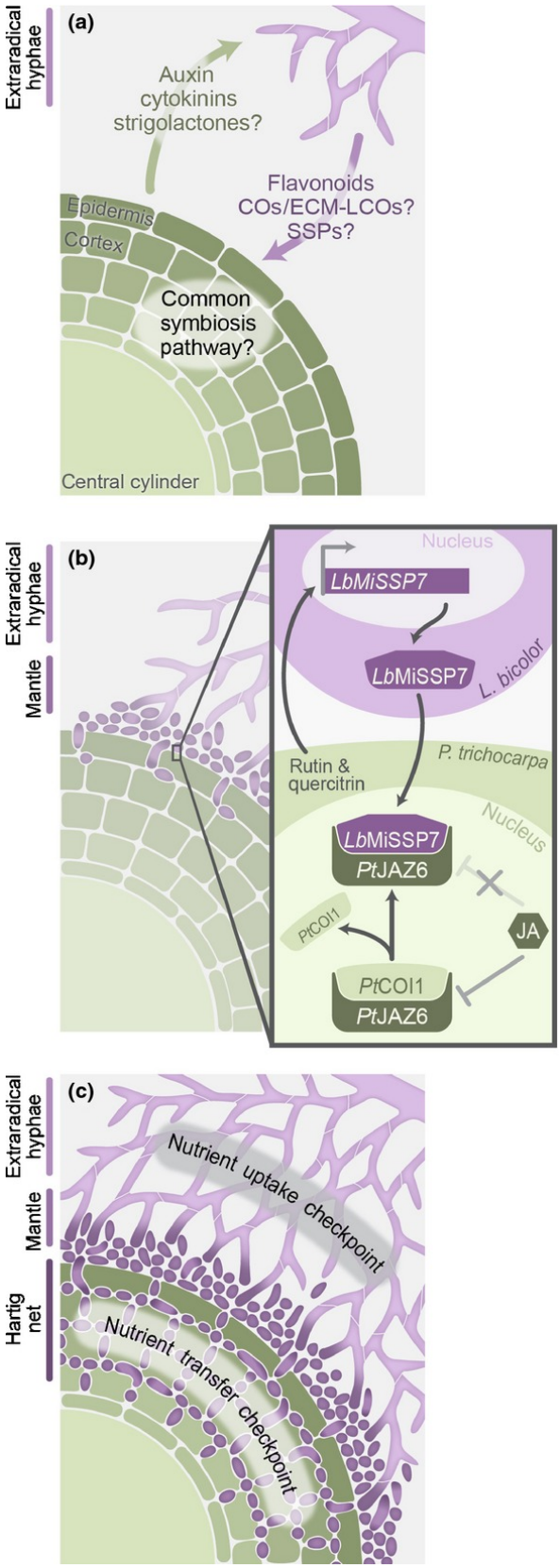

Figure 1. Signaling and regulation of ectomycorrhizal (ECM) symbiosis development and function.

(a) The first recognition steps between plant roots and pre-symbiotic ECM fungi involve a chemical dialogue, involving the release of flavonoids and hormones. The involvement of fungal lipochitooligosaccharides (LCOs), chitooligosaccharides (COs) and small-secreted proteins (SSPs) in the early stages of the ECM interaction are unknown so far. Similarly, the common symbiosis pathway could be involved in some types of ECM associations.

(b) In the *Laccaria bicolor* – *Populus trichocarpa* interaction, the formation of the Hartig net is regulated by the fungal effector *Lb*MiSSP7. The expression of *Lb*MiSSP7 is induced by two plant flavonoids (rutin and quercitrin). Upon expression, *Lb*MiSSP7 is exported from the fungus and imported into the nucleus of the plant cell where it interacts with the protein *Pt*JAZ6. This interaction prevents the formation of the *Pt*JAZ6-PtCOI1 complex and protects *Pt*JAZ6 from degradation induced by jasmonic acid (JA).

(c) In order to maintain a long-term cooperative relationship, nutrient allocation from both plant and fungal partners need to be finely regulated in mature ectomycorrhizae. Thus, regulatory checkpoints requiring transcriptional, post-transcriptional, and translational regulations of transport systems are needed for resource acquisition from soil and nutrient transfers between partners.

spore germination and hyphal branching of AM fungi have been identified only recently as strigolactones (Akiyama *et al.*, 2005). Strigolactone biosynthesis requires two enzymes involved in carotenoid cleavage, CCD7 and CCD8. Though strigolactones have not been detected in gymnosperms thus far, both their presence in all land plants investigated, including the earliest diverging ones, and the finding of CCD7 and CCD8 orthologs in available genomes and transcriptomes of gymnosperms strongly suggest their presence in these lineages (Delaux *et al.*, 2012; Fig. 2). The absence of a CCD8 ortholog in *Pinus massoniana* is likely due to the low transcriptomic coverage for this species.

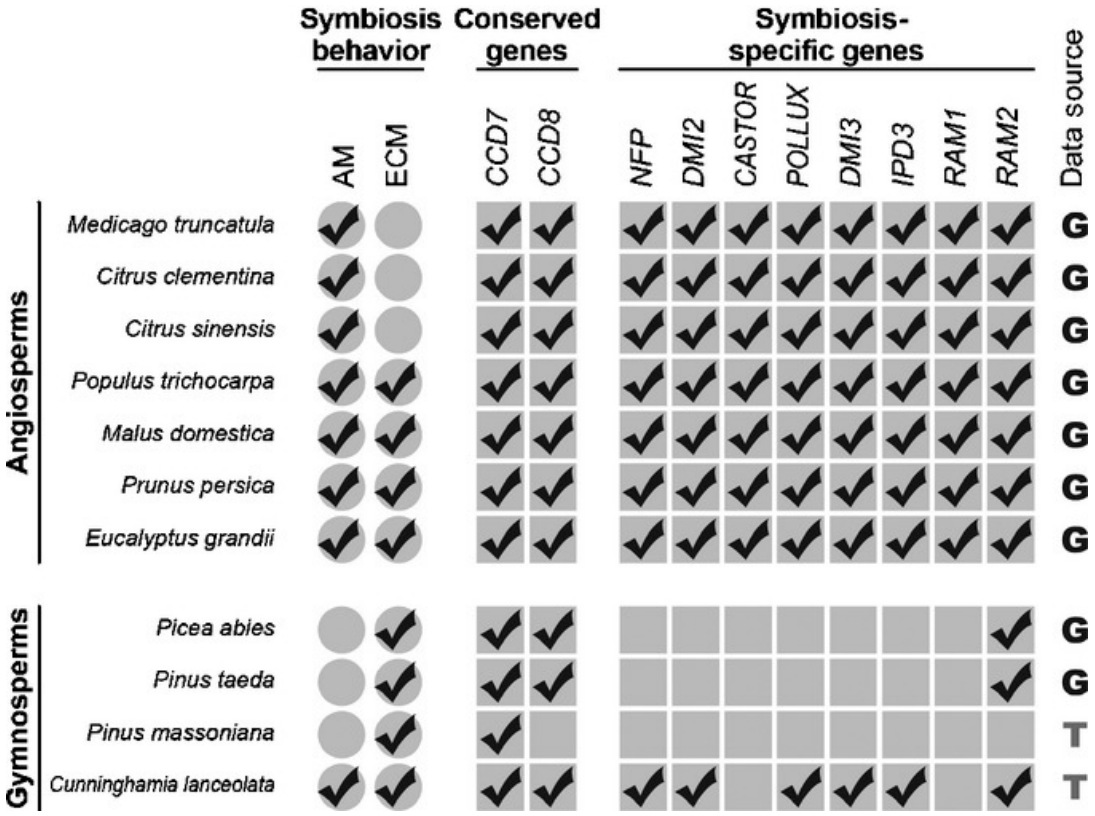

Figure 2. Loss of the common symbiosis pathway genes in Pinaceae. Most of the common symbiosis pathway genes are not detected in the genomes and transcriptomes of ECM-specific species belonging to the Pinaceae clade, except the transcription factor RAM2 identified in both the *Picea abies* and *Pinus taeda* genomes. CCD7 and CCD8 genes coding for enzymes involved in strigolactones production are also detected in these Coniferae genomes. The absence of CCD7, CCD8 and RAM2 genes in *Pinus massoniana* transcriptome does not mean this gene is absent in the genome of this species. Check marks indicate presence or absence of a gene or behavior trait.

When a synthetic strigolactone analog (GR24) was applied to various soil-borne fungi, including four ECM fungi, no growth response was observed (Steinkellner *et al.*, 2007). Despite these negative results, the involvement of strigolactones in ectomycorrhizal symbiosis cannot be ruled out. More than a developmental response, strigolactones could activate symbiotic pathways and the production of signals such as effectors or chitin-derived signals (Genre *et al.*, 2013). Generation of *ccd7* and *ccd8* knock-out or knock-down tree lines should allow a direct investigation of this hypothesis. Beyond strigolactones, the role of plant hormones in the early stages of ECM associations remains elusive. Various roles have been proposed for other phytohormones such as auxins that are known to stimulate hyphal branching of ECM fungi (Debaud & Gay, 1987). Auxin is produced by both plant and fungal partners and seems to play an early role in the control of root development prior to fungal colonization (Felten *et al.*, 2010). Cytokinins were described as stimulators of hyphal development in *Suillus variegatus* (Gogala, 1991). At later stages, treatment of ECM poplar roots with ethylene and jasmonic acid prevented fungal colonization while salicylic acid treatment did not (Plett *et al.*, 2014a). Again, reverse genetic approaches may help with evaluating the importance of phytohormones in the initiation of ECM associations.

Independent recruitment of the common symbiosis pathway in ectomycorrhizal associations

In AM associations, the fungus participates in the molecular dialogue with the plant by releasing a mixture of signaling molecules, including lipochitooligosaccharides and short chitooligosaccharides (Maillet *et al.*, 2011; Genre *et al.*, 2013). To date, there is no evidence that such molecules are produced by ECM fungi too. However, in order to allow cell wall plasticity, fungi produce several chitinases and glucanases. It seems likely that all fungi are able to release chitooligosaccharides as a byproduct of cell wall remodeling (Adams, 2004). In addition, ECM

fungi constitutively secrete chitin-derived molecules into their environment. *Amanita muscaria* and *Hebeloma crustuliniforme* release elicitors triggering defense reactions in the host plant *Picea abies* (Sauter & Hager, 1989; Salzer *et al.*¸ 1997). These elicitors may constitute one of the first steps in a molecular dialogue in ECM association. Interestingly, similar microbe-associated molecular patterns (MAMPs) are also required in the early steps of the rhizobia-legume symbiosis (Luo & Lu, 2014). Lipochitooligosaccharides from AM fungi are similar to those produced by rhizobia (referred to as Nod factors) (Maillet *et al.*, 2011). The backbone of lipochitooligosaccharides is synthesized by three *nod* genes present in most rhizobia: a chitin synthase (*nodC*), a chitin deacetylase (*nodB*) and an acyltransferase (*nodA*). In genomic databases for two ECM fungi, *L. bicolor* and *Tuber melanosporum*, many potential homologs of *nodA/B/C* genes can be found (Table 1; Martin *et al.*, 2008, 2010). As mentioned previously, it is possible that such enzymes are produced by fungi to allow cell wall remodeling. Biochemical screening of ECM exudates and genetic analyses will be needed to unravel the possible role of these enzymes and chitin-derived molecules in ECM associations. Although the ability of fungi to form ECM association arose at least 80 times independently in the Basidiomycota clade, the strict specificity of this symbiosis is very rare (Tedersoo & Smith, 2013). We can assume that plant and fungal signals may be widely distributed or easy to acquire through convergent evolution.

Table 1. Putative fungal *nodA/B/C-like* genes of ectomycorrhizal fungi *Laccaria bicolor* and *Tuber melanosporum*.

Gene annotation	*L. bicolor* (i)	*T. melanosporum* (ii)
Chitin synthase (*nodC-like*)	22	11
Chitin deacetylase (*nodB-like*)	21	14
Acyltransferase (*nodA-like*)	110	81

Several fungal genes putatively involved in chitin synthase (*nodC-like*), deacetylase (*nodB-like*) and acyltransferase (*nodA-like*) activity are annotated in the genomes of *Laccaria bicolor* and *Tuber melanosporum* genomes. Although the presence of ECM-lipochitooligosaccharides and chitooligosaccharides has yet to be determined, these genes may participate in the synthesis of such fungal chitin oligomers.
(i) http://genome.jgi-psf.org/Lacbi2/Lacbi2.home.html
(ii) http://genome.jgi.doe.gov/Tubme1/Tubme1.home.html

In the model legume *Medicago truncatula*, the perception and transduction of chitooligosaccharides and lipochitooligosaccharides produced by AM fungi and rhizobia requires a set of genes often referred to as the "common symbiosis pathway". Several LysM-receptor-like kinases are required to perceive these signals. Then, a series of signal transduction proteins, including a leucine-rich repeat receptor-like kinase (DMI2), which serves as a co-receptor, two nuclear ion channels (CASTOR and POLLUX), a calcium- and calmodulin-dependent protein kinase (DMI3) and at least one transcription factor (IPD3), are required for the activation of the plant symbiotic program. Downstream, a GRAS transcription factor (RAM1) and a glycerol-3-phosphate acyl transferase (RAM2) allow the establishment of AM symbiosis (reviewed in Venkateshwaran *et al.*, 2013). Genes encoding these proteins are highly conserved in angiosperm and gymnosperm species that form AM, and for some of them, ECM associations (Fig. 2). Recently, Delaux *et al.* (2014) demonstrated that the loss of these genes in several lineages is consistently correlated with the loss of AM symbiosis. Interestingly, with the exception of *RAM2,* the above mentioned symbiosis specific genes cannot be detected in available genomes and transcriptomes of plant species in the Pinaceae family. Although the potential AM colonization of such species was proposed (Wagg *et al.*, 2008), the lack of arbuscule observations combined with the absence of most or all of the genes in the common symbiosis pathway suggests that Pinaceae trees cannot form a *bona fide* AM symbiosis. These observations cannot exclude that some level of nutrient exchanges between the partners may occur. This finding strongly supports the idea that ECM symbiosis in Pinaceae does not rely on the common symbiosis pathway. ECM evolved independently in many other gymnosperm and angiosperm lineages and some ECM fungi associate with host plants within and outside the Pinaceae (Churchland & Grayston, 2014). Thus, it is possible that, in some lineages, the common symbiosis pathway was recruited to allow ECM symbioses (Fig. 1a). One could hypothesize that ECM fungi colonizing both Pinaceae and non-

Pinaceae trees would produce lipochitooligosaccharides whereas Pinaceae-specific colonizers would not. ECM fungi able to colonize both clades of trees could potentially up or down regulate the biosynthesis of lipochitooligosaccharides depending on the host with which it associates. An extensive biochemical survey of ECM fungal exudates coupled with massive sequencing of a large array of ECM trees should provide more insights into these mechanisms. At the same time, we cannot exclude that other signals (chemical or not) produced by ECM fungi may activate the common symbiosis pathway. There is strong evidence for instance that the common symbiosis pathway is involved in the transduction of mechanical signals produced by the hyphopodium of AM fungi (reviewed in Jayaraman *et al.*, 2014). Even if they do not form hyphopida, it seems possible that ECM fungi may apply mechanical forces on host cells too. Ultimately, knocking-down or knocking-out genes of the common symbiosis pathway in ECM host trees will provide the most definitive answer on their putative involvment in ECM associations. In addition to the common symbiosis pathway, it is worth mentioning the presence of *RAM2* in all the species examined, including those in the Pinaceae, thus suggesting its possible role in ECM symbiosis (Fig. 2). In AM associations, RAM2 catalyzes the synthesis of cutin monomers that are perceived by the fungus, leading to the formation of penetration structures. Therefore, cutin monomers could be applied on ECM fungi to test their potential role during fungal colonization as was shown for the colonization by some oomycetes (Wang *et al.*, 2012).

The central role of fungal effectors in ECM associations

Plants share their environment with many microbes and are constantly interacting with fungal, bacterial, and viral pathogens. Many of these pathogens secrete cocktails of effector proteins in order to counteract plant defenses including the jasmonic acid, ethylene, and salicylic acid pathways. The manipulation of plant immunity allows efficient colonization, rapid growth,

and propagation of the pathogen into host tissues (reviewed in Win *et al.*, 2012). During host colonization, many effectors encoded for by multiple genes are produced by the AM fungus *Rhizophagus irregularis* and the ECM fungus *L. bicolor* (Martin *et al.*, 2008; Tisserant *et al.*, 2013). Just like effectors produced by pathogens, small secreted peptides produced by mycorrhizal fungi target host defense mechanisms. The effector SECRETED PROTEIN 7 (SP7) from *R. irregularis* is secreted by the AM fungus into plant cells where it interacts with a nuclear ethylene-responsive transcription factor (ERF19) and keeps plant defense reactions under control (Kloppholz *et al.*, 2011). During the ECM interaction between *L. bicolor* and *P. trichocarpa*, the expression of MYCORRHIZAL iNDUCED SMALL SECRETED PROTEIN 7 (*MiSSP7*) is induced by two flavonoids produced by the plant (Plett & Martin, 2012; Fig. 1b). MiSSP7 is imported to the plant nucleus where it interacts with the JASMONATE ZIM-DOMAIN 6 (*Pt*JAZ6) protein (Plett *et al.*, 2011, 2014b). The fairly high concentrations of flavonoids used in this study make it difficult to conclude that they are the genuine signals triggering the expression of *MiSSP7* in natural conditions but the role of MiSSP7 in the control of plant defense reactions was very nicely demonstrated. The degradation of *Pt*JAZ6 mediated by its interaction with the CORONATINE-INSENSITIVE 1 (*Pt*COI1) protein in response to jasmonic acid triggers plant immune responses. By decreasing the formation of *Pt*JAZ6-*Pt*COI1 complex and preventing the jasmonic acid-dependent degradation of *Pt*JAZ6, the MiSSP7-*Pt*JAZ6 interaction reduces the plant immune response (Fig. 1b). Given that jasmonic acid is a negative regulator of ECM associations, counteracting this plant defense pathway allows hyphal development into the plant root and ultimately the formation of the Hartig net. Due to cell autonomous action of effectors, their effect is very local, thus avoiding a systemic alteration of jasmonic acid-dependent plant defenses. Once the Hartig net is formed, the ECM symbiosis becomes functional (Plett *et al.*, 2011). In addition to establishment, we may hypothesize that MiSSPs are also excreted in mature

ectomycorrhizae to keep plant defense reactions under control and maintain a long-term mutualistic association (Fig. 1a). Surprisingly, no such fungal effectors were found in the ectomycorrhiza-regulated transcript of *T. melanosporum*, reinforcing the view that the term "ECM associations" encompass a wide range of symbioses that are established and maintained through very different mechanisms (Martin *et al.*, 2010). The recent release of many ECM fungal genomes together with the rapid increase of genetically transformable fungal species will allow further studies to decipher the role of ECM effectors in a more comprehensive manner (Kohler *et al.*, 2015).

2.4 Nutrients as Regulators of Ectomycorrhizal Symbiosis

The nutrient marketplace of mycorrhizal symbiosis

Nutrient dynamics in AM symbioses were recently proposed to follow a "reciprocal reward" system governing resource allocation between host plants and AM fungi (Hammer *et al.*, 2011; Kiers *et al.*, 2011). This fine balance may be necessary for a long-term mutualistic association in AM symbiosis. In multi-compartment experiments using one plant and one fungal species, AM fungi providing the greater amount of phosphorous or nitrogen to the host plant were rewarded with more carbon, and reciprocally plants providing more carbon received more nutrients (Kiers *et al.*, 2011; Fellbaum *et al.*, 2012). The first molecular mechanisms controlling these nutrient dynamics have been identified recently through genetic studies. An AM-induced phosphorous transporter from *M. truncatula*, *Mt*PT4, was up-regulated in response to carbon allocation from the host plant (Harrison *et al.*, 2002; Fellbaum *et al.*, 2014). The corresponding *mtpt4* mutants displayed a premature degeneration of fungal arbuscules, indicating that phosphorous delivery from the fungus is crucial for the maintenance of AM symbiosis in *M. truncatula* (Javot *et al.*, 2007). Given that root-organ-cultures were used in these initial studies

and that such an experimental system may affect sink/source feedback loops between the two partners (Kiers *et al.*, 2011; Olsson *et al.*, 2014), other authors used entire plants to conduct similar experiments. Although these reciprocal rewards can act as a regulatory mechanism for avoiding cheaters and less cooperative partners, Walder *et al.* (2012) demonstrated that unequal trades occur in a mixed-culture experiment using both flax and sorghum (C_3 and C_4 plants, respectively) colonized by the same AM fungus. C_4 plants possess a more efficient photosynthetic machinery than C_3 plants; thus, sorghum could transfer a larger amount of carbon to the fungus than flax, partially explaining the observed phenotype. Another recent study contests this mutual rewards hypothesis as a general principle and showed that, when mycorrhizal wheat plants are shaded, fungal phosphorous allocation is not dependent on host carbon availability (Stonor *et al.*, 2014). We cannot exclude that, in some experimental conditions, reward mechanisms involve other nutrients or benefits that may be sufficient to stabilize the mutualism. Other authors showed that shading *M. truncatula* or *Allium vineale* host plants affects carbon and phosphorus allocation but not the colonization rate during AM associations (Fellbaum *et al.*, 2014; Zheng *et al.*, 2015). Altogether these studies suggest that reciprocal rewards in AM symbiosis are not always observed in natural ecosystems. Nutrient dynamics may be affected by growth conditions but also the genetic, developmental or physiological status of the organisms involved. Finally, the existence of mycoheterotrophic plants that are non-chlorophyllic species receiving both phosphorus and carbon from mycorrhizal fungi, illustrates that co-evolution can lead to breaching the barriers built against non-rewarding partners (Selosse & Rousset, 2011; Smith & Smith, 2014).

In ECM associations, no reciprocal rewards between fungi and host trees have been reported so far. Nevertheless, it can be assumed that nutrient markets occurring in ECM symbioses might depend on the degree of specificity between hosts and mycorrhizal symbionts

(Bruns *et al.*, 2002). The vast majority of trees growing in temperate and boreal forests are associated with dozens of ECM fungi at the same time. However, the degree of host specificity is highly variable between fungal lineages and strict host specificity is rare (Churchland & Grayston, 2014). Moreover, some trees such as poplars can interact with both AM and ECM fungi (Loth-Pereda *et al.*, 2011). As a consequence, the allocation of nutrients between partners in AM and ECM symbiosis might be dependent of environmental, developmental and physiological factors. Interestingly, Näsholm *et al.* (2013) recently demonstrated unequal carbon:nitrogen trades in boreal forests between ECM fungi and their host plants under low nitrate availability. In these conditions, ECM fungi transferred a limited amount of nitrogen to trees even if a large quantity of carbon was provided by the host plant. As a consequence, mycorrhizal trees displayed reduced performance due to the "non-cooperative" behavior of their ECM fungal partners. This reduction in mutualistic behavior could be explained by the regulatory role of nutrient availability on hyphal development. Several reports showed reduced ECM mycelium growth under high nitrogen conditions, which was likely due to the large amount of carbon required to assimilate this nutrient at the expense of growth (reviewed in Ekblad *et al.*, 2013). Because ECM fungi need more carbon to efficiently assimilate nitrogen under non-limiting conditions, this could result in an increase in nitrogen transfer to the host in order to prevent an over-accumulation of nitrogen and to ensure a constant source of carbon (Fig. 3a). In contrast, the production of ECM fungal biomass is much more important under low nitrogen conditions due to a low carbon requirement, further indicating that unequal carbon:nitrogen fluxes can affect host trees (Fig. 3). In addition, carbon cost is strongly related to the form of nitrogen available since more carbon is required to assimilate nitrate compared to ammonium (Plassard *et al.*, 2000). Although it was shown that the growth of some ECM fungi is also inhibited at high phosphorous levels, further experiments will be needed to understand how

phosphorous availability can affect carbon:phosphorous trades in ECM associations (Fig. 3; Torres Aquino & Plassard, 2004). Though reward mechanisms have been demonstrated for carbon versus phosphorus and nitrogen in some conditions, multiple other benefits may also be involved in the formation and the stabilization of this association. Additional research should seek to evaluate the degree of equal trades occurring in AM and ECM symbioses in natural

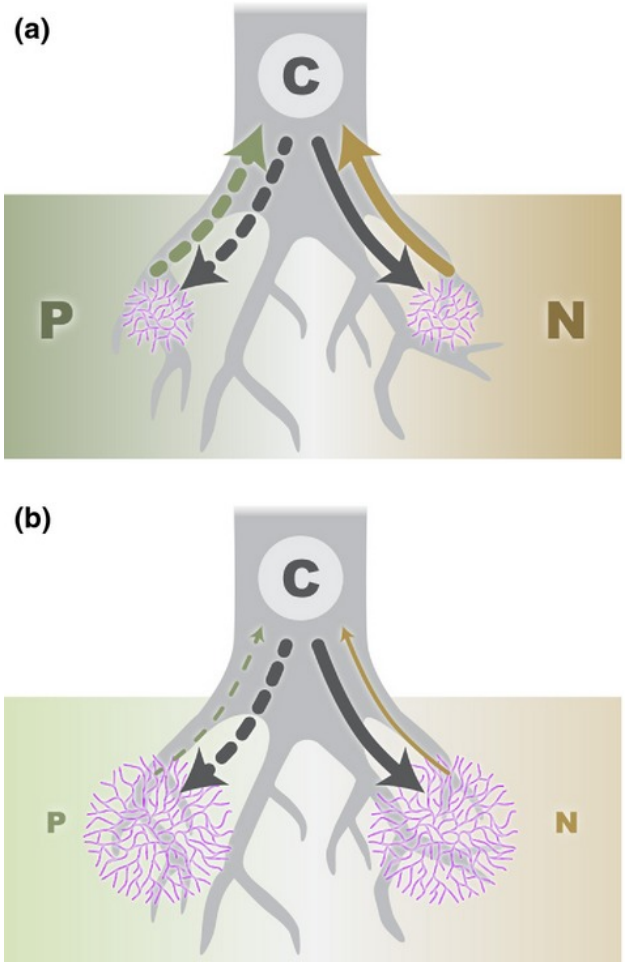

Figure 3. Model of the impact of phosphorous (P) and nitrogen (N) availability on ECM mycelium production and resource allocation between host and fungi in temperate and boreal forests.

(a) At high P and N, the growth reduction observed in ECM mycelium is probably due to the energy required for nutrient assimilation at the expense of growth (Ekblad *et al.*, 2013). Thus, equal nutrient trades are observed under N-sufficient conditions in boreal forest in order to ensure a sustainable source of carbon (C) to the fungal partner (Näsholm *et al.*, 2013).

(b) In contrast, at low P and N, fungal mycelium require a lower amount of C to grow. Thus, it could result in the unequal N allocations observed by Näsholm *et al.* (2013) in such conditions. Concerning P, similar results on the reciprocal allocation between plant and fungal partners can be assumed but have not been described so far (dotted arrows).

ecosystems while taking into account more mutual benefits than just carbon, phosphorus, and nitrogen. Altogether these studies indicate the existence of a central, active, but not always stable marketplace in ECM forests and reinforce the importance of nutrient availability in the homeostasis of mycorrhizal associations.

Plant transport systems involved in mycorrhizal nutrient trades

Nutrient fluxes between the host plant and the fungal partner are supported by a wide range of transport systems. On the plant side, these proteins need to be expressed specifically in arbuscule-containing cells or in cortical cells encompassed by the Hartig net for AM or ECM associations respectively. Although sucrose and mono-/di- saccharide transporters (SUT and SWEET proteins, respectively) may play a role in the release of plant carbon to the apoplasm in AM and ECM symbioses, there is no evidence so far that they are regulated in response to phosphorous or nitrogen provided by the fungus (Casieri *et al.*, 2013). Regarding nutrient fluxes from the fungal partner, several studies have reported AM-specific expression of plant genes involved in phosphorous and nitrogen transport (reviewed in Casieri *et al.*, 2013). Recently, Delaux *et al.* (2014) identified a suite of genes exclusively present in AM host plants. Interestingly, *M. truncatula* genes coding for the phosphate transporter *Mt*PT4, two ABC transporters and some other putative transport systems were present specifically in plants that can be colonized by AM fungi. Due to the strong degree of conservation of these genes in AM-hosts, we hypothesize that molecules transported by the corresponding proteins could play important trophic and/or regulatory functions in the establishment or the maintenance of AM associations. The poplar phosphate transporters *Pt*PT9, *Pt*PT10 and *Pt*PT12 are upregulated in AM roots and *Pt*PT9 and *Pt*PT12 are also up-regulated in ECM associations and phosphorus deficiency (Loth-Pereda *et al.*, 2011). This suggests a possible recruitment of AM phosphate transporters for ECM associations. However, no ECM-specific phosphate transporter has been identified so far. Recent studies tend to highlight the importance of phosphorous in the regulation of AM associations since fungal colonization is highly dependent on phosphorous availability (reviewed in Carbonnel & Gutjahr, 2014). Although a complete inhibition of plant association with AM fungi was observed in phosphorous-sufficient conditions, nitrogen, potassium, calcium or iron deprivation

partially restored the colonization process (Nouri *et al.*, 2014). In addition, the severe arbuscule degeneration phenotype observed in *M. truncatula mtpt4* mutant was partially rescued under nitrogen deficiency (Javot *et al.*, 2011) and *Mt*PT4 expression is dependent on carbon transferred to the fungal partner (Fellbaum *et al.*, 2014). All these data suggest that resource availability and allocation considerably impact the establishment and maintenance of AM associations. In contrast, very little is known about how nutrients affect ECM associations and the molecular mechanisms involved. Although one nitrogen and two phosphate transporters from poplar were up-regulated during colonization by *L. bicolor* (Selle *et al.*, 2005; Loth-Pereda *et al.*, 2011), there is no evidence for the involvement of a carbon-mediated regulation of these proteins via a reciprocal reward mechanism. Investigating the expression of these transporters in response to plant carbon availability could provide the first molecular insights into reciprocal market dynamics in ECM symbiosis.

Fungal transport systems mycorrhizal nutrient trades

The molecular players allowing and regulating nutrient fluxes on the fungal side are still poorly described. In order to establish a functional association, a polarized localization of fungal transport systems at the uptake and release sites is needed. Two important checkpoints of nutrient flow can be described in the fungal partner (Fig. 1c). First, transporters that allow soil-fungus nutrient fluxes are probably expressed specifically in extra-radical hyphae. Due to their crucial role in soil nutrient uptake, it can be assumed that these proteins are key regulators of nutrient exchanges during mycorrhizal symbiosis. In the case of non-reciprocal trades with the host, the reduction in external nutrient acquisition could significantly affect plant nutrition to avoid the amplification of unequal fluxes. Few phosphate, nitrate and ammonium concentration-dependent transporters have been functionally characterized in ECM fungi so far (reviewed in Casieri *et al.*,

2013). Interestingly, Avolio *et al.* (2012) showed that organic and inorganic nitrogen transporters from *H. cylindrosporum* were up-regulated in pure culture under a high carbon:nitrogen ratio. A nitrate transporter in *H. cylindrosporum* (*Hc*NRT2) was up-regulated specifically by ECM associations and external carbon sources (Rékangalt *et al.*, 2009). These studies suggest a carbon-dependent modulation of fungal nitrogen transporters, but further experiments will be needed to determine if this regulation is also dependent on host carbon allocation. Regarding phosphorous, the expression of the phosphate transporter *Hc*PT1.1 from *H. cylindrosporum* was induced under phosphorous and potassium deprivation (Garcia *et al.*, 2013, 2014). Moreover, the alteration of fungal potassium nutrition triggered by the overexpression of a potassium transporter of *H. cylindrosporum* affected both potassium and phosphorous nutrition of mycorrhizal plants. All these findings indicate that a fine control of fungal ion homeostasis through their uptake, assimilation, and mobilization is required for efficient nutrient transfer to the host.

On the other side, both host carbon acquisition and fungal nutrient discharge in the plant-fungus interface probably requires the specific expression and regulation of fungal transporters and channels. A second regulatory checkpoint of symbiotic nutrient fluxes probably takes place at this interface with the regulation of these transport systems (Fig. 1c). During AM symbiosis, *RiMST2* coding for a monosaccharide transporter from *R. irregularis* is expressed in intraradical hyphae, up-regulated at high carbon, and down-regulated at high phosphorous (Helber *et al.*, 2011). This suggests a fungal molecular response to a decrease of plant carbon allocation due to the alteration of fungal phosphorous transfer under phosphorous-sufficient conditions. To date, no transport systems specifically expressed at the plant-fungus interface have been characterized in ECM symbiosis. The identification and characterization of host carbon regulation of such transporters will be essential to unravel both the nutrient-flux molecular toolkit of ECM fungi and the impact of the host plant on fungal nutrient allocation.

2.5 Conclusion

The molecular bases of establishment and maintenance of ECM symbioses are still poorly understood. It is tempting to transfer our knowledge of AM symbiosis to ECM symbiosis as it appears that some mechanisms are indeed shared between the two types of mycorrhizal associations. However, many mechanisms seem very specific to one or the other symbiosis (Fig. 4). With the recent release of several ECM genomes combined with the development of molecular and genetic tools in higher fungi and host trees, key signaling and regulatory components controlling ECM associations will likely be decoded in the near future.

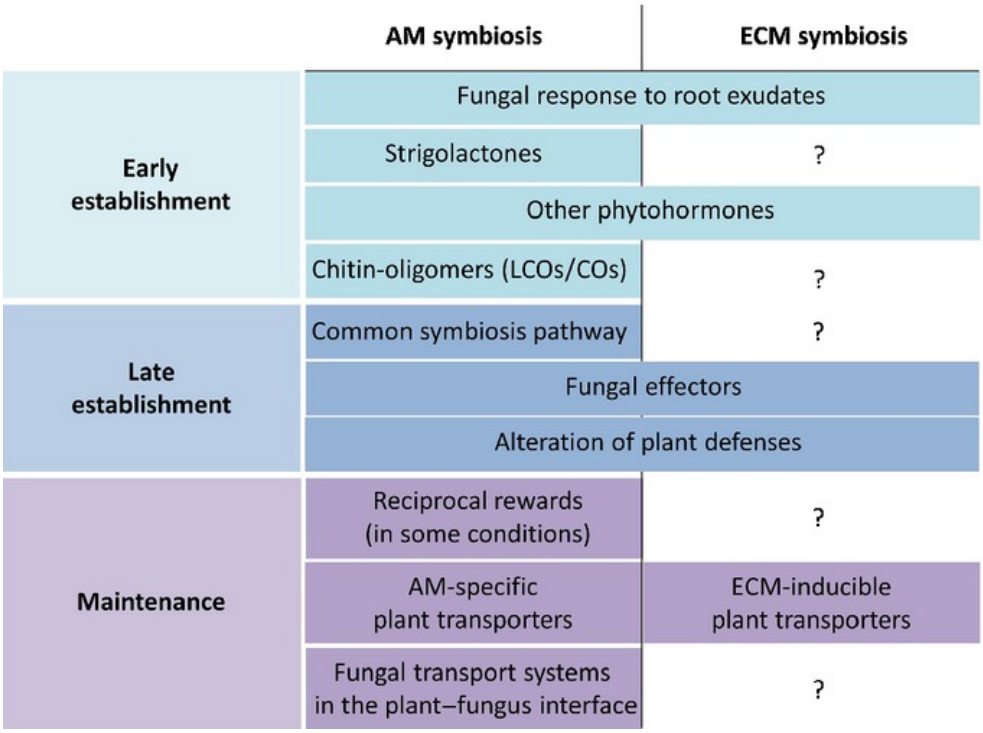

Figure 4. Comparison of the current knowledge dealing with molecular signaling events in AM and ECM symbioses. Our current understanding of the factors required for the establishment and maintenance of AM symbiosis far outweigh that of ECM symbiosis. For example, the role of plant strigolactones, fungal lipochitooligosaccharides (LCOs), and chitooligosaccharides (COs) in ECM symbiosis is still debated, and no evidence indicate that the "common symbiosis pathway" required for the establishment of AM symbiosis is also needed in ECM association. During the maintenance steps, the role of nutrients as regulators of ECM symbiosis through reciprocal reward mechanisms is still hypothetical. In addition, no ECM-specific plant transporters have been identified thus far, and no transport systems specifically expressed at the plant-ECM fungal interface have been characterized.

2.6 Acknowledgments

We thank Dr. Claude Plassard for her comments on the manuscript. K.G. was supported by a grant from the National Science Foundation (NSF-IOS#1331098) and K.R.C by a grant from the U.S. Department of Agriculture (USDA Hatch#WIS01695).

2.7 References

Abdel-Lateif K, Bogusz D, Hocher V. **2012**. The role of flavonoids in the establishment of plant roots endosymbioses with arbuscular mycorrhiza fungi, rhizobia and *Frankia* bacteria. *Plant Signaling & Behavior* **7**: 636–641.

Adams DJ. **2004**. Fungal cell wall chitinases and glucanases. *Microbiology* **150** : 2029–2035.

Akiyama K, Matsuzaki K, Hayashi H. **2005**. Plant sesquiterpenes induce hyphal branching in arbuscular mycorrhizal fungi. *Nature* **435**: 824–827.

Avolio M, Müller T, Mpangara A, Fitz M, Becker B, Pauck A, Kirsch A, Wipf D. **2012**. Regulation of genes involved in nitrogen utilization on different C/N ratios and nitrogen sources in the model ectomycorrhizal fungus *Hebeloma cylindrosporum*. *Mycorrhiza* **22**: 515–524.

Bruns TD, Bidartondo MI, Taylor DL. **2002**. Host specificity in ectomycorrhizal communities: What do the exceptions tell us? *Integrative and Comparative Biology* **42**: 352–359.

Carbonnel S, Gutjahr C. **2014**. Control of arbuscular mycorrhiza development by nutrient signals. *Frontiers in Plant Science* **5**: 462.

Casieri L, Lahmidi NA, Doidy J, Zimmermann S, Plassard C, Wipf D. **2013**. Biotrophic transportome in mutualistic plant – fungal interactions. *Mycorrhiza* **23**: 597–625.

Churchland C, Grayston SJ. **2014**. Specificity of plant-microbe interactions in the tree mycorrhizosphere biome and consequences for soil C cycling. *Frontiers in Microbiology* **5**: 261.

Debaud JC, Gay G. **1987**. *In vitro* fruiting under controlled conditions of the ectomycorrhizal fungus *Hebeloma cylindrosporum* associated with *Pinus pinaster*. *New Phytologist* **105**: 429–435.

Delaux P-M, Xie X, Timme RE, Puech-Pages V, Dunand C, Lecompte E, Delwiche CF, Yoneyama K, Bécard G, Séjalon-Delmas N. **2012**. Origin of strigolactones in the green lineage. *New Phytologist* **195**: 857–71.

Delaux P-M, Varala K, Edger PP, Coruzzi GM, Pires JC, Ané J-M. **2014**. Comparative phylogenomics uncovers the impact of symbiotic associations on host genome evolution. *PLoS Genetics* **10**: e1004487.

Ekblad A, Wallander H, Godbold DL, Cruz C, Johnson D, Baldrian P, Björk RG, Epron D, Kieliszewska-Rokicka B, Kjøller R, *et al.* 2013. The production and turnover of extramatrical mycelium of ectomycorrhizal fungi in forest soils: role in carbon cycling. *Plant and Soil* **366**: 1–27.

Fellbaum CR, Gachomo EW, Beesetty Y, Choudhari S, Strahan GD, Pfeffer PE, Kiers ET, Bücking H. **2012**. Carbon availability triggers fungal nitrogen uptake and transport in arbuscular mycorrhizal symbiosis. *Proceedings of the National Academy of Sciences, USA* **109**: 2666–71.

Fellbaum CR, Mensah JA, Cloos AJ, Strahan GE, Pfeffer PE, Kiers ET, Bücking H. **2014**. Fungal nutrient allocation in common mycorrhizal networks is regulated by the carbon source strength of individual host plants. *New Phytologist* **203**: 646–656.

Felten J, Legué V, Ditengou FA. **2010**. Lateral root stimulation in the early interaction between *Arabidopsis thaliana* and the ectomycorrhizal fungus *Laccaria bicolor*: Is fungal auxin the trigger? *Plant Signaling & Behavior* **5**: 864–7.

Fries N, Serck-Hanssen K, Dimberg LH, Theander O. 1987. Abietic acid, and activator of basidiospore germination in ectomycorrhizal species of the genus *Suillus* (*Boletaceae*). *Experimental Mycology* **11**: 360–363.

Garcia K, Haider MZ, Delteil A, Corratgé-Faillie C, Conéjero G, Tatry M-V, Becquer A, Amenc L, Sentenac H, Plassard C, *et al.* 2013. Promoter-dependent expression of the fungal transporter HcPT1.1 under Pi shortage and its spatial localization in ectomycorrhiza. *Fungal Genetics and Biology* **58**: 53–61.

Garcia K, Delteil A, Conéjéro G, Becquer A, Plassard C, Sentenac H, Zimmermann S. **2014**. Potassium nutrition of ectomycorrhizal *Pinus pinaster*: overexpression of the *Hebeloma cylindrosporum Hc*Trk1 transporter affects the translocation of both K(+) and phosphorus in the host plant. *New Phytologist* **201**: 951–60.

Genre A, Chabaud M, Balzergue C, Puech-Pagès V, Novero M, Rey T, Fournier J, Rochange S, Bécard G, Bonfante P, *et al.* 2013. Short-chain chitin oligomers from arbuscular mycorrhizal fungi trigger nuclear Ca^{2+} spiking in *Medicago truncatula* roots and their production is enhanced by strigolactone. *New Phytologist* **198**: 190–202.

Gogala N. 1991. Regulation of mycorrhizal infection by hormonal factors produced by hosts and fungi. *Experientia* **47**: 331–340.

Hammer EC, Pallon J, Wallander H, Olsson PA. **2011**. Tit for tat? A mycorrhizal fungus accumulates phosphorus under low plant carbon availability. *FEMS Microbiology Ecology* **76**: 236–244.

Harrison MJ, Dewbre GR, Liu J. **2002**. A phosphate transporter from *Medicago truncatula* involved in the acquisition of phosphate released by arbuscular mycorrhizal fungi. *The Plant Cell* **14**: 2413–2429.

Helber N, Wippel K, Sauer N, Schaarschmidt S, Hause B, Requena N. **2011**. A versatile monosaccharide transporter that operates in the arbuscular mycorrhizal fungus *Glomus* sp is crucial for the symbiotic relationship with plants. *The Plant Cell* **23**: 3812–23.

Jayaraman D, Gilroy S, Ané J-M. **2014**. Staying in touch: mechanical signals in plant-microbe interactions. *Current opinion in plant biology* **20C**: 104–109.

Javot H, Penmetsa RV, Terzaghi N, Cook DR, Harrison MJ. 2007. A *Medicago truncatula* phosphate transporter indispensable for the arbuscular mycorrhizal symbiosis. *Proceedings of the National Academy of Sciences* **104**: 1720–1725.

Javot H, Penmetsa RV, Breuillin F, Bhattarai KK, Noar RD, Gomez SK, Zhang Q, Cook DR, Harrison MJ. 2011. Medicago truncatula mtpt4 mutants reveal a role for nitrogen in the regulation of arbuscule degeneration in arbuscular mycorrhizal symbiosis. *The Plant Journal* 68: 954–965.

Kalinova J, Radova S. 2009. Effect of rutin on the growth of *Botrytis cinerea*, *Alternaria alternata* and *Fusarium solani*. *Acta Phytopathol Entomol Hung* **44**: 39–47.

Kiers ET, Duhamel M, Beesetty Y, Mensah JA, Franken O, Verbruggen E, Fellbaum CR, Kowalchuk GA, Hart MM, Bago A, *et al.* 2011. Reciprocal rewards stabilize cooperation in the mycorrhizal symbiosis. *Science* **333**: 880–882.

Kikuchi K, Matsushita N, Suzuki K, Hogetsu T. **2007**. Flavonoids induce germination of basidiospores of the ectomycorrhizal fungus *Suillus bovinus*. *Mycorrhiza* **17**: 563–570.

Kloppholz S, Kuhn H, Requena N. **2011**. A secreted fungal effector of *Glomus intraradices* promotes symbiotic biotrophy. *Current Biology* **21**: 1204–9.

Kohler A, Kuo A, Nagy LG, Morin E, Barry KW, Buscot F, Canback B, Choi C, Cichocki N, Clum A, *et al.* 2015. Convergent losses of decay mechanisms and rapid turnover of symbiosis genes in mycorrhizal mutualists. *Nature Genetics* doi:10.1038/ng.3223.

Lagrange H, Jay-Allgmand C, Lapeyrie F. 2001. Rutin, the phenolglycoside from eucalyptus root exudates, stimulates *Pisolithus* hyphal growth at picomolar concentrations. *New Phytologist* **149**: 349–355.

Loth-Pereda V, Orsini E, Courty P-E, Lota F, Kohler A, Diss L, Blaudez D, Chalot M, Nehls U, Bucher M, *et al.* 2011. Structure and expression profile of the phosphate Pht1 transporter gene family in mycorrhizal *Populus trichocarpa*. *Plant Physiology* **156**: 2141–54.

Luo L, Lu D. 2014. Immunosuppression during Rhizobium-legume symbiosis. *Plant Signaling & Behavior* **9**: e28197.

Maillet F, Poinsot V, André O, Puech-Pagès V, Haouy A, Gueunier M, Cromer L, Giraudet D, Formey D, Niebel A, *et al.* 2011. Fungal lipochitooligosaccharide symbiotic signals in arbuscular mycorrhiza. *Nature* **469**: 58–63.

Martin F, Aerts A, Ahren D, Brun A, Danchin EGJ, Duchaussoy F, Gibon J, Kohler A, Lindquist E, Pereda V, *et al.* 2008. The genome of *Laccaria bicolor* provides insights into mycorrhizal symbiosis. *Nature* **452**: 88–92.

Martin F, Kohler A, Murat C, Balestrini R, Coutinho PM, Jaillon O, Montanini B, Morin E, Noel B, Percudani R, *et al.* 2010. Perigord black truffle genome uncovers evolutionary origins and mechanisms of symbiosis. *Nature* **464**: 1033–1038.

Melin E. 1954. Growth factor requirements of mycorrhizal fungi of forest trees. *Svensk Bot Tidskr* **48**: 86–94.

Mosse B, Hepper C. **1975**. Vesicular-arbuscular mycorrhizal infections in root organ cultures. *Physiological Plant Pathology* **5**: 215–223.

Näsholm T, Högberg P, Franklin O, Metcalfe D, Keel SG, Campbell C, Hurry V, Linder S, Högberg MN. **2013**. Are ectomycorrhizal fungi alleviating or aggravating nitrogen limitation of tree growth in boreal forests? *New Phytologist* **198**: 214–221.

Olsson O, Olsson P, Hammer E. 2014. Phosphorus and carbon availability regulate structural composition and complexity of AM fungal mycelium. *Mycorrhiza* **24**: 443–451.

Plassard C, Bonafos B, Touraine B. **2000**. Differential effects of mineral and organic N sources, and of ectomycorrhizal infection by *Hebeloma cylindrosporum*, on growth and N utilization in *Pinus pinaster*. *Plant, Cell & Environment* **23**: 1195–1205.

Plett JM, Kemppainen M, Kale SD, Kohler A, Legué V, Brun A, Tyler BM, Pardo AG, Martin F. **2011**. A secreted effector protein of *Laccaria bicolor* is required for symbiosis development. *Current Biology* **21**: 1197–203.

Nouri E, Breuillin-sessoms F, Feller U, Reinhardt D. 2014. Phosphorus and nitrogen regulate arbuscular mycorrhizal symbiosis in *Petunia hybrida*. *PLoS ONE* **9(3)**: e90841. doi:10.1371/journal.pone.0090841.

Plett JM, Martin F. **2012**. Poplar root exudates contain compounds that induce the expression of MiSSP7 in *Laccaria bicolor*. *Plant Signaling & Behavior* **7**: 12–5.

Plett JM, Khachane A, Ouassou M, Sundberg B, Kohler A, Martin F. 2014a. Ethylene and jasmonic acid act as negative modulators during mutualistic symbiosis between *Laccaria bicolor* and *Populus* roots. *New Phytologist* **202(1):** 270–286.

Plett JM, Daguerre Y, Wittulsky S, Vayssières A, Deveau A, Melton SJ, Kohler A, Morrell-Falvey JL, Brun A, Veneault-Fourrey C, *et al.* 2014b. Effector MiSSP7 of the mutualistic fungus *Laccaria bicolor* stabilizes the Populus JAZ6 protein and represses jasmonic acid (JA) responsive genes. *Proceedings of the National Academy of Sciences, USA* **111**: 8299-8304.

Rékangalt D, Pépin R, Verner M-C, Debaud J-C, Marmeisse R, Fraissinet-Tachet L. 2009. Expression of the nitrate transporter *nrt2* gene from the symbiotic basidiomycete *Hebeloma cylindrosporum* is affected by host plant and carbon sources. *Mycorrhiza* **19**: 143–148.

Salzer P, Hebe G, Hager A. 1997. Cleavage of chitinous elicitors from the ectomycorrhizal fungus *Hebeloma crustuliniforme* by host chitinases prevents induction of K^+ and Cl^- release, extracellular alkalinization and H_2O_2 synthesis of *Picea abies* cells. *Planta* **203**: 470–479.

Sauter M, Hager A. 1989. The mycorrhizal fungus *Amanita muscaria* induces chitinase activity in roots and suspension-cultured cells of its host *Picea abies*. *Planta* **179**: 61–66.

Selle A, Willmann M, Grunze N, Geßler A, Weiß M, Nehls U. 2005. The high-affinity poplar ammonium importer PttAMT1.2 and its role in ectomycorrhizal symbiosis. *New Phytologist* **168**: 697–706.

Selosse M-A, Rousset F. 2011. Evolution. The plant-fungal marketplace. *Science* **333**: 828–829.

Smith SE, Read DJ. 2008. *Mycorrhizal symbiosis.* Cambridge, UK: Academic Press.

Smith FA, Smith SE. 2015. How harmonious are arbuscular mycorrhizal symbioses? Inconsistent concepts reflect different mindsets as well as results. *New Phytologist* **205**: 1381–1384.

Steinkellner S, Lendzemo V, Langer I, Schweiger P, Khaosaad T, Toussaint J-P, Vierheilig H. 2007. Flavonoids and strigolactones in root exudates as signals in symbiotic and pathogenic plant-fungus interactions. *Molecules* **12**: 1290–1306.

Stonor R, Smith S, Manjarrez M, Facelli E, Smith FA. 2014. Mycorrhizal responses in wheat: shading decreases growth but does not lower the contribution of the fungal phosphate uptake pathway. *Mycorrhiza* **24**: 465–472.

Tedersoo L, Smith ME. 2013. Lineages of ectomycorrhizal fungi revisited: foraging strategies and novel lineages revealed by sequences from belowground. *Fungal Biology Reviews* **27**: 83–99.

Tisserant E, Malbreil M, Kuo A, Kohler A, Symeonidi A, Balestrini R, Charron P, Duensing N, Frei dit Frey N, Gianinazzi-Pearson V, *et al.* 2013. Genome of an arbuscular mycorrhizal fungus provides insight into the oldest plant symbiosis. *Proceedings of the National Academy of Sciences, USA* **110**: 20117–20122.

Torres Aquino M, Plassard C. **2004**. Dynamics of ectomycorrhizal mycelial growth and P transfer to the host plant in response to low and high soil P availability. *FEMS Microbiology Ecology* **48**: 149–156.

van der Heijden MGA, Martin F, Selosse M-A, Sanders IR. 2015. Mycorrhizal ecology and evolution: the past, the present, and the future. *New Phytologist* **205**: 1406–1423.

Venkateshwaran M, Volkening JD, Sussman MR, Ané J-M. 2013. Symbiosis and the social network of higher plants. *Current opinion in plant biology* 16: 118–27.

Wagg C, Pautler M, Massicotte H, Peterson RL. **2008**. The co-occurrence of ectomycorrhizal, arbuscular mycorrhizal, and dark septate fungi in seedlings of four members of the Pinaceae. *Mycorrhiza* **18**: 103–110.

Walder F, Niemann H, Natarajan M, Lehmann MF, Boller T, Wiemken A. **2012**. Mycorrhizal networks: common goods of plants shared under unequal terms of trade. *Plant Physiology* **159**: 789–97.

Wang E, Schornack S, Marsh JF, Gobbato E, Schwessinger B, Eastmond P, Schultze M, Kamoun S, Oldroyd GED. **2012**. A common signaling process that promotes mycorrhizal and oomycete colonization of plants. *Current Biology* **22**: 2242–6.

Win J, Chaparro-Garcia A, Belhaj K, Saunders DGO, Yoshida K, Dong S, Schornack S, Zipfel C, Robatzek S, Hogenhout SA, *et al.* 2012. Effector biology of plant-associated organisms: concepts and perspectives. *Cold Spring Harbor Symposia on Quantitative Biology* **77**: 235–247.

Zheng C, Ji B, Zhang J, Zhang F, Bever JD. 2015. Shading decreases plant carbon preferential allocation towards the most beneficial mycorrhizal mutualist. *New Phytologist* **205**: 361–368.

Chapter 3: The ectomycorrhizal fungus *Laccaria bicolor* produces lipochitooligosaccharides and uses the common symbiosis pathway to colonize *Populus*

This chapter has been submitted for publication in The Plant Cell.

Kevin R. Cope[1,2], Adeline Bascaules[3], Muthusubramanian Venkateshwaran[2,a], Junko Maeda[1,2], Kevin Garcia[1,2,b], Cathleen Ma[4], Jessy Labbé[5], Sara Jawdy[5], Edward Steigerwald[1], Jonathan Setzke[1], Emmeline Fung[1,2], Kimberly Schnell[1,2], Yunqian Wang[1], Nathaniel Schlief[1,2], Angad Dhariwal[1], Steven H. Strauss[5], Patricia Jargeat[6], Guillaume Bécard[3], Virginie Puech-Pagès[3], and Jean-Michel Ané[1,2,*]

[1]Department of Bacteriology, University of Wisconsin–Madison, Madison, WI 53706
[2]Department of Agronomy, University of Wisconsin–Madison, Madison, WI 53706
[3]Laboratoire de Recherche en Sciences Végétales, Université de Toulouse, CNRS, UPS, France
[4]Department of Forest Ecosystems and Society, Oregon State University, Corvallis, OR 97331
[5]Biosciences Division, Oak Ridge National Laboratory, Oak Ridge, TN 37831
[6]Laboratoire Evolution et Diversité Biologique, Université de Toulouse, UPS, CNRS, IRD, France

Present address:
[a]School of Agriculture, University of Wisconsin–Platteville, Platteville, WI 53818
[b]Department of Crop and Soil Sciences, North Carolina State University, Raleigh, NC 27695

*Corresponding author: Dr. Jean-Michel Ané (jeanmichel.ane@wisc.edu)

Contributions:
K.R.C., M.V., S.H.S., G.B., V.P.P., and J.-M.A. designed the research; **K.R.C**., A.B., M.V., J.M., K.G., C.M., J.L., S.J., J.S., K.G.S., N.S., A.D. and P.J. performed the experiments; **K.R.C.**, A.B., M.V., J.M., E.S., E.F., Y. W., P.J., G.B., and J.-M.A. analyzed the data; and **K.R.C.** wrote the paper with input from A.B., M.V., K.G., J.L., S.H.S., G.B., P.J., V.P.P., and J.-M.A.

3.1 Abstract

Mycorrhizal fungi form mutualistic associations with the roots of most land plants and provide them with increased access to limited mineral nutrients in the soil in exchange for carbon derived from photosynthesis. The “common symbiosis pathway” (CSP) is required not only for the arbuscular mycorrhizal symbiosis, but also for the rhizobia–legume and actinorhizal symbioses. Given its role in such diverse symbiotic associations, we hypothesized that the CSP might also play a role in ectomycorrhizal associations. We showed that the ectomycorrhizal fungus *Laccaria bicolor* produces an array of lipochitooligosaccharides (LCOs) that can trigger both root hair branching in legumes and, most importantly, calcium spiking in the host plant *Populus* in a *CASTOR/POLLUX*-dependent manner. Non-sulfated LCOs enhanced lateral root development in *Populus* in a *CCaMK*-dependent manner and sulfated LCOs enhanced the colonization of *Populus* by *L. bicolor*. The colonization of *Populus* roots by *L. bicolor* was reduced in both *CASTOR*/*POLLUX* and *CCaMK* RNA interference lines and the expression of a mycorrhiza-induced phosphate transporter, *PT12*, was reduced in the *CCaMK*-RNA interference line compared to wild-type. Altogether, our work demonstrates that *L. bicolor* uses the CSP for full establishment of its mutualistic association with *Populus*.

3.2 Introduction

Mycorrhizal fungi are filamentous microorganisms that establish symbiotic associations with the roots of approximately 90% of terrestrial plant species (Brundrett and Tedersoo, 2018). There are four major types of mycorrhizal associations, and the two most ecologically and economically important ones are arbuscular mycorrhizal (AM) and ectomycorrhizal (ECM) (van der Heijden et al., 2015; Martin et al., 2016). AM fungi, which belong to the phylum Mucoromycota, subphylum Glomeromycotina (Spatafora et al., 2016), likely played a crucial role in the successful colonization of land by plants at least 450 million years ago (Remy et al., 1994; Redecker et al., 2000; Heckman et al., 2001; Delaux et al., 2013; Feijen et al., 2018). Today, AM fungi colonize approximately 72% of plant species, including most crops (Brundrett and Tedersoo, 2018). Fossil evidence of ECM associations date back to only 50 million years ago but likely evolved at least 130 million years ago based on molecular clock analyses (Berbee and Taylor, 1993; Lepage et al., 1997; Wang and Qiu, 2006; Hibbett and Matheny, 2009). ECM fungal species belong to one of three fungal phyla, including Ascomycota, Basidiomycota, or Mucoromycota. They associate with 2% of plant species, including mostly woody plants, and are essential for the well-being of temperate and boreal forests, which cover approximately 20% of the global terrestrial surface (Tedersoo et al., 2010).

In both AM and ECM associations, mycorrhizal fungi not only provide their host plant with mineral nutrients mined from the soil, especially phosphorus, nitrogen, and potassium, but they also provide protection against a wide range of biotic and abiotic stresses (Jeffries et al., 2003; Smith and Read, 2008; Garcia and Zimmermann, 2014; Garcia et al., 2017). In exchange, the plant provides the fungus with various forms of carbon fixed through photosynthesis (Casieri et al., 2013). Although AM and ECM fungi provide similar services to their host plants, the

structures they utilize to complete the task are quite different. AM fungi use hyphopodia as penetration structures to traverse the cell wall of root epidermal cells and enter inside of plant roots where they proliferate both inter- and intracellularly. Ultimately, they form highly branched hyphal structures called arbuscules in root cortical cells. In contrast, ECM fungi form a hyphal sheath or mantle that encases the entire root tip with an underlying network of hyphae called the Hartig net, which surrounds but does not penetrate plant epidermal and cortical cells (Balestrini and Bonfante, 2014). The arbuscule and Hartig net both provide interfaces for the exchange of nutrients between host and fungus. In the case of the arbuscule, a unique membrane is formed called the peri-arbuscular membrane that is enriched in symbiosis-specific transporters (Garcia et al., 2016). Some of these are phosphate transporters that are expressed specifically during AM symbiosis (Rausch et al., 2001; Harrison et al., 2002; Paszkowski et al., 2002; Karandashov et al., 2004; Glassop et al., 2005). Further characterization of these phosphate transporters revealed that they are required for AM fungal colonization (Maeda et al., 2006; Javot et al., 2007). Similarly, during the *Populus–Laccaria bicolor* ECM symbiosis, multiple phosphate transporters are upregulated in *Populus* roots and may be essential for the persistence of the symbiotic association (Loth-Pereda et al., 2011).

Given the crucial role of mycorrhizal associations in both natural and agricultural environments, extensive research has focused on determining their evolutionary origin, the molecular mechanisms regulating their development, and the benefits that they provide to plants (Bonfante and Genre, 2010; Garcia et al., 2015; Strullu-Derrien et al., 2018). Over the past two decades, significant advances have been made in elucidating the molecular signaling mechanisms required for AM fungi to colonize plants (Kamel et al., 2017; MacLean et al., 2017; Luginbuehl and Oldroyd, 2017). In brief, low phosphorus availability in the soil leads to reduced

phosphorus levels within plant tissues (Marschner and Rengel, 2011). This deficiency triggers increased biosynthesis of strigolactones, a class of plant hormones that also function as signaling molecules for AM fungi (Akiyama and Hayashi, 2006; Yoneyama et al., 2007; Umehara et al., 2008; Gomez-Roldan et al., 2008). These strigolactones are exported across the plasma membrane into the rhizosphere by the ATP-binding cassette transporter PDR1 (Kretzschmar et al., 2012). Upon detection, strigolactones induce both AM fungal spore germination and hyphal branching (Akiyama et al., 2005; Besserer et al., 2006, 2008). Through an unknown signaling mechanism, they also stimulate the production of short-chain (four- to five-chain) chitin oligomers (CO) which are one class of molecules contained in the complex "Myc factors" produced by AM fungi (Genre et al., 2013). Another class of molecules contained in Myc factors are lipochitooligosaccharides (LCOs) (Maillet et al., 2011).

Originally, LCOs have been identified as an essential signaling molecule produced by most rhizobia (Lerouge et al., 1990). Their discovery was made possible by using a bioassay known as "root hair branching", which is a phenomenon characterized by a transient cessation of polarized root hair growth and the subsequent re-polarization of growth in a different direction leading to a characteristic root hair deformation (Heidstra et al., 1994). Root hair branching was used to study the activity of Nod factors produced by rhizobia on the roots of legumes (Bhuvaneswari and Solheim, 1985). The first chemical structure of a Nod factor from *Rhizobium meliloti* was revealed by mass spectrometry as a sulfated β-1,4-tetrasaccharide of D-glucosamine with three acetylated amino groups and one acylated with a C_{16} bis-unsaturated fatty acid. This purified LCO specifically induced root hair branching at nanomolar concentrations in the host alfalfa (*Medicago sativa*) but not in the non-host vetch (*Vicia sativa*) (Lerouge et al., 1990). This host-specific induction of root hair branching in alfalfa was conferred by a sulfate group on the

reducing end of the LCO (Truchet et al., 1991). Thus, root hair branching is an excellent bioassay for LCO detection because specific leguminous plant species are extremely sensitive to and are only induced by specific LCO structures. The same root hair branching assays with *V. sativa* were later used to detect the presence and activity of non-sulfated LCOs purified from germinating spore exudates (GSE) of the AM fungus *Rhizophagus irregularis*. Mass spectrometry was also used to further characterize the precise LCO structures (Maillet et al., 2011).

During AM symbiosis, both short-chain COs and LCOs are released into the rhizosphere and function as signaling molecules to the plant. They are perceived on the plasma membrane of the host plant by lysine-motif receptor-like kinases (LysM-RLK) that function in concert with a leucine-rich repeat receptor-like kinase (LRR-RLK) co-receptor, termed NORK/DMI2/SymRK (Stracke et al., 2002; Op den Camp et al., 2011; Miyata et al., 2014; Zhang et al., 2015). NORK/DMI2/SymRK interacts with and activates 3-Hydroxy-3-Methylglutaryl CoA Reductase1 (HMGR1) leading to the production of mevalonate (Kevei et al., 2007; Venkateshwaran et al., 2015). Through an unknown cascade of events, mevalonate activates a suite of nuclear ion channels including CASTOR, DMI1/POLLUX, and cyclic nucleotide-gated calcium channels which allow for the flow of calcium ions (Ca^{2+}) into the nucleoplasm and around the nucleus (Ané et al., 2004; Charpentier et al., 2008, 2016, Venkateshwaran et al., 2012, 2015). A calcium ATPase, MCA8, then removes Ca^{2+} thus inducing repetitive oscillations in Ca^{2+} concentration within and around the nucleus (Capoen et al., 2011). This phenomenon is commonly referred to as "Ca^{2+} spiking" and is dependent on all of the components described above. COs and LCOs are capable of triggering Ca^{2+} spiking even in the absence of the fungus (Genre et al., 2013; Sun et al., 2015). Repetitive Ca^{2+} spikes in the nucleus lead to the activation of the calcium- and

calmodulin-dependent protein kinase DMI3/CCaMK, which then phosphorylates its main target, the transcription factor IPD3/CYCLOPS (Lévy et al., 2004; Messinese et al., 2007; Yano et al., 2008; Horváth et al., 2011; Singh and Parniske, 2012). Upon phosphorylation, IPD3/CYCLOPS regulates the expression of multiple transcription factors required for the development of AM symbiosis (MacLean et al., 2017; Luginbuehl and Oldroyd, 2017). This elaborate molecular signaling pathway is referred to as the "common symbiosis pathway" (CSP) because all of the described components are required not only for AM symbiosis but also for the rhizobia-legume and actinorhizal symbioses (Venkateshwaran et al., 2013; Martin et al., 2017).

A significant body of research on signaling mechanisms does exist in ECM associations too (Martin et al., 2016). In regard to diffusible signals released by plants, strigolactones do not appear to affect hyphal branching in the ECM fungal species *Laccaria bicolor* and *Paxillus involutus* (Steinkellner et al., 2007). However, the flavonol rutin stimulated hyphal growth in *Pisolithus* and the cytokinin zeatin altered hyphal branch angle (Lagrange et al., 2001). On the fungal side, multiple diffusible signals produced by ECM fungi altered plant growth and development: hypaphorine from *Pisolithus tinctorius* inhibited root hair elongation and induced increased cytosolic Ca^{2+} concentration in *Eucalyptus* (Ditengou et al., 2000; Dauphin et al., 2007); auxin released by an overproducing mutant of *Hebeloma cylindrosporum* exhibited increased mycorrhizal activity (Gay et al., 1994); and auxin released by *L. bicolor* enhanced lateral root formation in *Populus* (Felten et al., 2009, 2010; Vayssières et al., 2015). Diffusible signals from AM fungi were also shown to stimulate enhanced lateral root development in *M. truncatula* (Oláh et al., 2005). Later, these signals were identified as non-sulfated and sulfated LCOs, and both induced lateral root formation in a CSP-dependent manner (Maillet et al., 2011).

Before our work, it was not known if ECM fungi produce LCOs like AM fungi as signaling molecules that are perceived by their host plants via the CSP. However, given the role of the CSP in three very different beneficial plant–microbe associations—the AM, rhizobia–legume, and actinorhizal symbioses—we hypothesized that ECM fungi also produce LCOs and use the CSP to colonize plants. To test this hypothesis, we focused on the ECM fungus *L. bicolor*, a basidiomycete, which colonizes *Populus*, a woody plant species that contains all of the components of the CSP in its genome (Garcia et al., 2015). Here, we present data that confirm our hypothesis using biological, biochemical, and molecular techniques.

3.3 Results

Laccaria bicolor produces lipochitooligosaccharides

To determine if LCOs are produced by the ECM fungus *L. bicolor*, we first performed root hair branching assays with two species of legumes, including a close relative of alfalfa, *Medicago truncatula*, and common vetch (*V. sativa*). These bioassays allowed us to screen for both sulfated (s) and non-sulfated (ns)LCOs, respectively, in hyphal exudates from *L. bicolor*. In response to the exudates, root hair branching in both *M. truncatula* and *V. sativa* that was comparable to the positive controls, which included sLCOs (10^{-8} M) on the roots of *M. truncatula* and nsLCOs (10^{-8} M) on the roots of *V. sativa*. As an additional positive control, we applied germinating spore exudates (GSE) from *R. irregularis* which also induced root hair branching. We did not observe root hair branching in either plant species in response to mock treatment or tetra-N-acetyl chitotetraose (CO4; 10^{-6} M) (**Figure 1A**). These results suggested that *L. bicolor* produces both sLCOs and nsLCOs.

We then used mass spectrometry to confirm the presence of LCOs in the culture medium of *L. bicolor* and to determine their structure. Previous analyses of LCOs have shown that these molecules are naturally produced in very low concentrations (Maillet et al., 2011; Poinsot et al., 2016). As such, we performed the LCOs analysis using the targeted mass spectrometry approach called Multiple Reaction Monitoring (MRM) mode. This mode is highly sensitive but requires the selection of an already known LCO structure to then search for its possible product ions. In this way, we detected LCOs having various lengths of chitin chains (III, IV and V) with several classes of fatty acids (C16:0, C18:0 and C18:1) and multiple functional groups on both the non-reducing end (N-methyl [N-Me] and carbamoyl [Cb]) and the reducing end (deoxy-hexose, proposed as fucose [Fuc]) (**Figure 1B**, **Supplemental Table 1**; see also **Supplemental Figures**

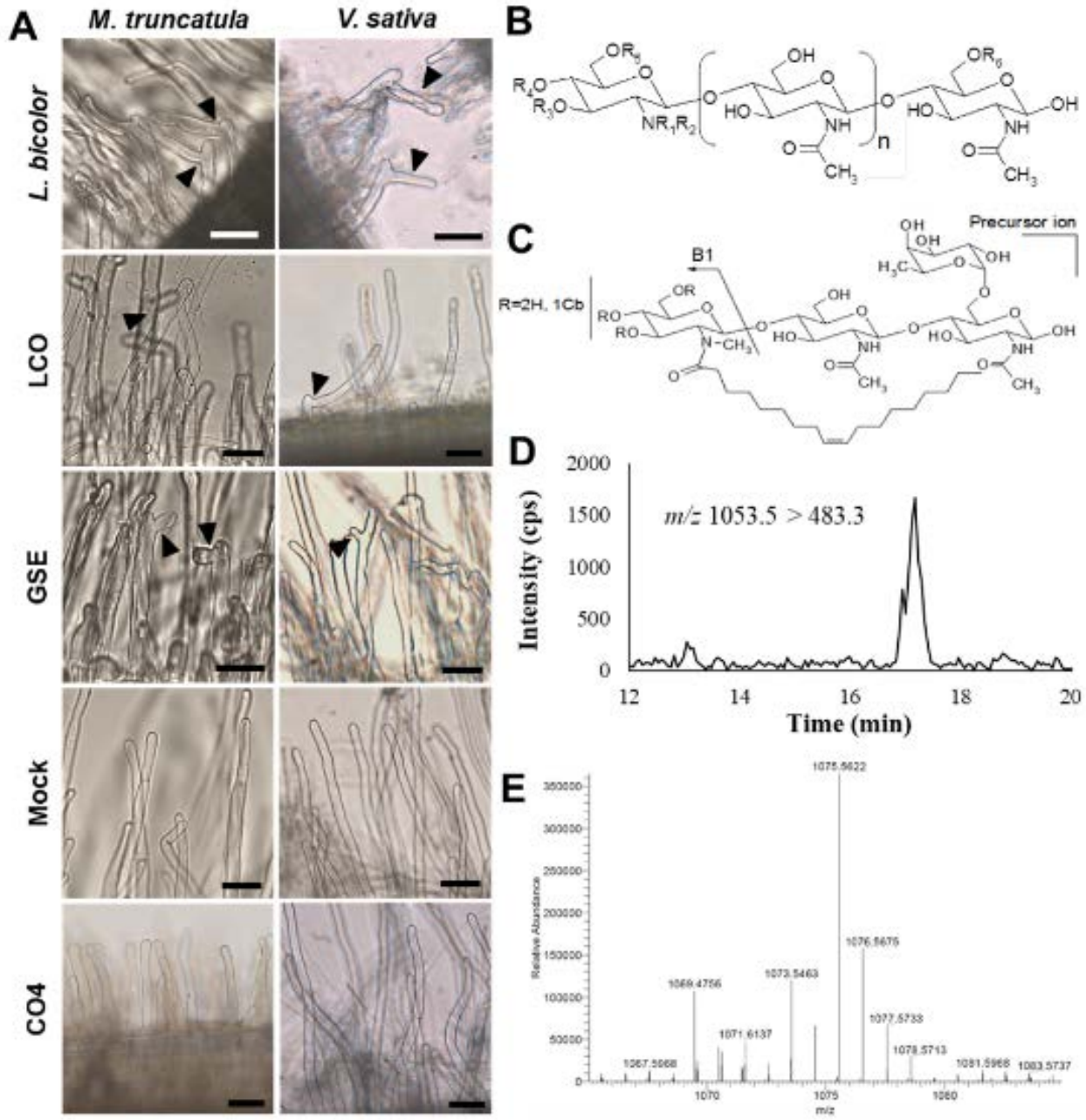

Figure 1 Detection of lipochitooligosaccharides produced by the ectomycorrhizal fungus *Laccaria bicolor* using root hair branching assays and mass spectrometry

(A) Representative images from root hair branching assays with two species of legumes, *Medicago truncatula* (***left***) and *Vicia sativa* (***right***). Exudates from *L. bicolor* induced root hair branching in both species comparable to that induced by the positive controls, which include sulfated LCOs (10^{-8} M) for *M. truncatula* and non-sulfated LCOs (10^{-8} M) for *V. sativa*. Germinating spore exudates (GSE) from the arbuscular mycorrhizal fungus *Rhizophagus irregularis* were applied as an additional positive control and induced root hair branching in both plant species. No branching occurred in response to mock treatment (water + 0.005% ethanol) or to the negative control, CO4 (10^{-6} M). Black arrows indicate branched root hairs. Scale bars = 50 µm. **(B)** Global structure of LCOs detected by mass spectrometry in the culture medium of *L.*

bicolor. Among the LCOs detected were different lengths of short-chain chitin oligomers (COs; *n* = 1, 2, or 3 corresponding to CO length III, IV or V, respectively) with different combinations of functional groups (R_1 = H or methyl [Me], R_2 = fatty acid [C16:0, C18:0 or C18:1], $R_{3,\,4,\,5}$ = H or carbamoyl [Cb], R_6 = H or deoxy hexose, proposed as fucose [Fuc]). **(C)** Proposed structure of one of the most representative LCO molecules detected: LCO-III C18:1, NMe, Cb, Fuc, based on known Nod factors (Price et al., 1992). The deoxy-hexose on the reducing end of the structure is proposed as an L-Fucose and the unsaturation of the fatty acid is proposed as Δ9. Calculated precursor ion $(M+H)^+$ *m/z* 1053.5, calculated B1 ion $(M+H)^+$ *m/z* 483.3. **(D)** Single reaction monitoring chromatogram obtained in LC-MS/MS (reverse phase HPLC-ESI-Q-Trap) with detection of the precursor ion $(M+H)^+$ *m/z* 1053.5 giving, after fragmentation, the product ion B1 *m/z* 483.3. The observed peak is at a retention time of 17.1 minutes. **(E)** High resolution LC-MS (U-HPLC-ESI-Q-Exactive) in scanning mode (*m/z* 350-1900) with detection of the precursor ion $(M+Na)^+$ *m/z* 1075.5622 (calculated for $C_{48}H_{84}N_4O_{21}Na$ = *m/z* 1075.5520) (7.64 minutes).

1 to **7**). The most abundant LCOs were LCO-IV, C18:1, N-Me and LCO-III, C18:1, N-Me, Cb, Fuc. Because of the low sensitivity of High Resolution (HR) MS analysis in complex matrices, only LCO-III, C18:1, NMe, Cb, Fuc was visible in the positive mode, in a sodium adduct $(M+Na)^+$ *m/z* 1075.5622 (calculated for $C_{48}H_{84}N_4O_{21}Na$ = *m/z* 1075.5520) (**Figure 1C** to **1E**). We looked for sulfated forms of the major LCOs detected in the samples and found that they were less abundant than the non-sulfated form. For example, sulfated LCO-IV, C18:1, N-Me was approximately half the intensity of non-sulfated LCO-IV, C18:1, N-Me (**Supplemental Figures 6** and **7**). These mass spectrometry data confirm the root hair branching results and demonstrate, for the first time, that the ECM basidiomycete *L. bicolor* produces a wide variety of both sLCOs and nsLCOs.

The arbuscular mycorrhizal fungus *Rhizophagus irregularis* and purified symbiotic signals trigger Ca^{2+} spiking in *Populus*

Given our finding that *L. bicolor* produces LCOs, we hypothesized that it could, therefore, trigger Ca^{2+} spiking in a compatible host plant species like *Populus*. However, since calcium spiking has not been reported in *Populus* previously, we first transformed *Populus* using

Agrobacterium rhizogenes with the coding sequence of nuclear-localized green (G)-GECO, a Ca^{2+}-sensitive fluorescent sensor (Zhao et al., 2011) (**Supplemental Figure 8**). We then evaluated the ability of GSE from the AM fungus *R. irregularis* to trigger Ca^{2+} spiking in epidermal cells of lateral roots from this *Populus* G-GECO line. GSE induced Ca^{2+} spiking in *Populus* that was comparable to that reported in other plant species (**Figures 2A** and **B**, **Supplemental Movie 1**). Since GSE contain a mixture of both short-chain COs and LCOs, both of which can trigger Ca^{2+} spiking in legumes and non-legumes even in the absence of the fungus (Maillet et al., 2011; Genre et al., 2013; Sun et al., 2015), we sought to dissect which of these symbiotic signals could induce Ca^{2+} spiking in *Populus*. We tested sLCOs, nsLCOs, and CO4 and all three induced Ca^{2+} spiking whereas the mock treatment did not (**Figure 2C**, **Supplemental Movies 2-5**). There was no difference in the ratio of spiking nuclei between treatments compared to GSE; however, the average number of spikes per nucleus was higher for the GSE and nsLCOs treatments compared to the sLCOs and CO4 treatments (p-value < 0.05; **Figure 2D**). These results confirmed that Ca^{2+} spiking occurs in *Populus* in response to AM fungi and the known symbiotic signals that they produce. Furthermore, they suggest that *Populus* is likely more responsive to nsLCOs than the other purified symbiotic signals tested.

Rhizophagus irregularis*-induced Ca^{2+} spiking in *Populus* is dependent on *CASTOR*/*POLLUX

To confirm that the CSP is intact in *Populus* and that Ca^{2+} spiking is dependent on both CASTOR and POLLUX, we used RNAi to simultaneously knock-down the expression of the genes encoding both proteins. Due to genome duplication, *Populus* contains two copies for both *CASTOR* and *POLLUX*. As such, we designed two RNAi constructs: one targeting both

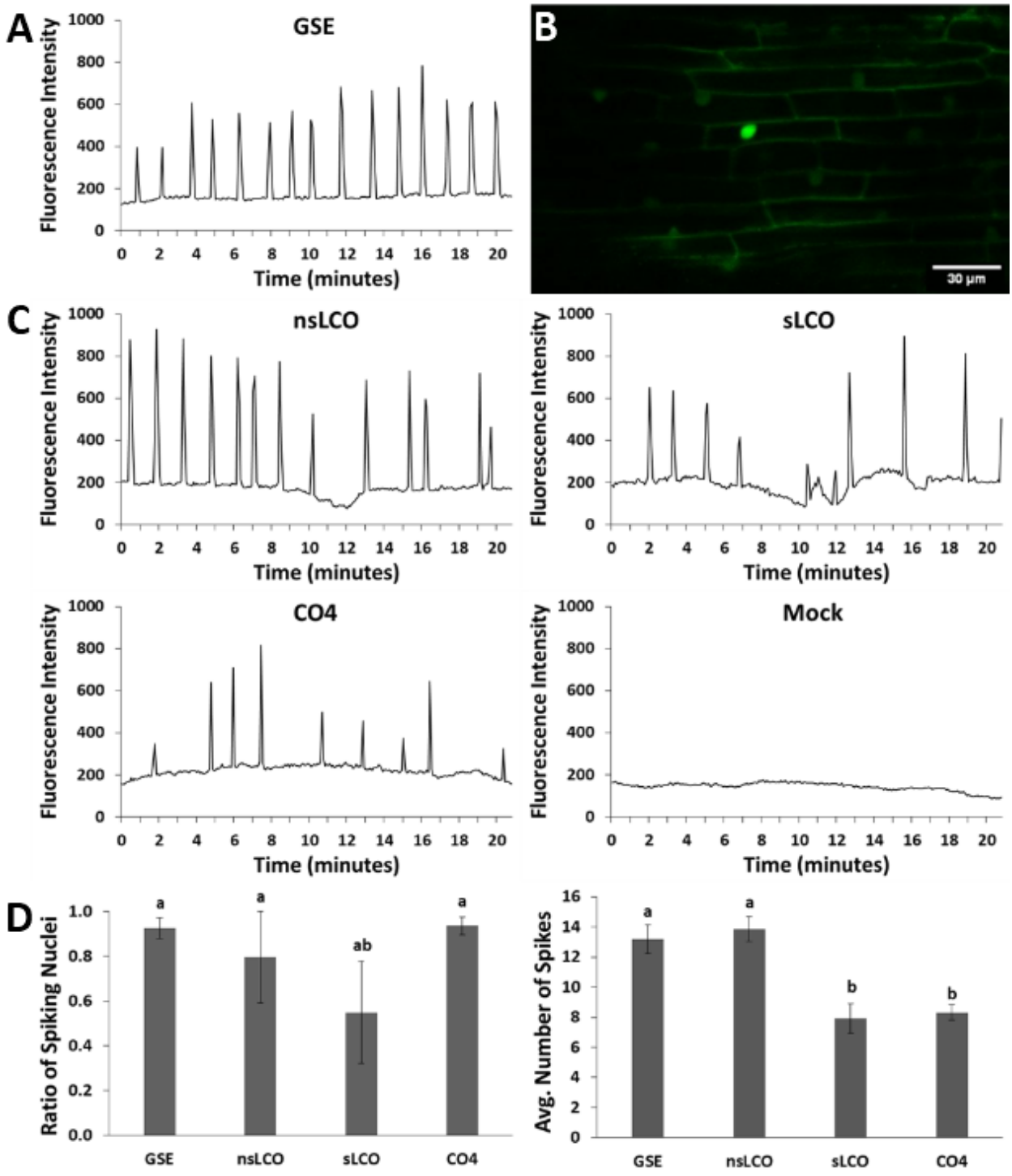

<u>Figure 2</u> Ca^{2+} spiking in *Populus* in response to the arbuscular mycorrhizal fungus *Rhizophagus irregularis* and to purified symbiotic signals

(A) Representative plot of Ca^{2+} spiking in response to germinating spore exudates (GSE) from the arbuscular mycorrhizal fungus *R. irregularis*. **(B)** Representative confocal image of a spiking nucleus in a *Populus* epidermal cell from a first-order lateral root treated with GSE and imaged with a confocal microscope. Scale bar = 30 µm. Note the elevated fluorescence of the spiking

nucleus compared to the basal fluorescence of non-spiking nuclei (see also **Supplemental Movie 1**). **(C)** Representative plots of Ca^{2+} spiking in response to purified signals that are present in GSE of *R. irregularis*, including: nsLCOs (10^{-7} M), sLCOs (10^{-7} M), and CO4 (10^{-6} M). No spiking was observed in the mock treatment (water + 0.005% ethanol) (see also **Supplemental Movies 2 to 5**). **(D)** Summary of *Populus* Ca^{2+} spiking data in response to GSE and purified signals. The ratio of spiking nuclei per root (n=3) was no different in any of the treatments (***left***); however, the average spiking frequency of nuclei in response to GSE (n=59) and nsLCOs (n=104) was higher than for sLCOs (n=32) and CO4 (n=92) (p-value < 0.05; ***right***). For both graphs, bars represent the mean of the data and error bars represent the standard error of the mean. The data were statistically analyzed by one-way ANOVA with Tukey pairwise comparison to assign significance groups (p-value < 0.05).

homologs of *CASTOR* and the other targeting both homologs of *POLLUX*. Both RNAi constructs were separately introduced into *Populus* using *Agrobacterium tumefaciens*. We recovered 21 independent transformation events for *CASTOR* and 32 for *POLLUX*. Shoots were regenerated from calli from each of these transformation events and were propagated to establish stably transformed RNAi lines. Each line was screened via quantitative reverse transcription polymerase chain reaction (qRT-PCR) to determine the degree of gene knock-down. Due to high sequence similarity between *CASTOR* and *POLLUX*, we measured the expression of both genes in all of the RNAi lines. Ultimately, we identified one RNAi line that, compared to wild-type *Populus*, had 89% and 71% reduction in the expression of *CASTOR* and *POLLUX*, respectively (**Supplemental Figure 9**). After identifying this single *CASTOR*/*POLLUX*-RNAi line with reduced expression of both genes, we subsequently transformed it with G-GECO as described previously with wild-type *Populus*. We successfully generated three independent *CASTOR*/*POLLUX*-RNAi G-GECO lines and used these for our Ca^{2+} spiking assays (**Supplemental Figure 10**).

We applied GSE onto lateral roots from all three *CASTOR*/*POLLUX*-RNAi G-GECO lines and on the wild-type G-GECO line of *Populus* (**Figure 3A** and **B**; **Supplemental Movies 7** and **8**). In all three RNAi G-GECO lines, we did not observe a reduction in the ratio of spiking

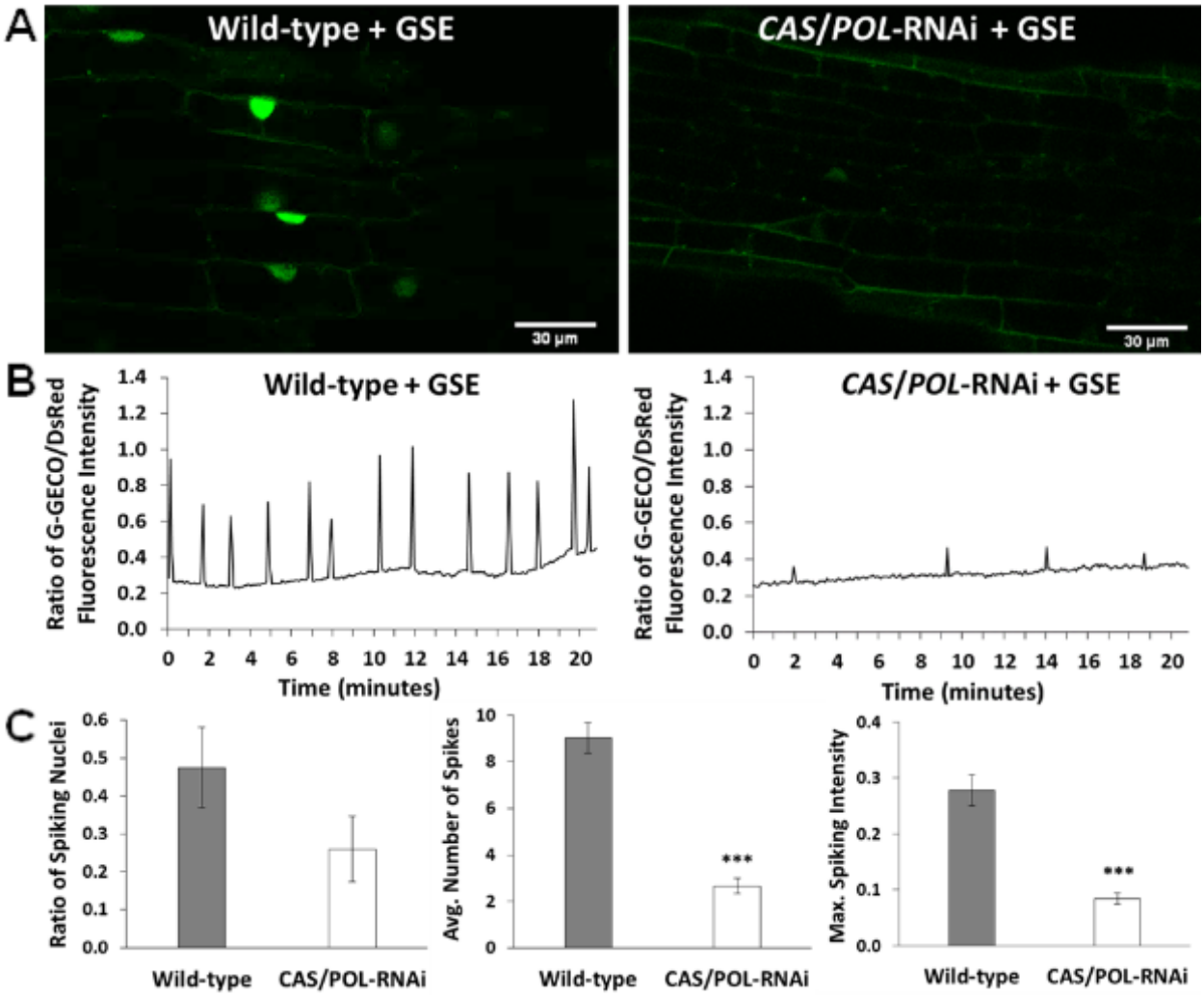

Figure 3 Dependence of *Rhizophagus irregularis*-induced Ca^{2+} spiking in *Populus* on *CASTOR* and *POLLUX*

(A) Representative confocal images of spiking nuclei in first-order lateral roots from both wild-type (***left***) and *CASTOR*/*POLLUX*-RNAi *Populus* (***right***) transformed with nuclear-localized G-GECO and treated with germinating spore exudates (GSE) from *R. irregularis*. Note the elevated fluorescence of the spiking nuclei in the wild-type root compared to the weakly spiking nucleus in the *CASTOR*/*POLLUX*-RNAi root. Scale bars = 30 µm (see also **Supplemental Movies 6** and **7**). **(B)** Representative plots of Ca^{2+} spiking showing the ratio of G-GECO to DsRed fluorescence intensity in wild-type (***left***) and *CASTOR*/*POLLUX*-RNAi (***right***) *Populus* G-GECO lines treated with GSE. **(C)** Summary of Ca^{2+} spiking data. The ratio of spiking nuclei per root was determined for wild-type (n=10) and all three *CASTOR*/*POLLUX*-RNAi lines combined (n=13), but the difference was not statistically significant (***left***; p-value = 0.12). However, both the average number of spikes per nucleus (***middle***) and the spiking intensity of the largest spike for each nucleus (***right***; wild-type: n=77 and *CASTOR*/*POLLUX*-RNAi: n=45) were highly statistically significant (p-value < 0.001). For all three graphs, bars represent the mean of the data and error bars represent the standard error of the mean. The data were statistically analyzed by Welches two-sample t-test.

nuclei compared to the wild-type G-GECO line; however, we did see a substantial decrease in both the average number of spikes and the intensity of the largest spike for each nucleus based on the ratio of G-GECO fluorescence to baseline DsRed fluorescence (p-value < 0.05; **Figure 3C**). These results indicate that the simultaneous RNAi-mediated knock-down of both *CASTOR* and *POLLUX* expression was sufficient to interfere with their activity thereby compromising the full activation of the CSP by GSE. Furthermore, these results also show that *CASTOR* and/or *POLLUX* contribute to Ca^{2+} spiking in *Populus* induced by GSE from *R. irregularis.*

The ectomycorrhizal fungus *Laccaria bicolor* triggers Ca^{2+} spiking in *Populus*

To directly test our hypothesis that *L. bicolor* can trigger Ca^{2+} spiking, we applied *L. bicolor* hyphae on first-order lateral roots from the wild-type *Populus* G-GECO line. As a positive control, we used GSE from *R. irregularis* and for a negative control, we used mock treatment. Both controls were applied separately on lateral roots from the same primary root. *L. bicolor* hyphae triggered Ca^{2+} spiking that was comparable to that observed in response to the GSE while mock treatment did not induce spiking at all (**Figures 4A** to **4C**; **Supplemental Movies 8** to **10**). The ratio of spiking nuclei in response to *L. bicolor* hyphae was lower than in response to GSE from *R. irregularis* (p-value < 0.01); however, the frequency of spiking nuclei was the same between the two treatments (**Figure 4D**). These data show for the first time that an ECM fungus is capable of triggering Ca^{2+} spiking comparable to that induced by the AM fungus *R. irregularis*.

Given that Ca^{2+} spiking induced by GSE from *R. irregularis* was dependent on *CASTOR* and/or *POLLUX*, we hypothesized that Ca^{2+} spiking induced by *L. bicolor* hyphae would be as well. To confirm this, we applied *L. bicolor* hyphae onto lateral roots from all three *CASTOR*/

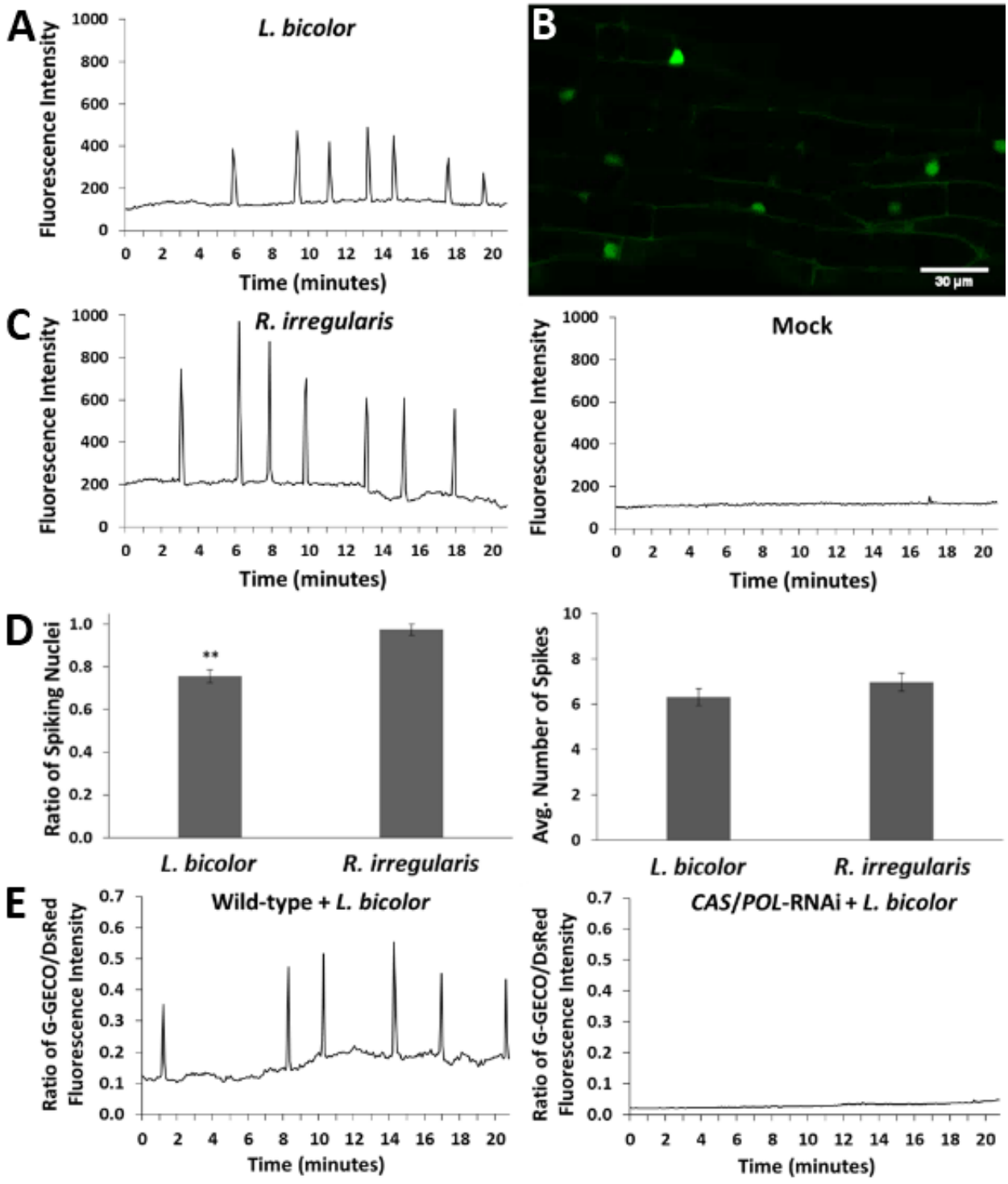

<u>Figure 4</u> Ca^{2+} spiking in *Populus* in response to the ectomycorrhizal fungus *Laccaria bicolor* and its dependence on *CASTOR* and *POLLUX*

(A) Representative plot of Ca^{2+} spiking in response to hyphae from *L. bicolor*. **(B)** Representative confocal image of a spiking nucleus in a *Populus* epidermal cell from a first-order lateral root treated with *L. bicolor* hyphae and imaged with a confocal microscope. Scale bar = 30 µm. Note the elevated fluorescence of the spiking nucleus compared to the basal fluorescence

of non-spiking nuclei (see also **Supplemental Movie 8**). **(C)** Representative plots of Ca^{2+} spiking in response to germinating spore exudates (GSE) from the arbuscular mycorrhizal fungus *R. irregularis* (***left***) and mock treatment (water; ***right***) (see also **Supplemental Movies 9** and **10**). **(D)** Summary of Ca^{2+} spiking data. The ratio of spiking nuclei in roots treated with *L. bicolor* hyphae (n=4) was lower (p-value < 0.01) than for roots treated with the GSE from *R. irregularis* (n=3; ***left***); however, the spiking frequency for both treatments was the same (***right***). For both graphs, bars represent the mean of the data and error bars represent the standard error of the mean. The data were statistically analyzed by Welches two-sample t-test. **(E)** Representative plots of Ca^{2+} spiking showing the ratio of G-GECO to DsRed fluorescence intensity in wild-type (***left***) and *CASTOR*/*POLLUX*-RNAi (***right***) *Populus* G-GECO lines treated with *L. bicolor* hyphae. No spiking was detected in the *CASTOR*/*POLLUX*-RNAi G-GECO roots (see also **Supplemental Movies 11** and **12**).

POLLUX-RNAi G-GECO lines and onto to wild-type G-GECO *Populus* as a positive control. Ca^{2+} spiking did not occur in any of the RNAi roots but did in the wild-type *Populus* roots transformed with G-GECO (**Figure 4E**; **Supplemental Movies 11** and **12**). Based on these results, we concluded that Ca^{2+} spiking in *Populus* induced by *L. bicolor* hyphae is also dependent on *CASTOR* and/or *POLLUX*.

Lipochitooligosaccharides affect *Populus* root development

Given that *L. bicolor* produces LCOs and that LCOs from AM fungi enhance lateral root formation in other plant species (Oláh et al., 2005; Gutjahr et al., 2009; Mukherjee and Ané, 2011; Maillet et al., 2011; Sun et al., 2015), we hypothesized that the enhancement of lateral root development in *Populus* by *L. bicolor* (Felten et al., 2009) can partially be attributed to LCOs. Furthermore, we hypothesized that if LCOs enhance lateral development in *Populus*, the enhancement would be dependent on the CSP. To test these hypotheses, we used wild-type *Populus* and the *CASTOR*/*POLLUX*-RNAi line described previously as well as a *CCaMK*-RNAi line that we developed with 83% reduction in *CCaMK* expression compared to the wild-type *Populus* line (**Supplemental Figure 9**). Before treating all three *Populus* lines with LCOs, we

first confirmed that native primary and lateral root development was unchanged in the transgenic RNAi lines compared to wild-type (**Figure 5A**). Next, we treated all three *Populus* lines with mock, purified nsLCOs, or sLCOs and observed their effect on both primary and lateral root development (**Figures 5B** and **5C**). Primary root length was the same for all of the *Populus* lines regardless of treatment except for an increase (p-value < 0.05) in the *CASTOR*/*POLLUX*-RNAi line when treated with sLCOs. For lateral root development, in response to nsLCOs, the number of lateral roots per length of primary root increased in both the wild-type and *CASTOR*/*POLLUX*-RNAi lines (p-value < 0.05), whereas the *CCaMK*-RNAi line was non-responsive to all of the treatments. These data suggest that LCOs affect root development in a CSP-dependent manner. In particular, they suggest that *L. bicolor* may use nsLCOs as a signal to trigger an increase in lateral root development independent of *CASTOR*/*POLLUX* but dependent on *CCaMK*, thereby maximizing root surface area for subsequent colonization.

Application of lipochitooligosaccharides enhances ectomycorrhizal colonization in *Populus*

After discovering that AM fungi produce LCOs, Maillet *et al.* (2011) also found that the application of LCOs significantly enhanced AM colonization. We hypothesized that we would observe a similar response in *Populus* when colonized with *L. bicolor*. We treated established *Populus* roots with mock, purified nsLCOs, or sLCOs and subsequently co-culture them with *L. bicolor* using a well-established sandwich system (Felten et al., 2009; **Supplemental Figure 11**). As a negative control, we co-cultured mock-treated *Populus* roots as well. After three weeks of colonization, we harvested the ectomycorrhizal root systems of all treated plants and used a stereomicroscope to observe external mantle formation. There was no obvious effect of LCOs (**Figure 6A**), nor was there any alteration in primary root length among treatments. However,

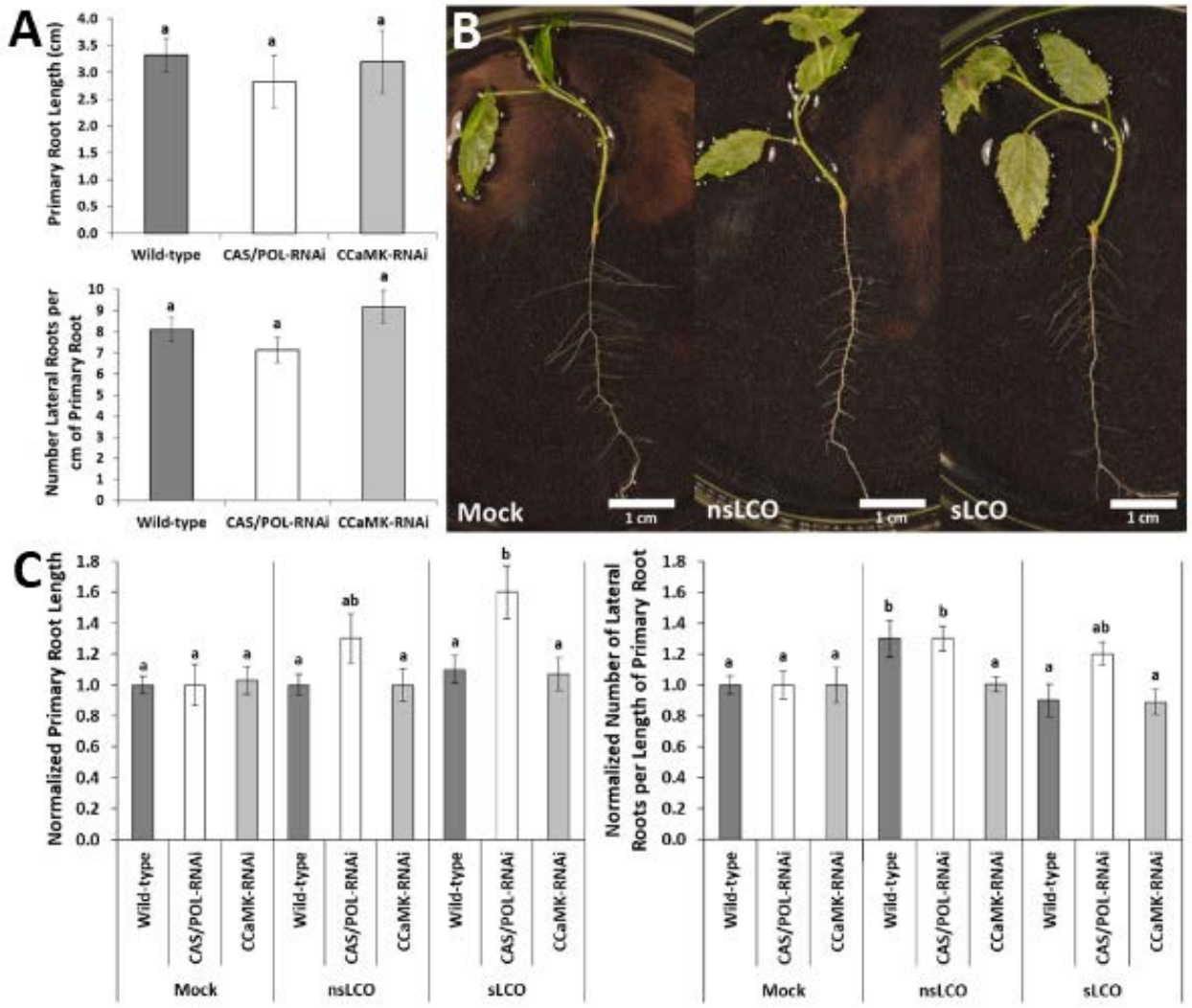

Figure 5 Primary and lateral root development in wild-type, *CASTOR*/*POLLUX*-RNAi, and *CCaMK*-RNAi *Populus* lines treated with lipochitooligosaccharides

(A) Summary of primary root length (***left***) and number of lateral roots per length of primary root (***right***) in the wild-type (n=9), *CASTOR*/*POLLUX*-RNAi (n=9), and *CCaMK*-RNAi (n=10) *Populus* lines. No statistical difference was observed in the RNAi lines compared to wild-type. **(B)** Representative images of wild-type *Populus* in response to mock treatment (***left***), nsLCOs (***middle***), and sLCOs (***right***). Scale bar = 1 cm. **(C)** Summary of normalized primary root length (***left***) and normalized number of lateral roots per length of primary root (***right***) for wild-type (n=28, 19, or 16), *CASTOR*/*POLLUX*-RNAi (n=19, 19, or 16), and *CCaMK*-RNAi (n=15, 16, or 18) *Populus* in response to one of three treatments: mock, nsLCOs (10^{-8} M), or sLCOs (10^{-8} M), respectively. For primary root length, sLCOs induced an increase in only the *CASTOR*/*POLLUX*-RNAi line (p-value < 0.05); and for the number of lateral roots per length of primary root, nsLCOs induced an increase in both wild-type and *CASTOR*/*POLLUX*-RNAi lines (p-value < 0.05). For all graphs, bars represent the mean of the data and error bars represent the standard error of the mean. The data were statistically analyzed by one-way ANOVA with Tukey pairwise comparison to assign significance groups (p-value < 0.05).

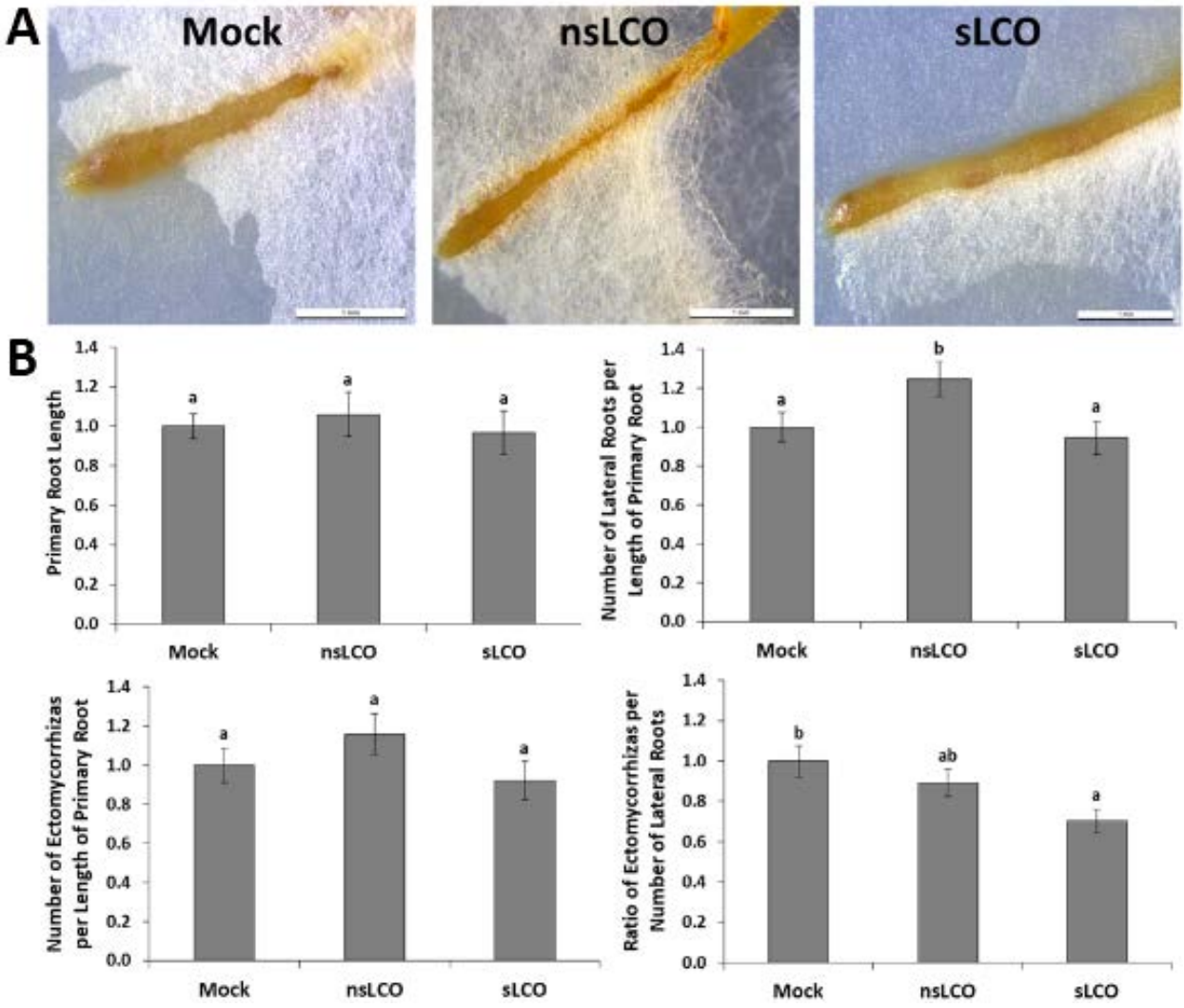

<u>Figure 6</u> Effect of lipochitooligosaccharides on both lateral root and ectomycorrhiza formation during *Laccaria bicolor* colonization

(A) Representative stereomicroscope images of wild-type *Populus* roots treated with mock (***left***), nsLCOs (10^{-8} M; ***middle***), or sLCOs (10^{-8} M; ***right***) and subsequently co-cultured with hyphae of *L. bicolor* for three weeks. Scale bars = 1 mm. **(B).** Summary plots of normalized data for root development and ectomycorrhiza formation in response to mock (n=17), nsLCOs (n=15), and sLCOs (n=15), including primary root length (***top left***), number of lateral roots per length of primary root (***top right***), number of ectomycorrhizas per length of primary root (***bottom left***), and the ratio of ectomycorrhizas per number of lateral roots (***bottom right***). The nsLCOs induced an increase in the number of lateral roots per length of primary root (p-value < 0.05). The sLCOs induced a decrease in the ratio of ectomycorrhizas to total lateral roots (p-value < 0.05). For all graphs, bars represent the mean of the data and error bars represent the standard error of the mean. The data were statistically analyzed by one-way ANOVA with Tukey pairwise comparison to assign significance groups (p-value < 0.05).

the nsLCO treatment again induced an increase in the number of lateral roots per length of primary root compared to mock treatment (p-value < 0.05; **Figure 6B**). Surprisingly, this did not result in a significant increase in the number of ectomycorrhizal lateral roots. In the sLCOs treatment compared to mock, we saw a decrease (p-value < 0.05) in the ratio of ectomycorrhizal lateral roots to the total number of lateral roots (**Figure 6B**). These data show that nsLCOs induce an increase in lateral root formation even in the presence of the fungus.

To identify other potential effects of LCOs, we analyzed further a subset of twenty ectomycorrhizal lateral roots per treatment using confocal microscopy. Using a vibratome, we generated ten 50 µm cross sections from each ectomycorrhiza and then stained the fungal tissue with wheat germ agglutinin conjugated with Alexafluor-488 and the plant tissue with propidium iodide (**Figure 7A**). Following confocal imaging of entire cross sections, we evaluated four parameters: mantle width, root diameter, Hartig net boundary, and root circumference (**Supplemental Figure 12**). Based on these measurements we calculated the ratio of mantle width to root diameter and the ratio of Hartig net boundary to root circumference and plotted the results. Compared to mock treatment, sLCOs induced a 15% and 8% increase in both ratios, respectively (p-value < 0.05; **Figure 7B**). These results suggest that exogenous application of sLCOs, but not nsLCOs, enhances ectomycorrhizal colonization in *Populus*.

Laccaria bicolor **uses the "common symbiosis pathway" to colonize** ***Populus***

Based on our previous data, we hypothesized that *L. bicolor* could use the CSP to colonize *Populus* roots. We co-cultured both the *CASTOR*/*POLLUX*-RNAi and *CCaMK*-RNAi *Populus* lines with *L. bicolor* as described above. We also co-cultured wild-type *Populus* with *L. bicolor* as a control (**Figure 8A**). After three weeks, we harvested, prepared, and observed

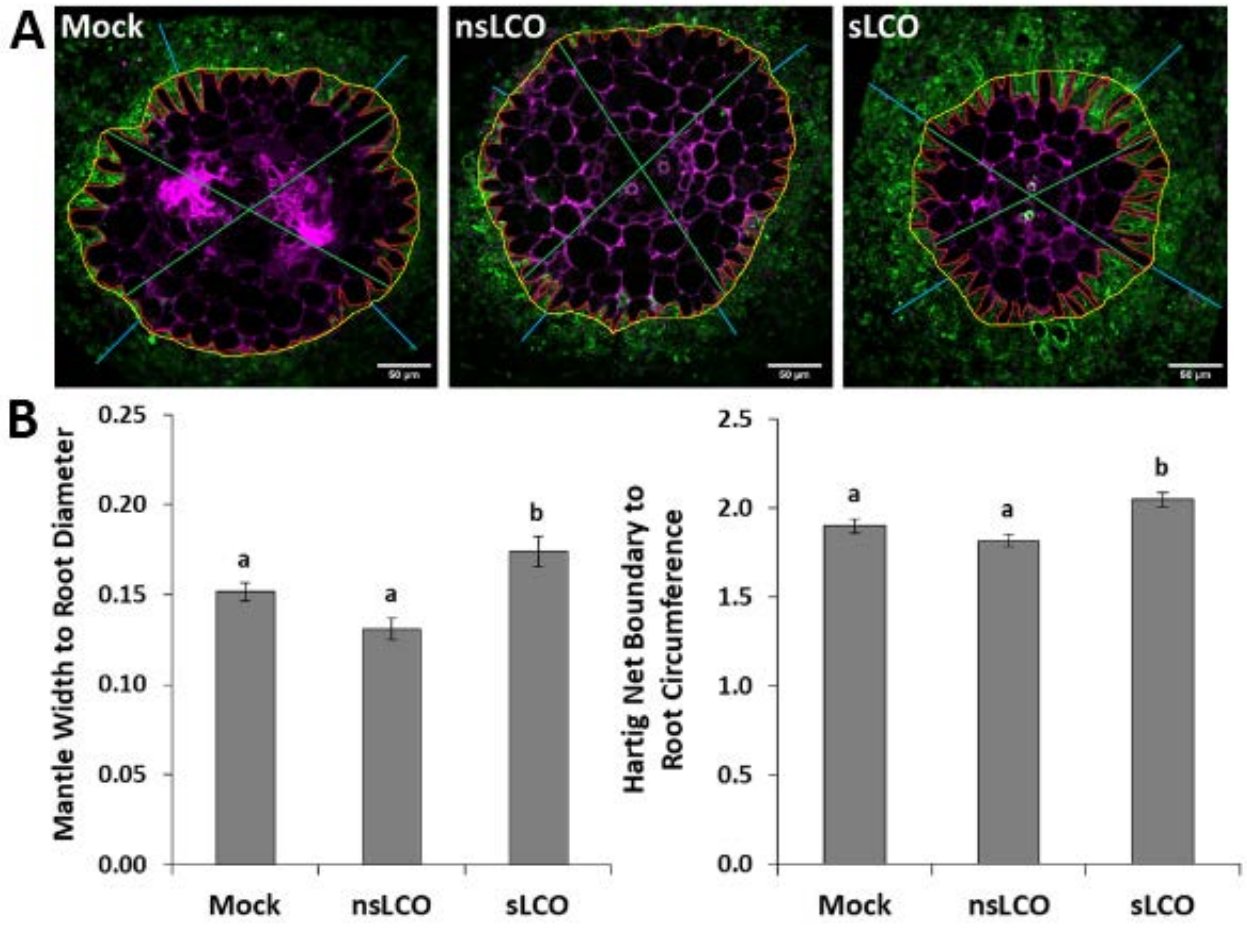

Figure 7 Effect of lipochitooligosaccharides on both mantle and Hartig net formation during *Laccaria bicolor* colonization

(A) Representative transverse cross sections of *Populus* roots treated with mock (***left***), nsLCOs (10^{-8} M; ***middle***), or sLCOs (10^{-8} M; ***right***) and co-cultured with *L. bicolor* for three weeks. Colonized roots were sectioned and stained with wheat germ agglutinin conjugated with Alexafluor-488 (green) and propidium iodide (purple) and imaged on a confocal laser scanning microscope. Scale bars = 50 µm. For each image, four types of measurements were obtained using ImageJ, including: mantle width (light blue), root diameter (green), Hartig net boundary (red), and root circumference (yellow). These measurements were used to calculate both the ratio of average mantle width to average root diameter and average Hartig net boundary to average root circumference. **(B)** Summary plots of the ratios of both mantle width to root diameter (***left***), and Hartig net boundary to root circumference (***right***), revealed that sLCOs (n=109), but not nsLCOs (n=77), induced an increase (p-value < 0.05) in ectomycorrhizal colonization compared to the mock treatment (n=111). For both graphs, bars represent the mean of the data and error bars represent the standard error of the mean. The data were statistically analyzed by one-way ANOVA with Tukey pairwise comparison to assign significance groups (p-value < 0.05).

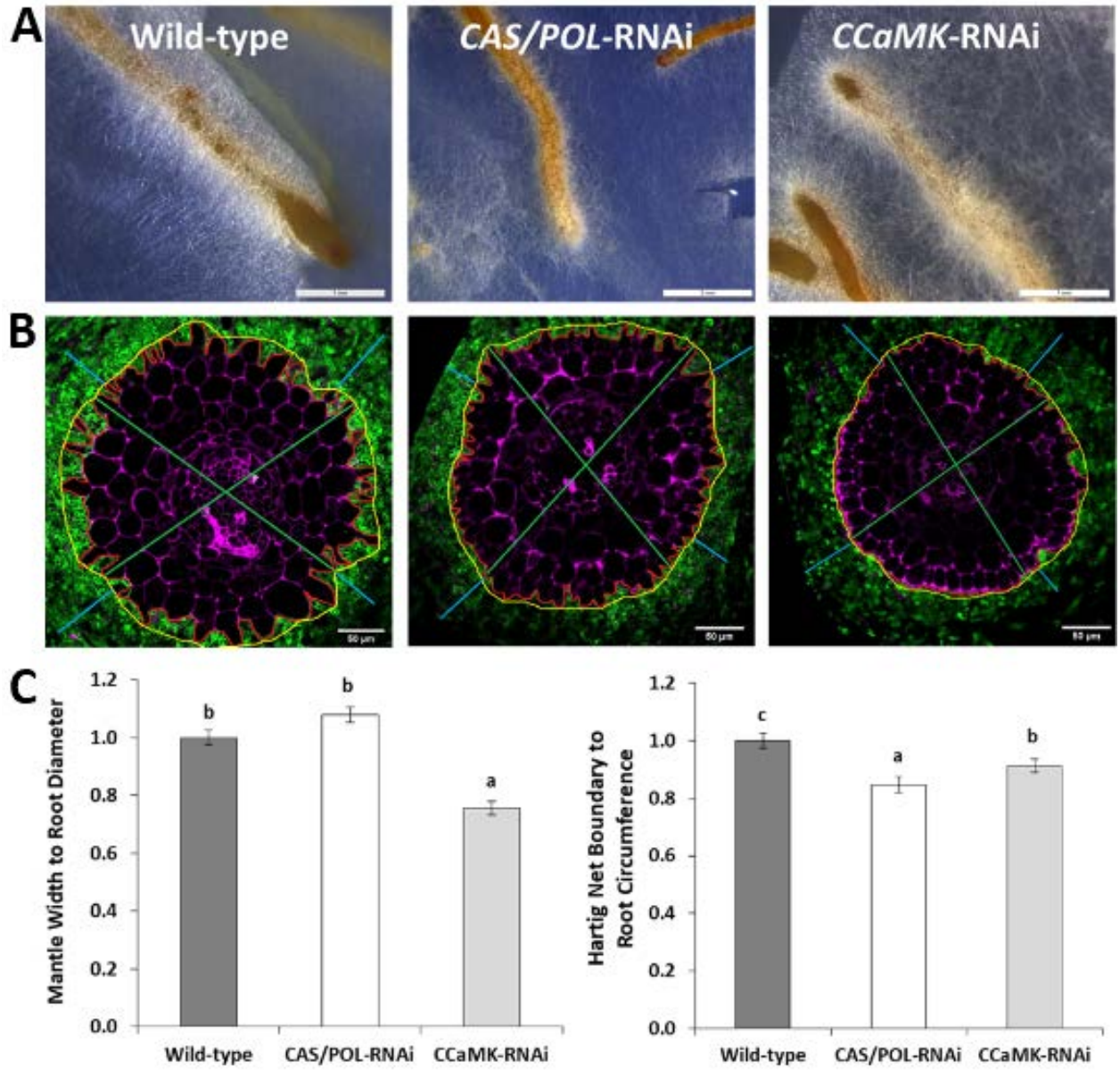

Figure 8 Role of the common symbiosis pathway in the colonization of *Populus* by the ectomycorrhizal fungus *Laccaria bicolor*

(A) Representative stereomicroscope images of wild-type (***left***), *CASTOR*/*POLLUX*-RNAi (***middle***), and *CCaMK*-RNAi *Populus* roots co-cultured with *L. bicolor* for three weeks. Scale bars = 1 mm. **(B)** Representative transverse cross sections of wild-type (***left***), *CASTOR*/*POLLUX*-RNAi (***middle***), and *CCaMK*-RNAi (***right***) *Populus* roots co-cultured with *L. bicolor*. Colonized roots were sectioned and stained with wheat germ agglutinin conjugated with Alexafluor-488 (green) and propidium iodide (purple) and imaged on a confocal laser scanning microscope. Scale bars = 50 µm. For each image, four types of measurements were obtained using ImageJ, including: mantle width (light blue), root diameter (green), Hartig net boundary (red), and root circumference (yellow). These measurements were used to calculate both the ratio of average mantle width to average root diameter and average Hartig net boundary to average root circumference. **(C)** Summary plots of the normalized ratios of mantle width to root diameter

(***left***), and Hartig net boundary to root circumference (***right***), in wild-type (n=240), *CASTOR*/*POLLUX*-RNAi (n=173), and *CCaMK*-RNAi *Populus* (n=149) lines are shown. Compared to wild-type, both ratios were lower in the *CCaMK*-RNAi line whereas only the ratio of Hartig net boundary to root circumference was lower in the *CASTOR*/*POLLUX*-RNAi line (p-value < 0.05). For both graphs, bars represent the mean of the data and error bars represent the standard error of the mean. The data were statistically analyzed by one-way ANOVA with Tukey pairwise comparison to assign significance groups (p-value < 0.05).

ectomycorrhizal roots (**Figure 8B**) and analyzed the same colonization parameters as described previously (**Supplemental Figure 12**). The ratio of mantle width to root diameter in the *CCaMK*-RNAi line decreased by 24% compared to wild-type *Populus* (p-value < 0.05); this decrease did not occur in the *CASTOR*/*POLLUX*-RNAi line. However, the ratio of Hartig net boundary to root circumference decreased by 15% and 16%, respectively, in the *CASTOR*/*POLLUX*-RNAi and *CCaMK*-RNAi lines compared to wild-type (p-value < 0.05; **Figure 8C**). These data confirmed our hypothesis and showed for the first time that an ectomycorrhizal fungus uses *CCaMK* for full establishment of the mantle and both *CCaMK* and *CASTOR*/*POLLUX* for Hartig net development during the colonization of its host.

Since the primary purpose of mycorrhizal associations is the exchange of nutrients, previous studies have evaluated the expression, localization, and function of nutrient transports during mycorrhizal symbioses. Phosphate transporters are particularly well-characterized in the AM symbiosis (Rausch et al., 2001; Harrison et al., 2002; Paszkowski et al., 2002; Karandashov et al., 2004; Glassop et al., 2005; Maeda et al., 2006; Javot et al., 2007). Some, including *PT12*, are upregulated in *Populus* during both AM and ECM colonization (Loth-Pereda et al., 2011). We, therefore, hypothesized that *PT12* expression would likely be reduced during ectomycorrhization in CSP-impaired *Populus*. To test this hypothesis, we performed qRT-PCR with RNA extracted from wild-type and *CCaMK*-RNAi roots colonized by *L. bicolor*. The expression of *PT12* in the *CCaMK*-RNAi line decreased nearly five-fold compared to wild-type

(p-value < 0.05; **Figure 9**). This finding suggests that not only is *L. bicolor* colonization impaired in the *CCaMK*-RNAi *Populus* line, but nutrient exchange may also be impaired as well. Therefore, the CSP likely contributes to both the establishment and the proper function of the ectomycorrhizal association between *Populus* and *L. bicolor*.

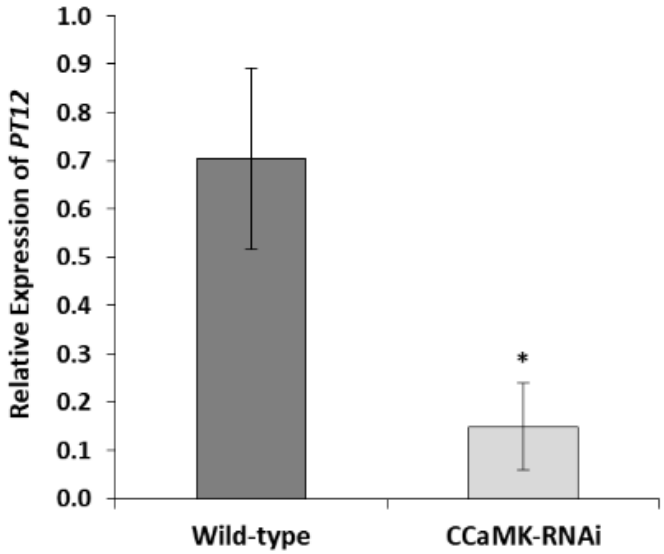

Figure 9 Relative expression of the *Populus* mycorrhiza-induced phosphate transporter *PT12* in wild-type and *CCaMK-RNAi* lines
Based on quantitative reverse transcription PCR, there was a nearly five-fold decrease in the expression of *PT12* in the *CCaMK*-RNAi *Populus* line (n=5) compared to the wild-type line (n=4; p-value < 0.05). In the graph, bars represent the mean of the data and error bars represent the standard error of the mean. The data were statistically analyzed by Welches two-sample t-test.

3.4 Discussion

Our work demonstrated, for the first time, that the ECM fungus *L. bicolor* produces both nsLCOs and sLCOs (**Figure 1**). We also showed that *L. bicolor* hyphae trigger Ca^{2+} spiking in *Populus* comparable to the spiking induced by GSE from the AM fungus *R. irregularis* (**Figures 2** and **4**). The Ca^{2+} spiking response in *Populus* to AM and ECM fungi was dependent on *CASTOR*/*POLLUX* as observed in both legumes and rice (Peiter et al., 2007; Charpentier et al., 2008; Chen et al., 2009; Sun et al., 2015) (**Figures 3** and **4**). Non-sulfated LCOs enhanced *Populus* lateral root development in a *CCaMK*-dependent manner as observed in *M. truncatula* and rice; however, for *Populus*, this response was *CASTOR*/*POLLUX*-independent whereas it was not in *M. truncatula* and rice (Maillet et al., 2011; Sun et al., 2015) (**Figure 5**). Even in the presence of the fungus, nsLCOs again induced an increase in lateral root formation, but this did not result in a significant increase in the ratio of mycorrhizas formed (**Figure 6**). Although the application of sLCOs caused a decrease in the ratio of mycorrhizas formed by *L. bicolor* on *Populus* roots (**Figure 6**), sLCOs still stimulated a slight increase in mantle and Hartig net formation (**Figures 7**). Interestingly, the colonization of *M. truncatula* by *R. irregularis* was also moderately increased by the application of LCOs (Maillet et al., 2011). Furthermore, we showed that *L. bicolor* uses *CCaMK* for full establishment of the mantle and both *CCaMK* and *CASTOR*/*POLLUX* for complete Hartig net development during the colonization of *Populus* roots. This provides the first evidence that the CSP is used in part by the ECM fungus *L. bicolor* to colonize its host plant (**Figure 8**). Finally, we demonstrated that the expression of the mycorrhiza-induced phosphate transporter *PT12* was significantly reduced in *CCaMK*-RNAi *Populus* compared to wild-type *Populus* thus demonstrating that not only does the CSP

contribute to the colonization of *Populus* by *L. bicolor*, but also plays a role in establishing a fully functional symbiosis (**Figure 9**).

Laccaria bicolor produces a suite of lipochitooligosaccharides with unique functions

Although several substitutions on LCOs differ between *R. irregularis* and *L. bicolor*, both mycorrhizal fungi produce a mixture of sLCOs and nsLCOs (Maillet et al., 2011). Different structures of LCOs are more active at different steps of the *Populus-L. bicolor* association. Purified nsLCOs enhanced lateral root development, while sLCOs did not; reciprocally, purified sLCOs enhanced ECM colonization, but nsLCOs did not. The role of different LCO structures at different stages of the symbiotic associations has been well described in the rhizobia–legume symbiosis. For instance, *Sinorhizobium meliloti* produces LCOs O-acetylated and N-acylated by C16-unsaturated fatty acids that are absolutely required for infection thread formation and nodule organogenesis. Double mutants of *nodF* and *nodL* produce LCOs with saturated fatty acids and that lack the O-acetyl substitution at the non-reducing end. This *S. meliloti nodF/L* mutant is able to elicit root hair curling and initiate nodule organogenesis but unable to initiate infection threads, indicating that different structures of LCOs are required for different stages of the symbiotic association. These observations led to the hypothesis that different receptor complexes recognizing different LCO structures may control different steps of the symbiotic association (Ardourel et al., 1995). Given the effect of different LCO structures on lateral root development and ECM colonization, we can speculate that different LCO receptor complexes may control lateral root formation and ECM colonization in response to fungal signals. In future studies, it would be interesting to develop *L. bicolor* mutants producing specific types of LCOs and to dissect the role of different LCO receptor complexes at different stages of the ECM association.

Ca^{2+} spiking is conserved in *Populus* and induced by both arbuscular mycorrhizal and ectomycorrhizal fungi

Observing Ca^{2+} spiking *in vivo* requires the injection of Ca^{2+}-sensitive dyes or the expression of Ca^{2+} sensors (Ehrhardt et al., 1996; Krebs et al., 2012). For the past decade, the most commonly used sensor for observing Ca^{2+} spiking was the FRET-based Yellow Cameleon protein YC3.6 or one of its progenitors (Capoen et al., 2011; Krebs et al., 2012; Sun et al., 2015; Venkateshwaran et al., 2015). However, another class of genetically encoded, non-FRET-based, Ca^{2+}-sensitive fluorescent sensors known as GECO were recently developed (Zhao et al., 2011). When compared to FRET-based sensors, GECO can detect symbiosis-related variations in Ca^{2+} spiking with higher sensitivity (Kelner et al., 2018). As such, we used a nuclear-localized G-GECO to monitor Ca^{2+} spiking in the nuclei of epidermal cells from *Populus* lateral roots treated with symbiotic signals. We showed, for the first time, that Ca^{2+} spiking occurs in *Populus* in response to both GSE from the AM fungus *R. irregularis* and purified signals (e.g., LCOs and CO4). While the ratio of spiking nuclei was identical among treatments, the spiking frequency was significantly lower in the CO4 and sLCOs treatments, suggesting that *Populus* is perhaps most responsive to nsLCOs. In contrast, nsLCOs and CO4 were less active than sLCOs to initiate Ca^{2+} spiking in lateral roots from *M. truncatula* (Sun et al., 2015). In that study, for nsLCOs and CO4, spiking initiated at a concentration of 10^{-8} M with a maximum response at 10^{-6} M while for sLCOs spiking began at 10^{-13} M with a plateau response at 10^{-9} M. This observation is not surprising given that the LCOs produced by *S. meliloti*—the rhizobial symbiont for *M. truncatula*—are sulfated (Truchet et al., 1991). In contrast to *M. truncatula*, Ca^{2+} spiking in rice occurred primarily in response to CO4, but not at all in response to LCOs (Sun et al., 2015). Our

data coupled with these previous findings confirm that different plants respond to and require different signals for the activation of the CSP.

To our knowledge, our work provides the first observation of Ca^{2+} spiking inhibition using RNAi to knock-down the expression of *CASTOR* and *POLLUX* as opposed to the use of mutants. Previous studies with other plant species have all used mutants with complete genetic knock-outs of genes required for Ca^{2+} spiking (Charpentier et al., 2008; Capoen et al., 2011; Sun et al., 2015; Charpentier et al., 2016). At the time we began this study, this was not an option in *Populus* due to the difficulty of obtaining mutant lines. Regardless, we still observed a significant decrease in both spiking frequency and intensity in response to GSE from *R. irregularis*.

Lipochitooligosaccharides enhance lateral root development across species but with variable dependence on components of the "common symbiosis pathway"

Enhanced lateral root development is a well-documented response to both AM and ECM fungi (Gutjahr and Paszkowski, 2013; Sukumar et al., 2013; Fusconi, 2014). In response to AM fungal spores from *Gigaspora margarita,* increased lateral root development in *M. truncatula* was dependent on *DMI1* and *DMI2*, but not *CCaMK/DMI3* (Oláh et al., 2005). Identical results were obtained with GSE from *R. irregularis* (Mukherjee and Ané, 2011). In rice, *R. irregularis* induced an increase in lateral root development completely independent of the CSP (Gutjahr et al., 2009). Again, identical results were observed in response to GSE (Mukherjee and Ané, 2011). However, nsLCOs and sLCOs increased lateral root formation in *M. truncatula,* and this response was entirely dependent on not only *DMI1* and *DMI2*, but also *CCaMK/DMI3* (Maillet et al., 2011). Both nsLCOs and sLCOs, as well as CO4, enhanced lateral root formation in rice,

and this response to purified signals was dependent on the rice CCaMK (Sun et al., 2015). Based on these results, enhanced lateral root formation occurs in both *M. truncatula* and rice in response to AM fungal colonization, application of spores or GSE, and purified signals (COs and LCOs); however, the dependence of these responses on components of the CSP varies by species and by treatment. In our *Populus* experiment, we found that lateral root development was affected by nsLCOs and that this was dependent on *CCaMK* but not *CASTOR/POLLUX*. Surprisingly, the CASTOR/POLLUX-RNAi lines exhibited an enhanced response to LCOs in both primary root length and lateral root development, which was not observed before in other species using mutants.

Interactions between ethylene and auxin are required for lateral root development in multiple plant species (Ivanchenko et al., 2008; Negi et al., 2010). ECM fungi take advantage of this conserved mechanism of hormone balance and manipulate root morphology in various tree species by producing ethylene and auxin (Rupp and Mudge, 1985; Rupp et al., 1989; Karabaghli-Degron et al., 1998; Splivallo et al., 2009; Felten et al., 2009, 2010; Vayssières et al., 2015). Our findings indicate that manipulating hormone balance is not the only mechanism that *L. bicolor* uses to affect root architecture. Rather, similar to AM fungi (Oláh et al., 2005), *L. bicolor* also produces LCOs to stimulate an increase in lateral root formation thereby potentially maximizing root surface area available for colonization.

The "common symbiosis pathway" is likely not used for all ectomycorrhizal associations

AM colonization assays have traditionally been performed with plant mutants to evaluate the role of the core CSP genes in the colonization process (Stracke et al., 2002; Ané et al., 2004; Lévy et al., 2004). Given the inability to produce mutant lines in *Populus* at the time we initiated

this study, the best method for manipulating gene expression was RNAi. This method was used previously to knock-down the expression of *CCaMK* in tobacco resulting in a decrease in AM colonization (Groten et al., 2015). Using RNAi in *Populus*, we generated RNAi lines targeting *CASTOR*, *POLLUX*, and *CCaMK* with 89%, 71%, and 83% knock-down, respectively, compared to wild-type *Populus*. Due to the time and cost of producing transgenic *Populus*, we did not generate an empty-vector control line but instead used wild-type poplar since its root development was no different than that observed in the RNAi lines (**Figure 5A**). Compared to wild-type, the *CASTOR*/*POLLUX*- and CCaMK-RNAi lines exhibited a decrease in colonization with both the AM fungus *R. irregularis* (**Supplemental Figure 13**) and the ECM fungus *L. bicolor* (**Figure 8**), thus further demonstrating that RNAi is a useful tool for evaluating the role of genes involved in plant-microbe interactions. However, the degree of inhibition in the RNAi lines was greater for AM colonization than for ECM colonization, especially in the CCaMK-RNAi line. There are multiple reasons that may explain why this occurred. A previous study on genes involved in AM symbiosis revealed that high-density inoculum partially overcame the mutant phenotype of multiple CSP genes (Morandi et al., 2005). In our study, we used the well-established sandwich system (Felten et al., 2009), which allows for the uniform formation of multiple ectomycorrhizas on the same root system. This method of inoculation exposes plant roots to a density of ECM hyphae that exceeds that present in nature. As such, the expected phenotype of reduced colonization may have been somewhat masked by the ability of high-density inoculum to partially overcome the knock-down of the CSP genes. Regardless, colonization was reduced in the RNAi lines compared to the wild-type control, thus demonstrating that *L. bicolor* uses the CSP to colonize *Populus.*

Our observation that the CSP plays a role in the establishment of the *Populus–L. bicolor* association is probably not a general rule for all ECM associations. Many genes of the CSP are absent in the genome of pine, a host plant for the ECM fungus *H. cylindrosporum* (Garcia et al., 2015). In support of this, the addition of LCOs on roots of *Pinus pinaster* did not affect lateral root development, suggesting that pine is perhaps incapable of perceiving or responding to LCOs (**Supplemental Figure 14**). Moreover, the co-culture of LCO-treated *P. pinaster* roots with *H. cylindrosporum* did not affect the number of ectomycorrhizas that formed (**Supplemental Figure 15**). Since *L. bicolor* produces LCOs and requires the CSP for full colonization of *Populus*, in future studies it would be interesting to test if *L. bicolor* colonization of a host plant that lacks the CSP, e.g., Norway spruce (*Picea abies*), is increased with the application of LCOs (Karabaghli-Degron et al., 1998; Garcia et al., 2015). Furthermore, the presence of LCOs in *L. bicolor* raises the question if other ECM fungal species also produce LCOs and potentially use them to activate the CSP as part of their mechanisms for plant colonization. The methods described in this paper could serve as a platform for future studies in evaluating the presence of LCOs in additional species of ECM fungi and evaluating their role during colonization with a compatible host plant.

Some molecular mechanisms required for individual ectomycorrhizal associations are likely species-specific

Fossil evidence and molecular studies suggest a single origin for AM symbioses (Brundrett, 2002; Delaux et al., 2014; Bravo et al., 2016); however, phylogenetic studies with ECM fungi suggest that ECM symbioses have arisen independently in 78-82 fungal lineages (Tedersoo and Smith, 2013; Martin et al., 2016; Hoeksema et al., 2018). It is therefore very

likely that the molecular mechanisms required for one ECM fungus to colonize one plant species differ from those required by even the same fungus to colonize another plant species. As evidence of this, in addition to a core regulon, a variable gene regulon was identified in *L. bicolor* during the colonization of two distinct host plants, black cottonwood (*Populus trichocarpa*) and douglas fir (*Pseudotsuga mensiezii*) (Plett et al., 2015). Furthermore, another study that compared the transcriptome of both extraradical mycelium and hyphae derived from mature ectomycorrhizae from 13 ECM fungal species found that some groups of genes based on gene ontology were similarly regulated (Kohler et al., 2015). However, symbiosis-induced genes were mostly restricted to individual species. In fact, even two ECM species of *Laccaria* that diverged ~20 million years ago only shared one-third of *Laccaria* symbiosis-induced orphan genes. This observation suggests that even after the evolution of the ECM habit within a genus, individual species diverged and developed their own 'toolkit' of symbiosis-specific proteins (Kohler et al., 2015; Hoeksema et al., 2018).

It is also likely that host-specific responses may be related to the production of small secreted proteins (SSPs). In *L. bicolor*, two mycorrhiza-induced (Mi)SSPs have been characterized (MiSSP7 and MiSSP8) and both function as effectors in the host plant *Populus* (Plett et al., 2011; Pellegrin et al., 2017). The expression of MiSSP7 is induced by the plant-derived flavonoid rutin and modulates jasmonic acid signaling (Plett and Martin, 2012; Plett et al., 2014). To add more complexity to the *Populus–L. bicolor* symbiosis, *Populus* also releases SSPs that enter ECM hyphae and alter their growth and morphology (Plett et al., 2017). All of these findings combined with ours provide a more complete view of how the *Populus–L. bicolor* association forms. However, a significant amount of research still needs to be performed to determine how many ECM fungi produce LCOs and whether they use them like *L. bicolor* to

colonize their host plants via activation of the CSP. If they do, then the common symbiosis pathway should be considered as more common than we previously thought in regulating not only the rhizobia–legume, Frankia–actinorhizal, and AM symbioses, but also some ECM symbioses as well.

3.5 Material and Methods

Plant material and culture. Seeds from *Medicago truncatula* Jemalong A17 and *Vicia sativa* (L.A. Hearne Company, California) were used for root hair branching experiments. Hybrid *Populus* (*P. tremula* x *P. alba* clone INRA 717-1-B4) was used for all other experiments. *M. truncatula* seeds were germinated as described previously (Mukherjee and Ané, 2011). *Vicia sativa* seeds were surface sterilized with 2.4% (w/v) calcium hypochlorite for two minutes, rinsed three times with sterile water, and then soaked for four hours. Imbibed seeds were placed on moist germination paper (38 lb; Anchor Paper Co.) on 1% agar (Sigma-Aldrich) containing 1 mM gibberellic acid (Sigma-Aldrich) and placed at 4 °C for seven days to synchronize germination. The seeds were then germinated at room temperature (25 °C) for up to four days. Fully germinated *M. truncatula* and *V. sativa* seeds were plated on moist germination paper on Fahraeus medium (Fåhraeus, 1957) supplemented with 0.1 µM 2-aminoethoxyvinyl glycine (AVG; Sigma Aldrich). *Populus* plants were maintained in axenic conditions using Lloyd & McCown's woody plant medium (WPM; 2.48 g l^{-1} basal salts [Caisson Labs] supplemented with 5 mM NH_4NO_3, 2.5 mM $Ca(NO_3)_2$ • 4 H_2O, 3 µM D-Gluconic acid calcium salt, 20 g l^{-1} sucrose, pH 5.6, 3.5 g l^{-1} agar, 1.3 g l^{-1} Gelrite) and grown in glass bottles (6 cm x 10 cm) sealed with Magenta B-caps (Sigma-Aldrich). Unless indicated otherwise, for all experiments with *Populus*, 3 cm terminal cuttings were taken from four-week-old *Populus* plants and rooted for one week in

half-strength Murashige & Skoog (MS) medium with vitamins (Caisson Labs) supplemented with 10 µM indole-3-butyric acid (IBA; Fisher Scientific). All plants were grown in a growth chamber (Conviron PGC Flex) set to 25 °C with a 16-h day/8-h night photoperiod and ~100 µmol m^{-2} s^{-1} of light provided by fluorescent bulbs (Phillips Silhouette High Output F54T5/841).

Fungal material and culture. Germinating spore exudates from *R. irregularis* strain DAOM 197198 (Premier Tech Biotechnologies) were prepared as described previously using ~4,000 spores ml^{-1} (Mukherjee and Ané, 2011). *L. bicolor* strain S238N obtained from Francis Martin (INRA, Nancy, France) was maintained on Pachlewski P05 medium (Müller et al., 2013) with 2% agar (w/v) at 25 °C in the dark. For root hair branching assays, hyphal exudates from *L. bicolor* were obtained as follows: 9 cm x 9 cm sheets of cellophane were boiled in 1 mM EDTA (Sigma-Aldrich) for one hour, rinsed three times with milli-Q water, and then autoclaved for one hour while immersed in water. The cellophane sheets were then placed on Pachlewski P20 medium (Müller et al., 2013) with 2% agar (w/v) and nine, 8 mm, plugs of *L. bicolor* were placed on the cellophane equidistant from one another. After incubation for approximately two weeks, fungal hyphae covered the surface of the cellophane which was then floated on 30 ml of sterile milli-Q water in a square Petri dish (9 cm x 9 cm) and incubated for three days. Hyphal exudates were then collected by pouring off the liquid from multiple plates and concentrating it to 10% of the original volume using a rotary evaporator. The concentrated exudates were then stored at -20 °C and thawed as needed for root hair branching experiments. For Ca^{2+} spiking assays, *L. bicolor* hyphae from liquid cultures grown for two months in 50 ml of Pachlewski P05 broth were rinsed with sterile water three times. The hyphae were then re-suspended in 20 ml of sterile water and mechanically emulsified for five seconds to generate a liquid suspension of

hyphae that was used immediately for application directly onto *Populus* roots to induce Ca^{2+} spiking.

Root hair branching assays. We used nsLCOs and sLCOs suspended in water with 0.005% ethanol (v/v) at a concentration of 10^{-8} M. Also, we prepared mock treatment with water containing 0.005% ethanol (v/v). The mock, diluted nsLCOs or sLCOs, GSE, and *L. bicolor* hyphal exudates were individually applied onto root hairs from Zone II of developing roots (Heidstra et al., 1994) from *M. truncatula* and *V. sativa*. After 24 hours of horizontal incubation at room temperature on the bench, the treated regions of the roots were screened with an inverted transmission light microscope (Leica DMi1) using a 20×/0.30 Leica PH1 objective. Root hairs on the primary root of at least five plants were observed for each treatment.

Production of hyphal exudates for mass spectrometry. In our previous study of LCOs from *Rhizobium* sp. IRBG74, five liters of bacterial exudates was not sufficient to detect any LCOs by mass spectrometry (Poinsot et al., 2016). In that study, detection of LCOs was only possible after engineering the strain with extra copies of the regulatory *nodD* gene from *Sinorhizobium* sp. NGR234. Similarly, the detection of LCOs in *R. irregularis* was only possible after using 450 liters of sterile culture medium used for AM-colonized carrot roots and exudates from 40 million germinating AM fungal spores (Maillet et al., 2011). Here, we used a total volume of six liters of culture medium from 17 independent cultures of *L. bicolor* (**Supplemental Table 1**). Firstly, fungal cultures were initiated on MP medium (Jargeat et al., 2014) overlaid with cellophane membrane with one plug per 55 mm Petri dish or three plugs per 90 mm Petri dish. After two to three weeks, mycelia were transferred to liquid MP medium, in Petri dishes (6 independent series), or to liquid modified MP medium (MPM; 2.5 g l^{-1} glucose), in Petri dishes (11 independent series). All liquid cultures were incubated at 24°C in the dark for

four weeks without agitation. The fungal culture media (100 to 400 ml depending on the series) were extracted twice with butanol (1:1, v/v). The pooled butanol phases were washed with distilled water and evaporated under vacuum. The dry extract was re-dissolved in 4 ml water:acetonitrile (1:1, v/v) and dried under nitrogen.

Mass spectrometry analyses. Synthetic lipochitin standards (LCO IV-C16:0, LCO IV-C16:0 S, LCO IV-C18:1, LCO IV-C18:1 S) obtained from Hugues Driguez (CERMAV, Grenoble, France) were used to optimize HPLC/Q-TRAP tandem mass spectrometry detection by MRM, at 10^{-5} M in ACN:water (1:1, v/v), as described previously (Maillet et al., 2011). The HPLC 3000 (Dionex) was equipped with: i) in "HPLC" using a C18 reverse-phase column Acclaim 120 (2.1 x 250 mm, 5 µm, Dionex, Sunnyvale, USA). The separation was achieved with a gradient of ACN/water:acetic acid (1000/1, v/v), started at 30% ACN for one minute, followed by a 30 minute gradient to 100% ACN, followed by an isocratic step at 100% ACN for five minutes, at a constant flow rate of 300 µl.min^{-1}. ii) In "U-HPLC" using a C18 reverse-phase column C18 Acquity (2.1 x 100 mm, 1.7 µm, Waters). The separation was achieved with a gradient of ACN/water:acetic acid (1000/1, v/v), started at 30% ACN in water for one minute, followed by an eight minute gradient to 100% ACN, followed by an isocratic step at 100% ACN for two minutes, at a constant flow rate of 450 µl min^{-1}. Ten µl samples were injected. The mass spectrometer was a 4500 Q Trap mass spectrometer (Applied Biosystems, Foster City, USA) with electrospray ionization in the positive ion mode. The samples were analyzed in the multiple reactions monitoring (MRM) and Enhanced Mass Spectrometry-Enhanced Product Ion (EMS-EPI). The capillary voltage was fixed at 4500 V, source temperature at 400 °C. Fragmentation was performed by collision-induced dissociation (CID) with nitrogen at a collision energy between 22 and 54 V. Declustering potential was between 90 and 130 V, optimized for each

molecule. The MRM channels were set according to the transitions of the proton adduct ion $[M + H]^+$ to the fragment ions corresponding to the loss of one, two, or three N-Acetyl Glucosamine at the reducing end (sulfated or not).

RNAi-construct design for silencing CASTOR, POLLUX, and CCaMK. Due to genome duplication, two homologs of *CASTOR*, *POLLUX*, and *CCaMK* exist in the *Populus* genome (Tuskan et al., 2006). These include *PtCASTORa* (Potri.019G097000) and *PtCASTORb* (Potri.013G128100), *PtPOLLUXa* (Potri.003G008800) and *PtPOLLUXb* (Potri.004G223400), and *PtCCaMKa* (Potri.010G247400) and *PtCCaMKb* (Potri.008G011400). Given that neither copy of these genes had been characterized previously, both copies of each gene were targeted simultaneously for RNA-based gene silencing. For *PtCASTOR*, *PtPOLLUX*, and *PtCCaMK*, respectively, a 175, 153, and 200 bp DNA fragment was selected based on sequence similarity between both paralogs of each gene and amplified using compatible primers (**Supplemental Table 2**). PCR amplified products were cloned into the pENTR/D-TOPO entry vector following manufacturer guidelines (Invitrogen). Subsequently, the *PtCASTORa/b*-RNAi, *PtPOLLUXa/b*-RNAi and *PtCCaMKa/b*-RNAi fragments were each individually cloned into the pK7GWIWG2(II) binary vector using Gateway LR Clonase (Invitrogen) (**Supplemental Table 3**). Following insertion, the resulting RNAi constructs were verified for proper orientation and integrity through sequencing and were introduced into *Agrobacterium tumefaciens* strain AGL1 for transformation into *P. tremula* x *alba* clone INRA 717-1-B4.

Agrobacterium tumefaciens-mediated Populus transformation. *Agrobacterium tumefaciens* strain AGL1 was used to transform the RNAi binary vectors into *Populus* as described in (Filichkin et al., 2006). For the *PtCASTOR*-, *PtPOLLUX*- and *PtCCaMK*-RNAi constructs, 259, 303 and 259 independent transgenic events were generated, respectively. After

multiple rounds of initial selection based on resistance to kanamycin in the selection medium, 32, 21, and 82 events of *PtPOLLUX*-, *PtCASTOR*- and *PtCCaMK*-RNAi, respectively, were further confirmed for the presence of the transgene (RNAi cassette) in the transgenic plants using primers designed on the CaMV 35S promoter, terminator, and RNAi intron flanking the RNAi fragments (**Supplemental Table 3**). All of the transgenic RNAi lines were maintained as described above for further validation of the effect of RNAi-based gene silencing.

RNA extraction, cDNA synthesis, and quantitative reverse transcription (qRT)-PCR. RNA was extracted from ~100 mg of root tissue from at least three separate plants for each RNAi line by flash freezing them in liquid nitrogen and pulverizing them with two glass beads using a mixer mill (Retsch, model MM 400). Immediately after, 500 µl of RNA extraction buffer (4 M guanidine thiocyanate, 0.2 M sodium acetate [pH 5.0], 25 mM EDTA, 2.5% PVP-40 [v/v], 2% sarkosyl [v/v], and 1% β-mercaptoethanol [v/v] added just before use) was added to the pulverized root tissue and vortexed for five seconds. Then, 500 µl of 24:1 chloroform:isoamyl alcohol (v/v) was added to the solution and again vortexed for five seconds. Following a ten-minute centrifugation at 11,000 rpm and 4 °C, 450 µl of the aqueous phase of the solution was placed on a shearing column from the Epoch GenCatch™ Plant RNA Purification Kit. From this point forward, the manufacturer's protocol was strictly followed. Following the extraction, RNA quantity and quality were evaluated with a Nanodrop spectrophotometer (ThermoScientific; model ND100) and suitable RNA was stored at -80 °C. Contaminating DNA was removed from RNA samples using the TURBO DNA-*free*™ Kit (Invitrogen) and by following the manufacturer's protocol. RNA quantity and quality were again evaluated with a Nanodrop spectrophotometer to determine how much of each sample to use to obtain 1 µg of RNA.

To prepare the RNA to serve as a template for cDNA synthesis, 1 µg of RNA in 11.5 µl of RNase-free water was incubated at 65 °C with 1 µl of oligo$(dT)_{17}$ for five minutes and then placed on ice for another five minutes. To this solution, the following components were then added: 2 µl of 10 mM dNTP, 4 µl of 5x RevertAid Reverse Transcriptase buffer, 0.5 µl of RiboLock RNase Inhibitor, and 1 µl of RevertAid Reverse Transcriptase (ThermoFisher Scientific). After incubating at 42 °C for one hour and inactivating the transcriptase at 70 °C for 15 minutes, the resulting cDNA was stored at -20 °C. qRT-PCR was performed using the Bio-Rad CFX96™ Real-Time PCR System with the CFX Manager v3.0 software (Bio-Rad). Reactions were performed in 96-well plates using SsoAdvanced™ Universal SYBR® Green Supermix (Bio-Rad), 10 nM of each gene-specific primer (**Supplemental Table 3**), and 1:20 (v/v) cDNA:water. PCR cycling conditions were as follows: 95 °C for 3 minutes, followed by 40 cycles at 95 °C for 10 seconds, 58 °C for 25 seconds, and 72 °C for 30 seconds. The specificity and efficiency of primer pairs were confirmed by analysis of dissociation curves (65 to 95 °C) and serial dilution, respectively. Results were expressed as a threshold cycle (CT) value. At least three technical replicates and three biological replicates were performed for each sample, and their CT values were averaged. The standard curve method was used to analyze gene expression in each sample as described previously (El Yahyaoui, 2004). Ubiquitin- and putative protein-encoding genes were both used as reference genes as described previously (Felten et al., 2009).

Agrobacterium rhizogenes-mediated Populus transformation. *Agrobacterium rhizogenes* strain ARqua1 was transformed by electroporation with the binary vector pEC11579 provided by Dr. Giles Oldroyd (University of Cambridge, United Kingdom) encoding both a nuclear-localized version of G-GECO and the fluorescent protein DsRed (**Supplemental Figure 16**). Successfully transformed *A. rhizogenes* was used to generate transgenic *Populus* hairy roots

using a slightly modified method described by Yoshida et al. (2015). In brief, leaves from axenic cultures of hybrid *Populus* were wounded with a scalpel by making multiple perpendicular incisions 1 mm in length along the central vein on the abaxial surface of the leaf. Wounded leaves were inoculated for only five minutes on an inversion table with a liquid suspension of transformed *A. rhizogenes* strain ARqua1 diluted to an OD_{600} of 0.8 using induction broth. Inoculated leaves were placed on co-culture medium for two days and then transferred to antibiotic medium containing 200 mg ml^{-1} of cefotaxime and 300 mg ml^{-1} of Timentin. After approximately two weeks of incubation in the dark at 25 °C, transgenic roots appeared from wounded sites (**Supplemental Figure 8A**). These roots were screened using a fluorescent stereomicroscope (Leica M165 FC), and those visibly expressing DsRed were excised and placed on antibiotic medium containing 15 µM trans-zeatin (Cayman Chemical Company) to induce shoot formation as described previously (Son and Hall, 1990). Shoots appeared within as little as two months and were again screened using the same fluorescent stereomicroscope (**Supplemental Figures 8B** and **10**). Those expressing DsRed were excised from the roots and placed in half-strength MS medium supplemented with 10 µM IBA and 5 g l^{-1} of Gelrite (DOT Scientific Inc.). The resulting stable transgenic lines were maintained as described above and used for Ca^{2+} spiking experiments.

Ca^{2+} spiking experiments. Since lateral roots in *M. truncatula* are generally more responsive to LCOs than primary roots (Sun et al., 2015), for our experiments we used first-order lateral roots from *Populus*. Primary roots from axenic *Populus* with many lateral roots measuring at least 1 cm in length were extracted from solid WPM. The lateral roots were individually excised from the primary root and placed in WPM broth with reduced phosphorus (2.5 µM KH_2PO_4) and diminished nitrogen (no NH_4NO_3). To inhibit ethylene production, 0.1 µM AVG

was added to the broth. After at least two hours of incubation, lateral roots were removed from the broth, placed on a coverslip (48 mm x 60 mm), and held in place with high vacuum grease (Dow Corning) which was also used to form a square well around the root. Experimental treatments included: GSE, nsLCOs [10^{-7} M], sLCOs [10^{-7} M], CO4 [10^{-6} M; IsoSep], a liquid suspension of *L. bicolor* hyphae, or mock treatment (water with 0.005% ethanol). Approximately 200 µl of each treatment was applied individually onto separate lateral roots expressing G-GECO to evaluate their ability to induce Ca^{2+} spiking in root epidermal cells. After application of the treatment solution, lateral roots were overlaid with an additional coverslip (22 mm x 40 mm) and incubated for ~20 minutes. Following the incubation, Ca^{2+} spiking was observed for ~20 minutes using an LSM780 confocal laser scanning microscope (Carl Zeiss) with a LD C-Apochromat 40×/1.1 W Korr M27 objective. G-GECO was excited with the 488-nm line of an argon laser and GFP (490–535 nm) emission detected using a 488-nm primary dichroic mirror. DsRed was excited with the 561-nm line of an argon laser and RFP (579–624 nm) emission detected using a 561-nm primary dichroic mirror. The images were acquired at five-second intervals with a scanning resolution of 512 × 512 pixels. Settings (laser intensity, gain, offset, magnification, airy units) were similar between observations for all samples. Following the capture of each 20-minute time course experiment, spiking nuclei were designated as individual regions of interest (ROIs) using the ZEN software (version 2.3 SP1), and the fluorescence intensity of G-GECO and DsRed were recorded for each ROI. For all of the Ca^{2+} spiking experiments (**Figures 2, 3** and **4**), the total number of nuclei and the number of nuclei spiking more than once were used to calculate the ratio of spiking nuclei; furthermore, the fluorescence intensity of G-GECO was plotted for each spiking nucleus to determine the frequency of Ca^{2+} spiking events. For the Ca^{2+} spiking experiments with wild-type G-GECO compared to the *CASTOR*/*POLLUX*-RNAi G-

GECO line (**Figures 3** and **4**), maximum spiking intensity was clearly different between the two lines. As such, we tested two additional *CASTOR*/*POLLUX*-RNAi G-GECO lines to confirm our finding and we calculated the ratio of G-GECO to DsRed fluorescence by dividing the values for G-GECO fluorescence intensity from the corresponding values for DsRed fluorescence intensity within a given nucleus. This allowed us to confirm that variations in spiking intensity were not due to variation in the random insertion of the T-DNA into regions of the genome with varying degrees of expression.

Lateral root and colonization assays with Laccaria bicolor. Rooted *Populus* cuttings were plated on P20 medium in square Petri dishes (9 cm x 9 cm) sandwiched between two triangular pieces of cellophane. Plated cuttings were then placed in the growth chamber. For the native lateral root experiments with wild-type and RNAi *Populus* lines (**Figure 5A**), no treatment was applied, and the plants were grown for a total of three weeks; however, for the LCO-treated experiments (**Figure 5B, C**), after approximately one week, the adventitious root system of each plant was trimmed so that only one root remained. It was then immersed for one hour in mock treatment (water + 0.005% ethanol [v/v]), nsLCOs (10^{-8} M), or sLCOs (10^{-8} M). Treated plants were then plated on fresh Pachlewski P20 medium with cellophane and grown for an additional two weeks. At harvest, the number of lateral roots per primary root was counted manually, and the root system was photographed on each side with a DSLR camera (Nikon D3200). Both images of the root system were analyzed using ImageJ (https://imagej.nih.gov/ij/) to determine average primary root length. This number was also used to calculate the number of lateral roots per length of primary root.

For the colonization assays, *L. bicolor* was grown for ten days on triangular sheets of cellophane placed on Pachlewski P20 medium in square Petri dishes (9 cm x 9 cm) with seven

equally spaced 8 mm plugs per sheet and two sheets per dish (**Supplemental Figure 11A**). After the plugs were removed, the cellophane sheet was placed on fresh Pachlewski P20 medium. Then, either trimmed, LCO-treated wild-type *Populus* roots (**Figures 6**) or untrimmed and untreated wild-type or RNAi *Populus* roots (**Figure 8**) were placed on top of the hyphae-covered cellophane sandwiched in place with an additional sheet of cellophane placed on top (**Supplemental Figure 11B**). *Populus* plants co-cultured with *L. bicolor* were grown for three weeks in the growth chamber and then destructively harvested. Undisturbed ectomycorrhizal roots were imaged with a stereomicroscope (Leica M165 FC). A sub-sample of colonized lateral roots were harvested for analysis by confocal microscopy, and the remainder of the roots system was flash frozen in liquid nitrogen and stored at -80 °C for RNA extraction and subsequent qRT-PCR analysis of gene expression.

Microscopic analysis of ectomycorrhizal roots. Ectomycorrhizal lateral roots were fixed in 4% paraformaldehyde overnight at 4 °C, washed three times in phosphate buffered saline (PBS), and then embedded in 6% agarose as described previously (Felten et al., 2009). Using a vibratome (1000 Plus), ten 50 µm cross sections were taken beginning approximately 500 µm below the root tip to ensure that uniformly colonized root tissue was collected. The cross sections were then immersed in PBS with 2 µg ml^{-1} of wheat germ agglutinin (WGA) conjugated to Alexa Fluor™ 488 (Invitrogen) and 10 µg ml^{-1} of propidium iodide (MP Biomedicals). After overnight incubation at 4 °C, stained cross sections were rinsed with PBS and mounted on microscope slides in PBS for immediate observation with an LSM780 confocal laser scanning microscope (Carl Zeiss) equipped with an LD C-Apochromat 40×/1.1 W Korr M27 objective. WGA-Alexa Fluor™ 488 and propidium iodide were excited with the 488-nm line of an argon laser. Emission was detected between 493 and 534 nm for WGA-Alexa Fluor™ 488 and between 622 and 702

nm for propidium iodide. The images were acquired with a scanning resolution of 1024 × 1024 pixels. Settings (laser intensity, gain, offset, magnification, airy units) were similar between observations for all samples. Images of ectomycorrhizal cross sections were analyzed using ImageJ (https://imagej.nih.gov/ij/) to determine average root diameter from two perpendicular measurements, average mantle width from four separate measurements equidistant from one another along the mantle, root circumference as measured from the outer tip of root epidermal cells, and the Hartig net boundary as shown in **Supplemental Figure 12**.

Inoculation of Populus with arbuscular mycorrhizal fungi and measurement of colonization. For the colonization assays with arbuscular mycorrhizal (AM) fungi only, sterile wild-type and RNAi *Populus* (*P. tremula* x *P. alba* clone INRA 717-1B4) were grown in axenic conditions in half-strength Murashige and Skoog (MS) medium in magenta boxes (Sigma-Aldrich, USA) under a 16-h photoperiod at 25 ± 1 °C for four to six weeks prior to inoculation with arbuscular mycorrhizal fungi. These same *Populus* lines were also acclimated to greenhouse conditions in a peat-vermiculite soil substrate in 165-ml leach tube under a 16-h photoperiod at 25 ± 1 °C for four weeks prior to inoculation. *Rhizophagus irregularis* Schenck & Smith DAOM 197198 (syn: *Glomus intraradices*; Stockinger *et al.*, 2009; Tisserant *et al.*, 2012) was maintained in axenic carrot root organ cultures. Germinated spores were produced as described by Chabot *et al.* (1992). Two independent experiments of inoculation with *R. irregularis* were performed, one in axenic-*in vitro* conditions and the other in greenhouse conditions. A set of plants grown separately under identical conditions but without *R. irregularis* inoculation served as controls (four plants per line). For the axenic *in vitro* experiment, four six-week-old plants were inoculated with *R. irregularis* (100 spores per plant) in magenta boxes with 100 ml of half MS medium under a 16-h photoperiod at 25 ± 1 °C for six weeks. For the greenhouse experiment, four 4-week-old plants were inoculated with *R. irregularis* (800 spores per plant) in one liter pots with autoclaved (two times) peat-vermiculite under a 16-h photoperiod at 25 ± 1 °C for four weeks. Greenhouse plants were irrigated twice weekly with half-strength B&D solution (Broughton and Dilworth, 1971) containing a low

concentration of potassium phosphate (10 µM, K_2HPO_4) to favor AM colonization (Smith et al. 2003). Six weeks post-inoculation, plants were harvested and root systems rinsed with deionized-sterile water. Roots were sampled for staining with trypan blue according to a modified staining procedure by Koske and Gemma (1989). The stained roots were observed under a light microscope (Zeiss) to determine percentage of both arbuscular and root length colonization following the gridline-intersect method (McGonigle *et al.*, 1990).

Determination of root growth and ectomycorrhiza formation in Pinus pinaster treated with LCOs. Seeds of maritime pine (*Pinus pinaster* Soland in Ait. from Medoc, Landes-Sore-VG source, France) were surface sterilized with 37% H_2O_2 for 30 minutes and sown on Petri dishes containing 1% agarose. Two weeks later, germinated seeds were transferred individually into square Petri dishes containing solid modified MMN medium (3.67 mM KH_2PO_4, 0.45 M $CaCl_2$, 0.43 M NaCl, 0.22 M $(NH_4)_2HPO_4$, and 0.61 mM $MgSO_4 \cdot 7\ H_2O$; Morizet & Mingeau (1976) micronutrient solution, 2.5 g l^{-1} glucose, 10 g l^{-1} agarose) between two layers of damp germination paper (**Supplementary Figure 14**). Two days later, seedlings were treated with 1 ml of 10^{-8} M non-sulfated or sulfated LCOs, or 1 ml of mock treatment (0.005% ethanol). After three weeks of growth, the number of lateral roots per plant and the length of the primary root were determined from images of the root system using ImageJ software (https://imagej.nih.gov/ij/). Ectomycorrhizas were produced using a similar set up (**Supplementary Figure 15**). Once plants were placed in square Petri dishes, six plugs of the ECM fungus *Hebeloma cylindrosporum* Romagnesi (homokaryotic strain h7, Debaud & Gay, 1987) grown on solid YMG medium (Garcia *et al.*, 2014) were placed beside the primary root. These co-cultures were treated with 1 ml of 10^{-8} M non-sulfated or sulfated LCOs, or 1 ml of mock treatment (0.005% ethanol). Three weeks later, the number of ectomycorrhizas per plant was recorded.

Statistical analyses. Raw data from the Ca^{2+} spiking experiments were used directly for statistical analysis. In contrast, for the lateral root and colonization experiments, the data were normalized to the wild-type control to account for variation between experiments replicated in

time. All data were analyzed using R (version 3.2.4; http://www.R-project.org/). Welch's two-sample t-test was used for comparing two treatments while one-way ANOVA and Tukey pairwise comparison were used for comparing three or more treatments.

3.6 Acknowledgements

We thank the following individuals for their respective contribution: Tomás Rush for technical assistance with root hair branching assays, Dr. Sarah Swanson for training and support with confocal microscopy techniques, Dr. Francis Martin for providing a culture of *Laccaria bicolor* strain S238N, Dr. Giles Oldroyd for providing the binary vector pEC11579 carrying G-GECO, Dr. Fabienne Maillet for providing purified sLCOs and nsLCOs, and Dr. Hugues Driguez for providing synthetic LCO standards for mass spectrometry. Financial support for this project was primarily provided by the USDA (WIS01695) and NSF (DGE-1256259). Additional financial support was provided by: the French "Agence Nationale de la Recherche" under contract ANR-14-CE18-0008-01 and the Laboratoire d'Excellence entitled TULIP (ANR-10-LABX-41) for the mass spectrometry analyses; the Tree Genomics and Biosafety Cooperative at Oregon State University and the NSF I/UCRC Center for Advanced for Advanced Forestry Systems for partial support of RNAi line development; and the Plant–Microbe Interfaces Scientific Focus Area in the Genomic Science Program, the Office of Biological and Environmental Research in the US Department of Energy Office of Science (Oak Ridge National Laboratory is managed by UT-Battelle, LLC, the United States Department of Energy under contract DE-AC05-00OR22725) for the arbuscular mycorrhizal colonization assays.

3.7 Supplementary Figures

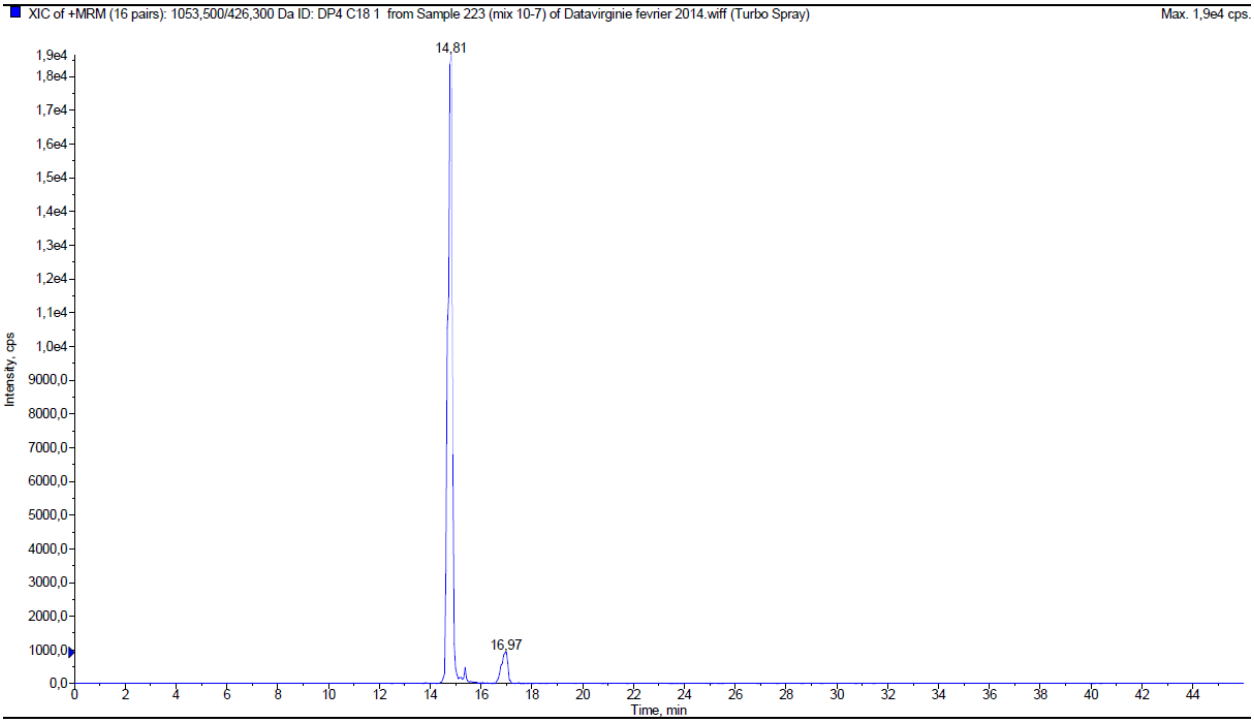

<u>Supplemental Figure 1</u> HPLC chromatogram showing the synthetic standard LCO-IV, C18:1 [10^{-7} M]

Reverse phase HPLC coupled to ESI-Q-Trap mass spectrometer, in the positive mode. Single reaction monitoring *m/z* 1053>426, corresponding to precursor ion $(M+H)^+$> product ion, peak retention time 14.8 min.

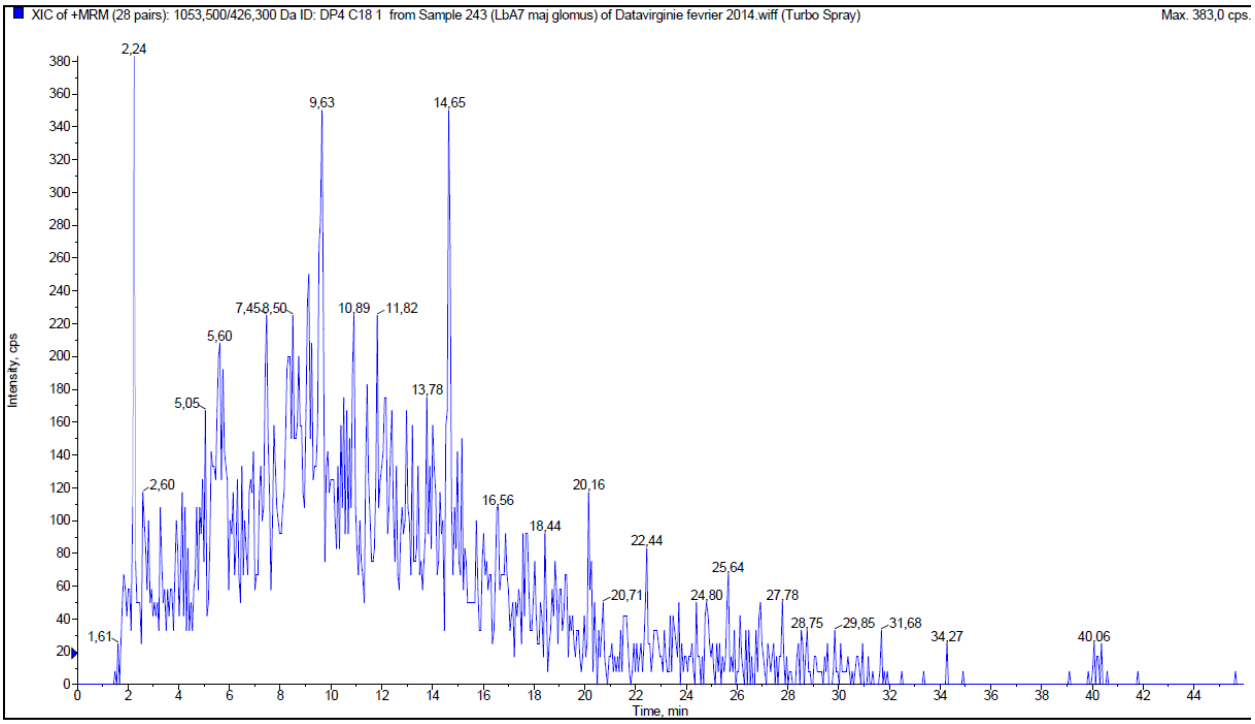

<u>Supplemental Figure 2</u> HPLC chromatogram showing LCO-IV, C18:1, from *Laccaria bicolor* sample (A7)

Reverse phase HPLC coupled to ESI-Q-Trap mass spectrometer, in the positive mode. Single reaction monitoring *m/z* 1053>426, corresponding to precursor ion $(M+H)^+$> product ion. Peak retention time 14.65 min.

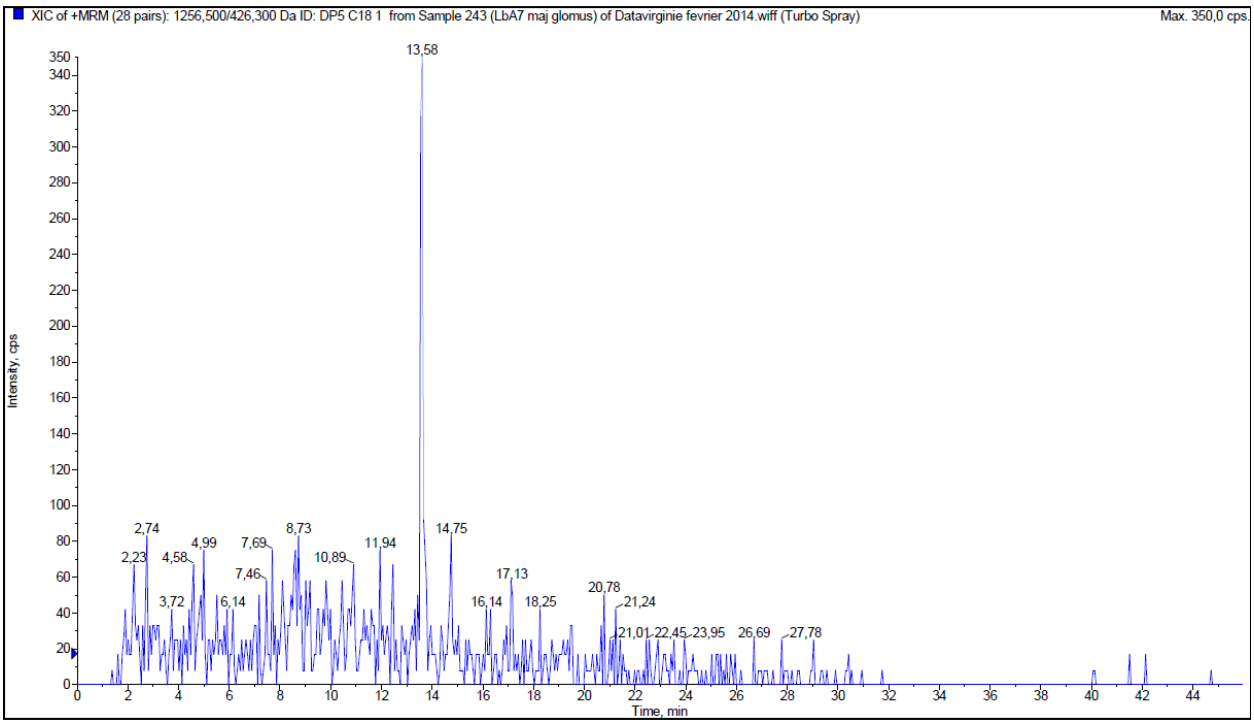

Supplemental Figure 3 HPLC chromatogram showing LCO-V, C18:1 from *Laccaria bicolor* sample (A7)

Reverse phase HPLC coupled to ESI-Q-Trap mass spectrometer, in the positive mode. Single reaction monitoring *m/z* 1256>426, corresponding to precursor ion $(M+H)^+$> product ion. Peak retention time 13.58 min.

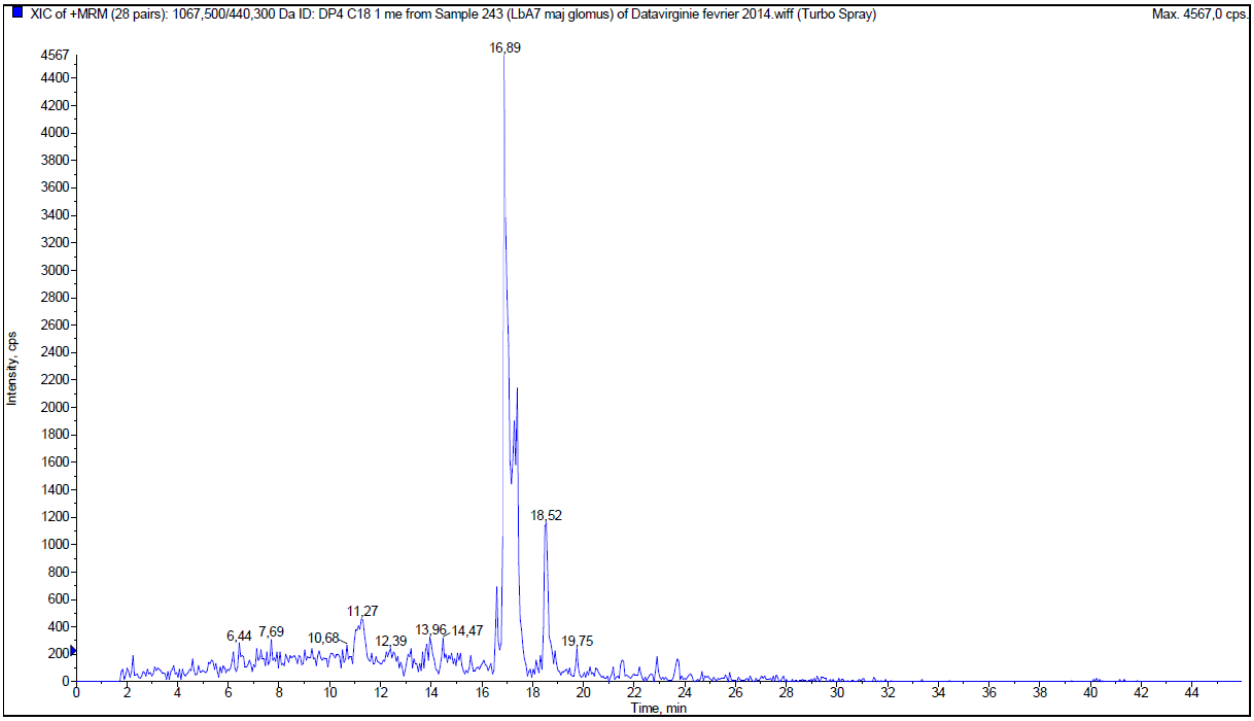

<u>Supplemental Figure 4</u> HPLC chromatogram showing LCO-IV, C18:1, NMe from *Laccaria bicolor* sample (A7)

Reverse phase HPLC coupled to ESI-Q-Trap mass spectrometer, in the positive mode. Single reaction monitoring *m/z* 1067>440, corresponding to precursor ion $(M+H)^+$> product ion. Peak retention time 16.89 min.

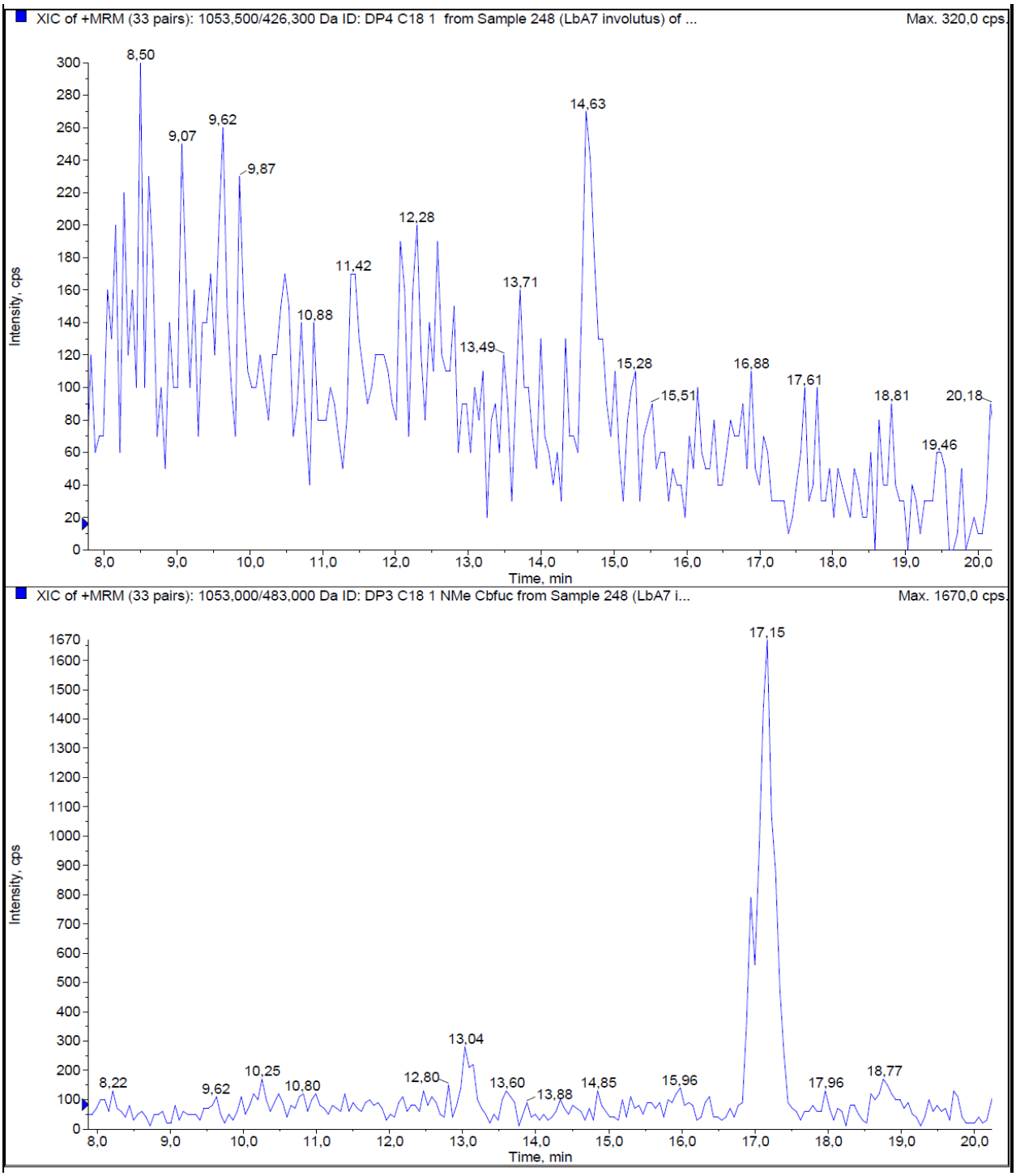

<u>Supplemental Figure 5</u> HPLC chromatograms showing LCO-IV, C18:1 and LCO-III, C18:1, NMe Cb Fuc from *Laccaria bicolor* sample (A7)

Reverse phase HPLC coupled to ESI-Q-Trap mass spectrometer, in the positive mode. Single reaction monitoring *m/z* 1053>426 for LCO-IV, C18:1 (***top***) and 1053>483 for LCO-III, C18:1, NMe Cb Fuc (***bottom***), corresponding to precursor ion $(M+H)^+$> product ion. Peak retention times of 14.63 and 17.15 min, respectively.

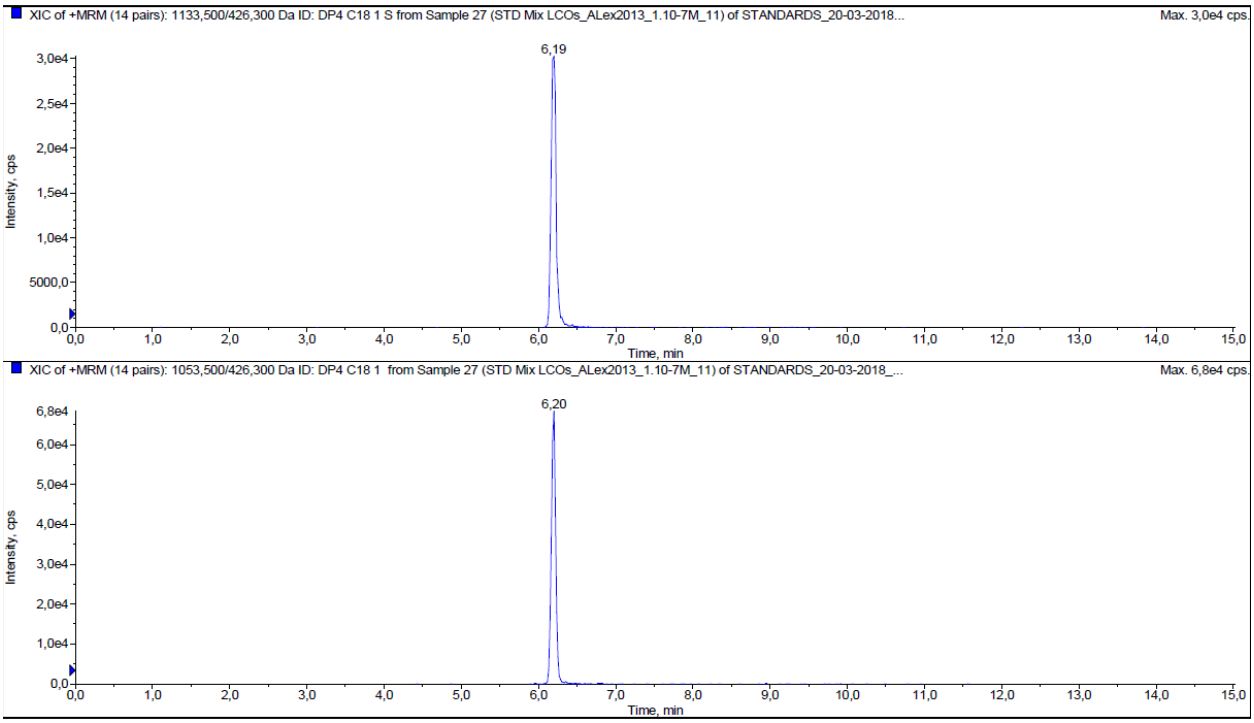

<u>Supplemental Figure 6</u> U-HPLC chromatograms showing the synthetic standards of sulfated and non-sulfated LCO-IV, C18:1 [10^{-7} M]

Reverse phase U-HPLC coupled to ESI-Q-Trap mass spectrometer, in the positive mode. Single reaction monitoring *m/z* 1133>426 for sulfated (***top***) and 1053>426 for non-sulfated (***bottom***), corresponding to precursor ion $(M+H)^+$> product ion. Peak retention times of 6.19 and 6.20 min, respectively.

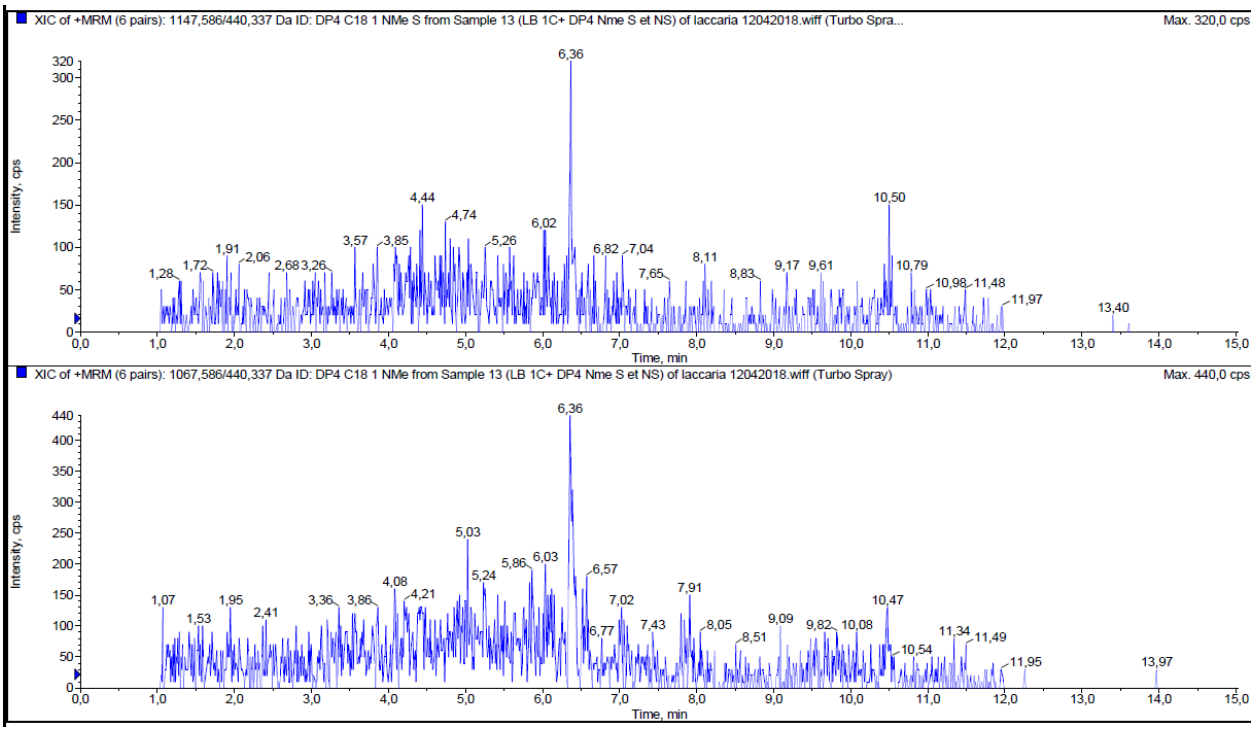

<u>Supplemental Figure 7</u> U-HPLC chromatogram showing the sulfated and the non-sulfated LCO-IV, C18:1 N-Me from *Laccaria bicolor* sample (MP-B1C)

Reverse phase U-HPLC coupled to ESI-Q-Trap mass spectrometer, in the positive mode. Single reaction monitoring *m/z* 1147>440 for sulphated (***top***) and 1067>440 for non-sulfated (***bottom***), corresponding to precursor ion $(M+H)^+$> product ion. Peak retention time of 6.36 min for both samples.

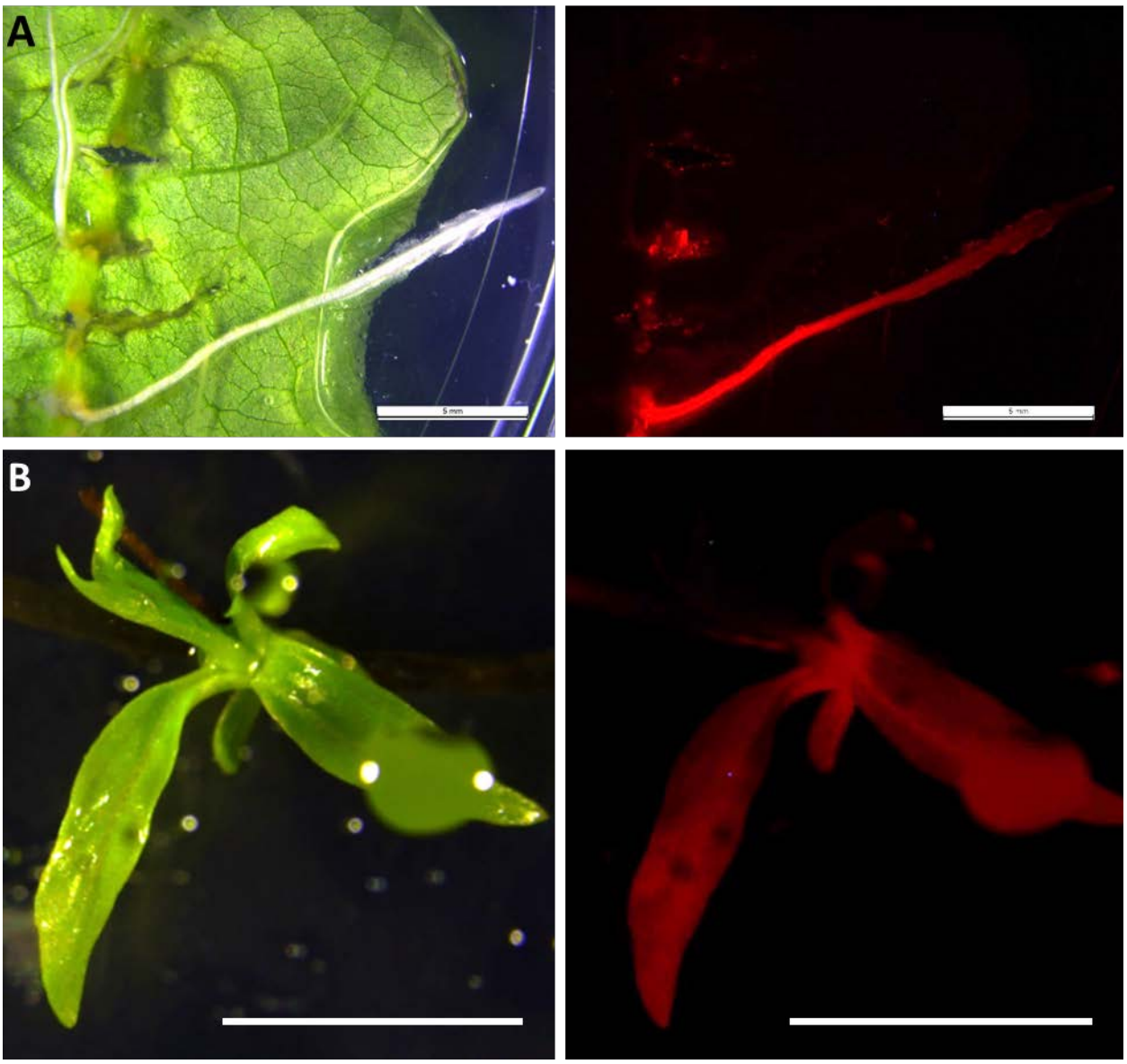

<u>Supplemental Figure 8</u> Images of wild-type *Populus* transformed with green-GECO

(A) Bright field (***left***) and DsRed (***right***) stereomicroscope images of a wild-type *Populus* leaf with a transgenic root arising from a small incision approximately three weeks post inoculation with *Agrobacterium rhizogenes* strain ARqua1 carrying the binary vector pEC11579 with the coding DNA sequence for both green-GECO and DsRed on the same T-DNA (**Supplemental Figure 17**). Scale bars = 5 mm. **(B)** Bright field (***left***) and DsRed (***right***) stereomicroscope images of a transgenic shoot arising from a root transformed with green-GECO after an approximately two month incubation on shoot induction medium containing 15 µM trans-zeatin. Scale bars = 5 mm.

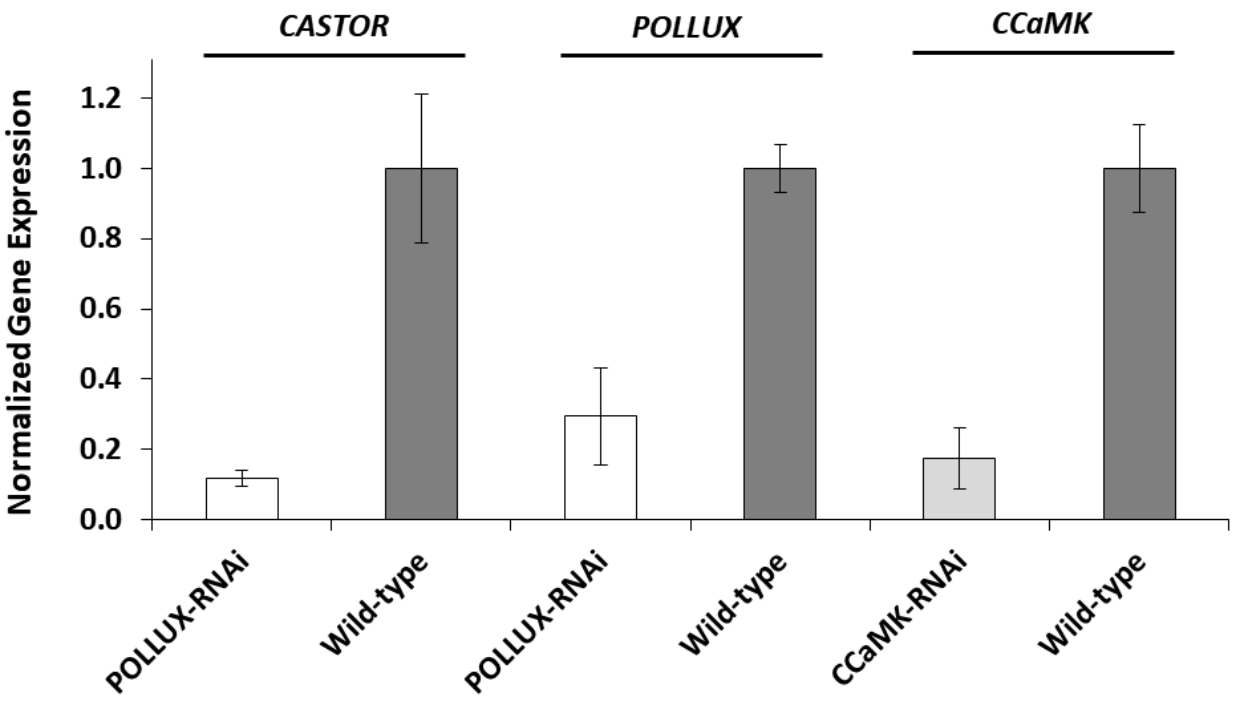

Supplemental Figure 9 Relative gene expression of *CASTOR*, *POLLUX*, and *CCaMK* in RNA interference lines of *Populus* compared to wild-type

Relative expression of *CASTOR* and *POLLUX* in a *POLLUX*-RNAi line (n=3) and *CCaMK* in a *CCaMK*-RNAi line (n=4) were obtained using quantitative reverse transcription (qRT)-PCR. Expression levels of each gene were determined based on three technical replicates (derived from the same RNA extraction) per biological replicate (RNA extracted from separate roots on different plants) and the expression levels of two reference genes, *Putative Protein* and *Ubiquitin* (**Supplemental Table 3**). All samples were normalized to the same wild-type control included within each qRT-PCR run. Bars represent the mean of the data and error bars represent the standard error of the mean.

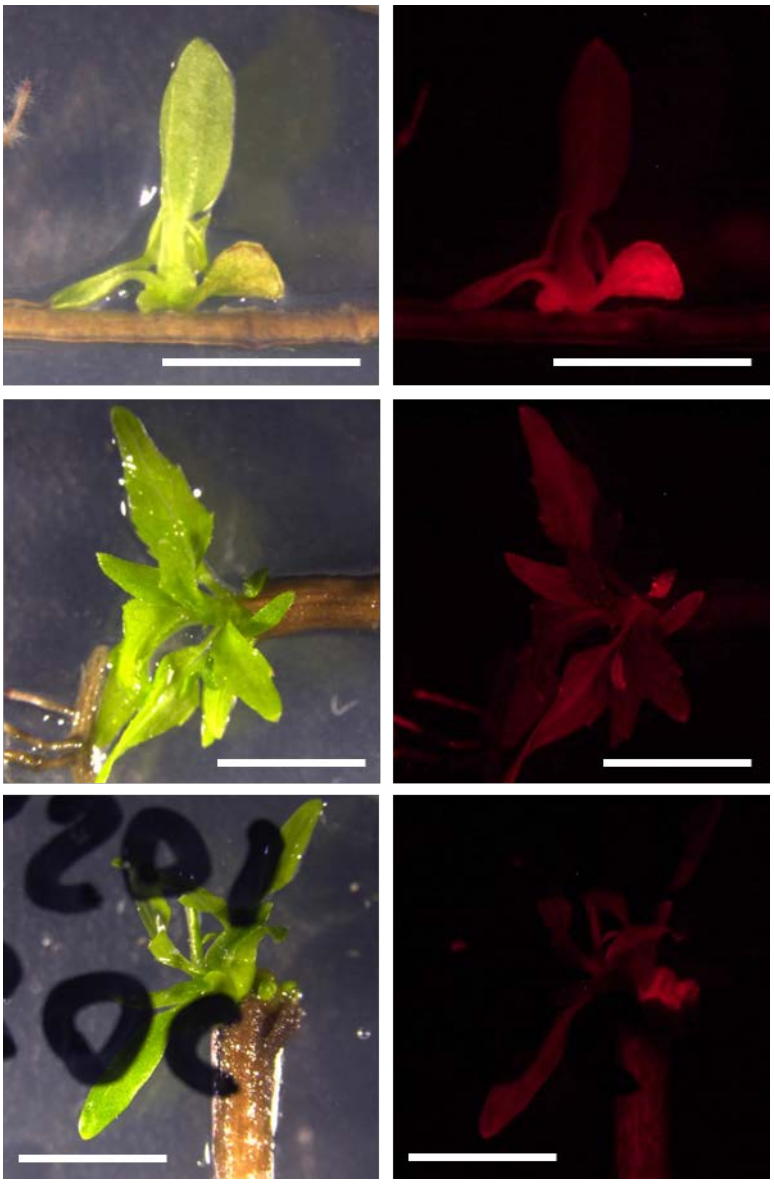

<u>Supplemental Figure 10</u> Images of three independent events of *CASTOR*/*POLLUX*-RNAi *Populus* transformation with green-GECO

Bright field (***left***) and DsRed (***right***) stereomicroscope images of transgenic shoots arising from roots transformed with *Agrobacterium rhizogenes* strain ARqua1 carrying the binary vector pEC11579 with the coding DNA sequence for both green-GECO and DsRed on the same T-DNA (**Supplemental Figure 17**). Shoots developed after approximately two-months of incubation on shoot induction medium containing 15 µM trans-zeatin. Scale bars = 5 mm.

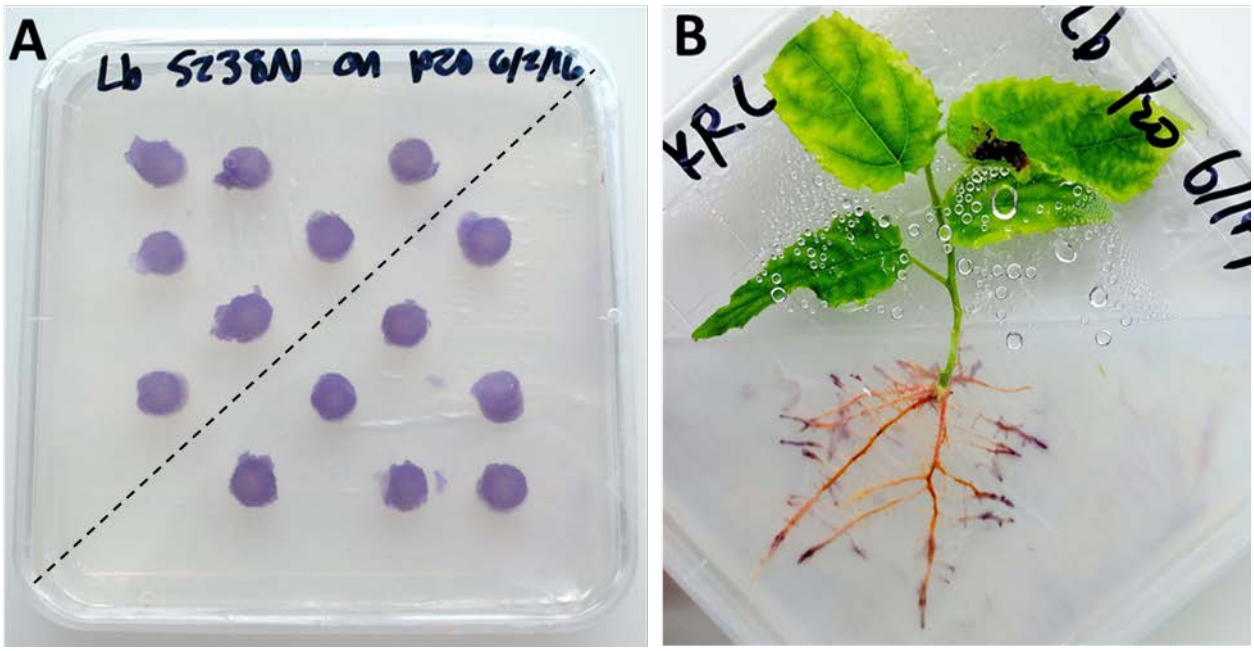

<u>Supplemental Figure 11</u> ***Laccaria bicolor*** **cellophane culture and co-culture with** ***Populus***
(A) Fourteen plugs from an active culture of *Laccaria bicolor* placed on two triangular sheets of cellophane and cultured on Pachlewski P20 medium for 10 days. The plugs were then removed, and the hyphae-covered cellophane sheets transferred to fresh Pachlweski P20 medium before being used to inoculate two *Populus* cuttings. **(B)** One-week-old co-culture of *Populus* with *L. bicolor*. The co-culture was established by placing a two-week-old rooted *Populus* cutting on top of a cellophane sheet containing *L. bicolor* and an additional sheet of cellophane placed on top. The co-culture was incubated for three weeks before the roots were harvested for analysis.

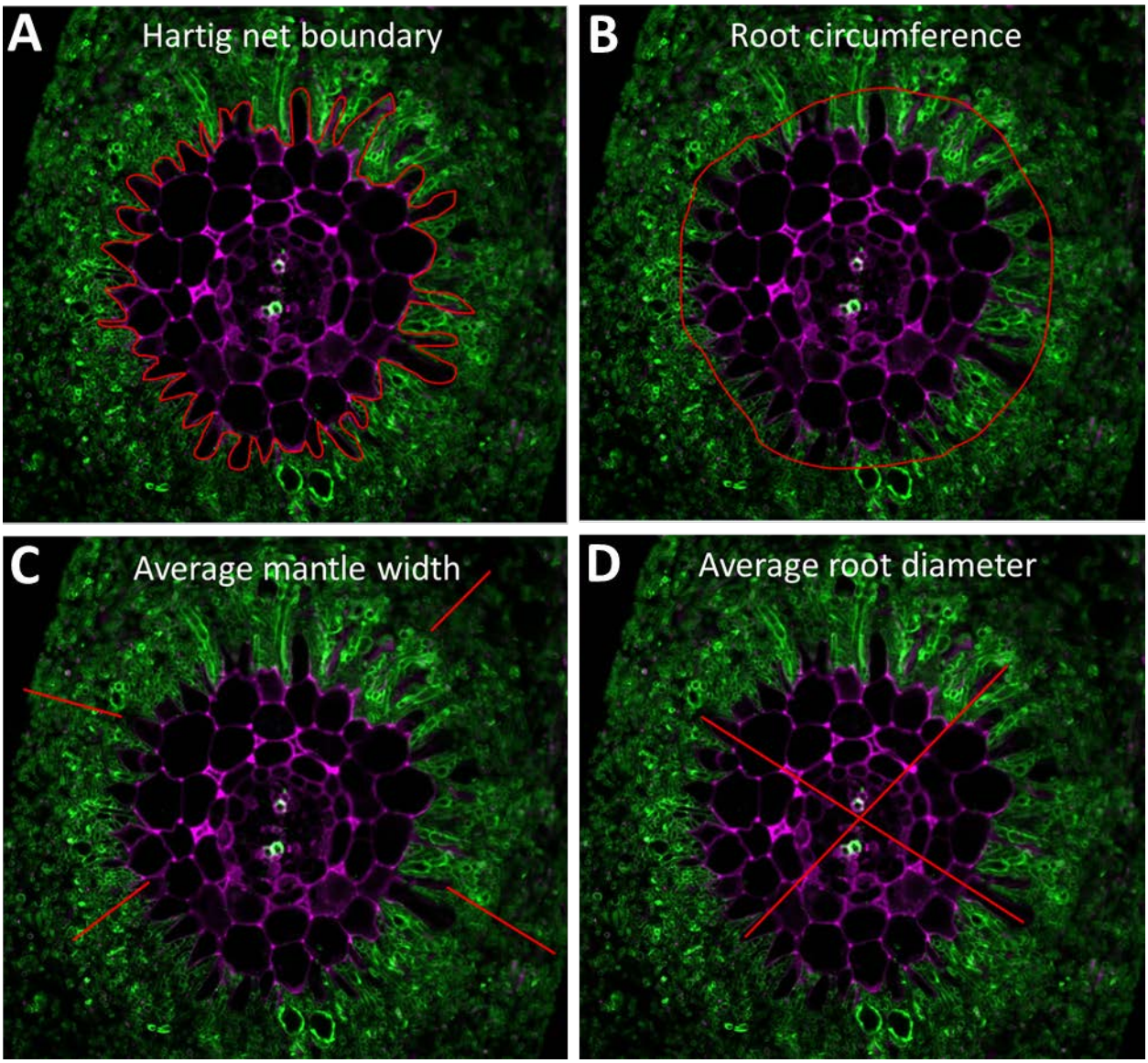

<u>Supplemental Figure 12</u> Example of the four measurements taken using ImageJ for all ECM root cross sections imaged with the confocal laser scanning microscope

(A) Hartig net boundary was measured by tracing the border between root epidermal cells and the fungal hyphae in direct contact with the epidermal cells. **(B)** Root circumference was measured by tracing the outer edge of every root epidermal cell around the entire root. **(C)** Average mantle width was obtained by measuring the width of the hyphal mat extending perpendicular to the root in four locations and calculating the average of all four measurements. **(D)** Average root diameter was obtained by measuring the width of the root in two locations from the outer edge of one epidermal cell to the outer edge of another epidermal cell directly across from it. Both lines intersected the middle of the root and the average of both measurements was calculated.

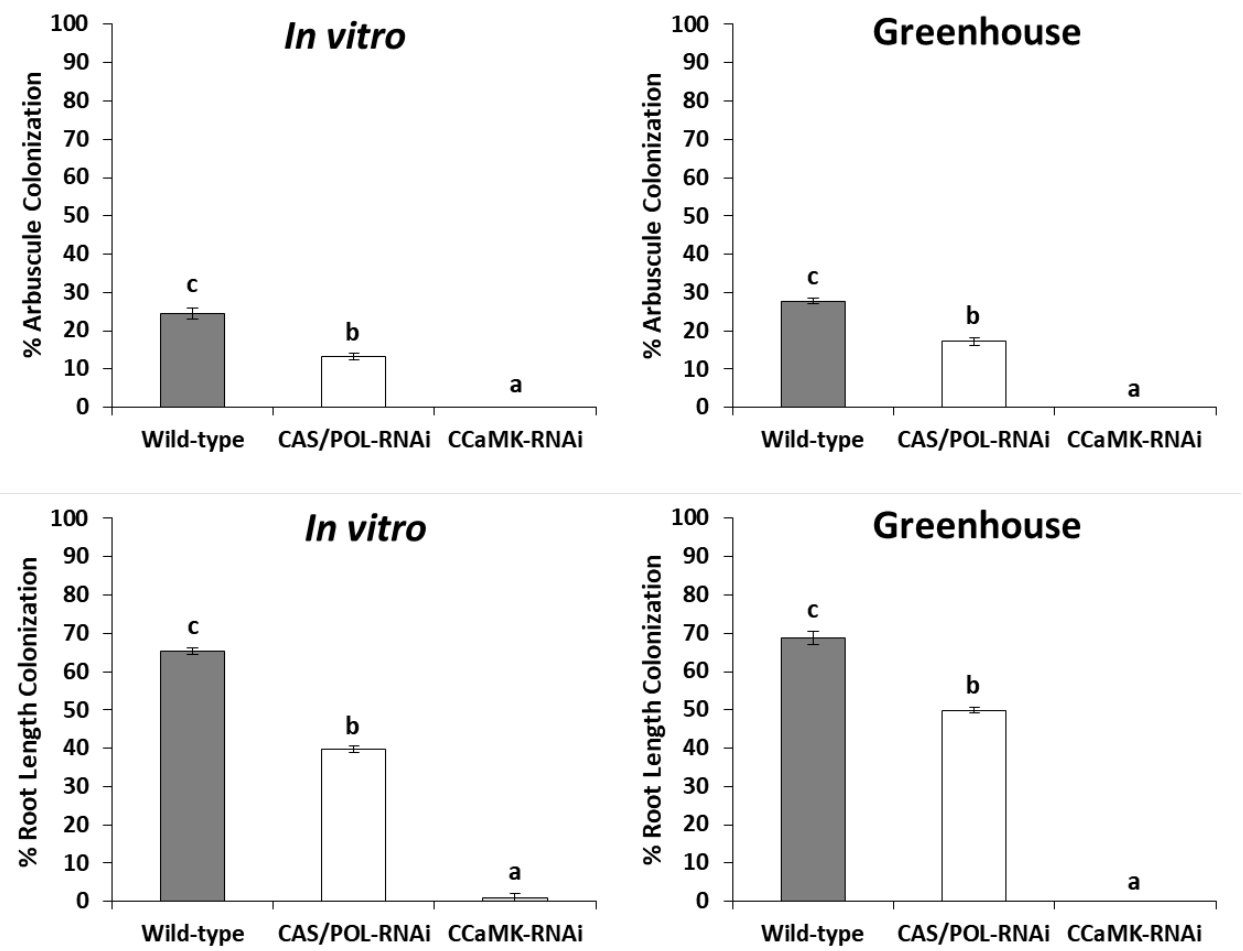

<u>Supplemental Figure 13</u> Arbuscular mycorrhizal–*Populus* colonization assays with wild-type, *CASTOR*/*POLLUX*-RNAi and *CCaMK*-RNAi lines

Summary of percent arbuscule colonization (***top***) and root length colonization (***bottom***) in both *in vitro* (***left***) and greenhouse (***right***) conditions for all three *Populus* lines (n=4). In all graphs, bars represent the mean of the data and error bars represent the standard error of the mean. The data were statistically analyzed by one-way ANOVA with Tukey pairwise comparison to assign significance groups (p-value < 0.05).

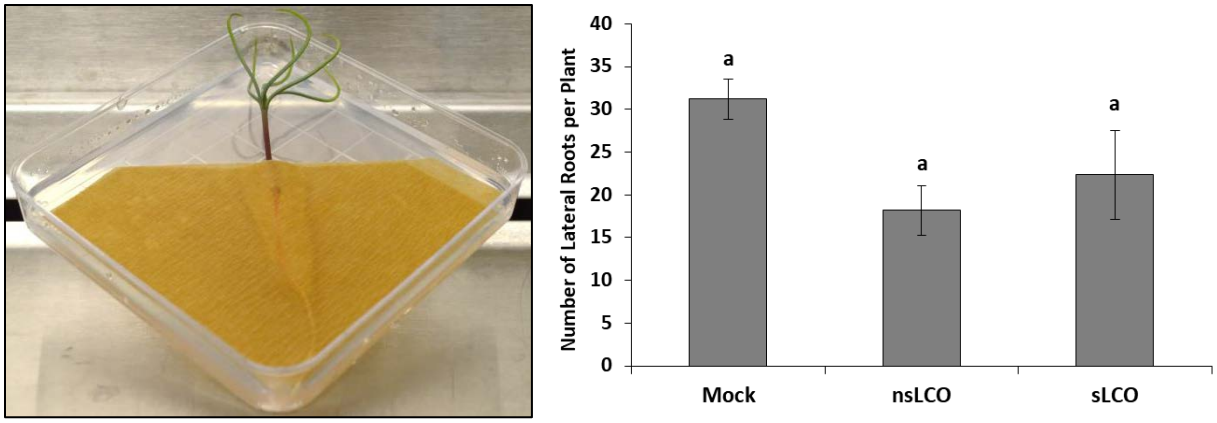

<u>Supplemental Figure 14</u> Effect of LCOs on lateral root development in *Pinus pinaster*
The roots of individual two-week-old pine seedlings were placed on moist germination paper on top of solid modified MMN medium in square Petri dishes (***left***). The roots were treated with a mock treatment (0.005% ethanol; n=5), non-sulfated (ns)LCOs (10^{-8} M; n=6), or sulfated (s)LCOs (10^{-8} M; n=6) and covered by another piece of moist germination paper. After incubating for three weeks, the number of lateral roots per plant was recorded (***right***). No significant difference was observed between treatments. Bars represent the mean of the data and error bars represent the standard error of the mean. The data were statistically analyzed by one-way ANOVA with Tukey pairwise comparison to assign significance groups (p-value < 0.05).

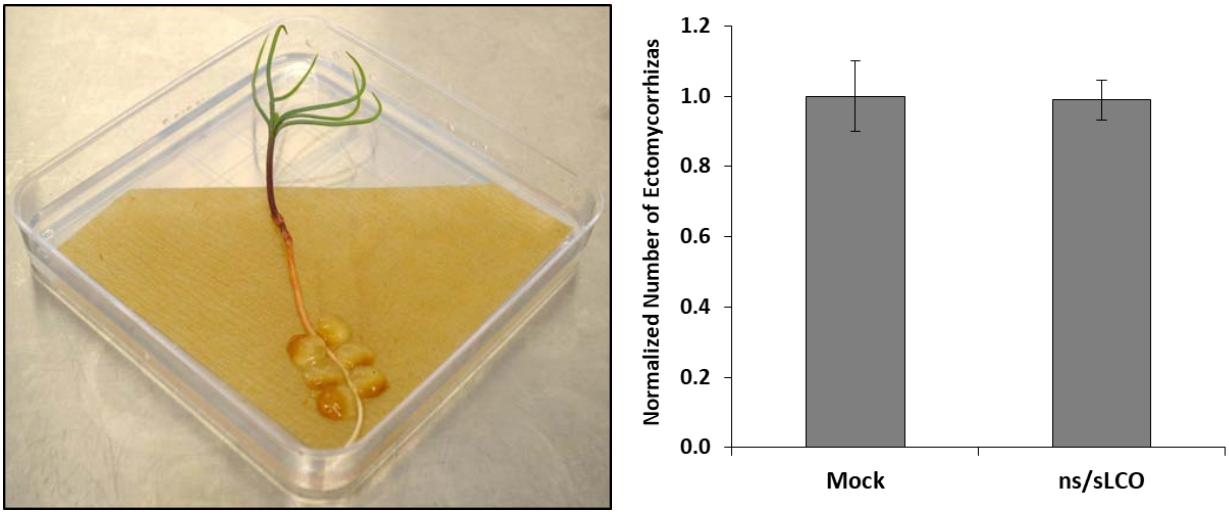

<u>Supplemental Figure 15</u> Effect of LCOs on ectomycorrhizal formation in *Pinus pinaster*
The roots of individual two-week-old pine seedlings were placed on moist germination paper on top of solid modified MMN medium in square Petri dishes. To produce ectomycorrhizas, six plugs of *Hebeloma cylindrosporum* were placed beside the primary root (***left***). The co-culture was treated with either a mock treatment (0.005% ethanol; n=11) or a 1:1 mixture of non-sulfated (ns) and sulfated (s)LCOs (10^{-8} M; n=11) and covered by another piece of moist germination paper. After incubating for three weeks, the number of ectomycorrhizae per plant was recorded (***right***). After completing two experiments replicated in time, the data were normalized and combined for statistical analysis using a Welch two-sample t-test. No significant difference was observed between treatments (p-value = 0.88). Bars represent the mean of the data and error bars represent the standard error of the mean.

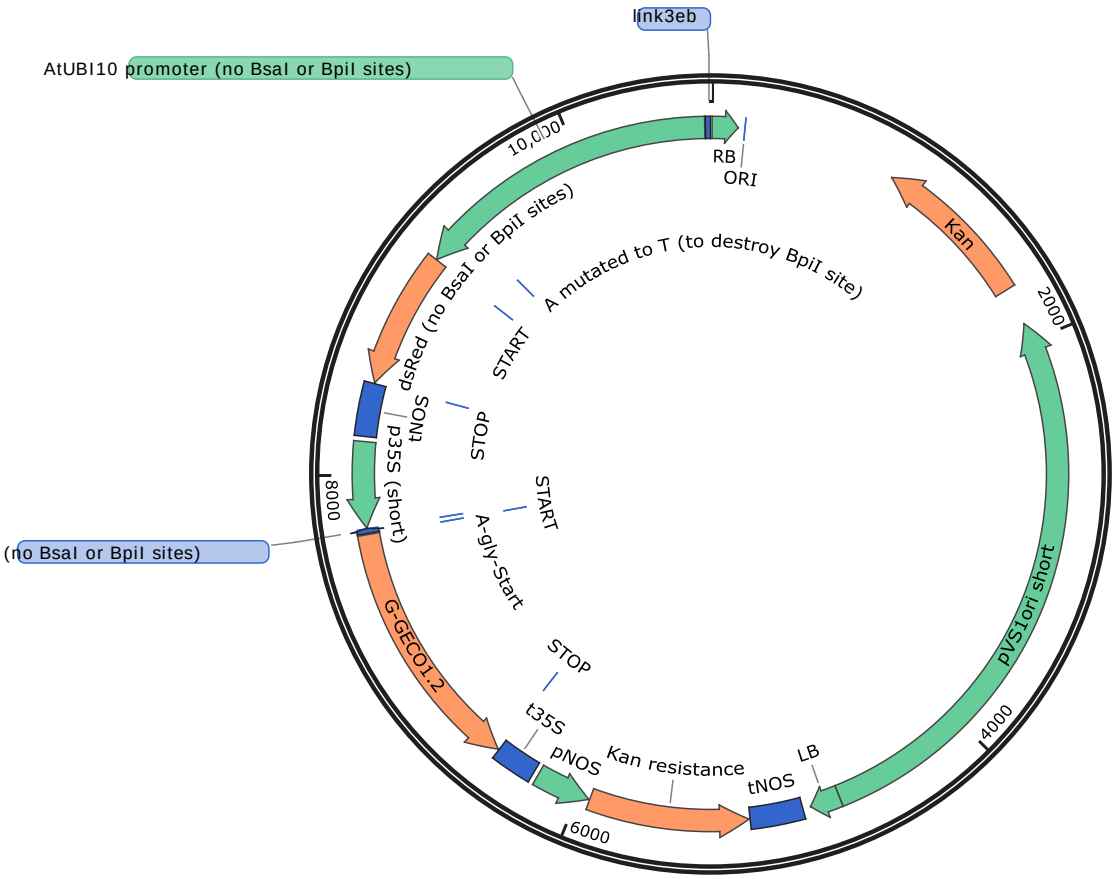

<u>Supplemental Figure 16</u> Vector map of the binary vector pEC11579 carrying the coding DNA sequence (CDS) for green-GECO and DsRed

The vector was originally assembled by Golden Gate cloning to contain the following: **1)** the CDS for DsRed with the *Arabidopsis thaliana* ubiquitin10 promoter and the *Agrobacterium tumefaciens* nopaline synthase (NOS) terminator; **2)** the CDS for green-GECO1.2 with the SV40 nuclear localization signal (NLS), the Cauliflower Mosaic Virus (CaMV) 35S promoter, and the CaMV 35S terminator; and **3)** the CDS for the kanamycin resistance gene with the NOS promoter and terminator.

3.8 Supplementary Tables

<u>Supplemental Table 1</u> Summary of lipochitooligosaccharides detected in the medium of 17 independent cultures of *Laccaria bicolor*.

					Culture Medium*															
	Functional Groups**				MPM										MP					
CO length	**R1**	**R2**	**R3, 4, 5**	**R6**	**A1**	**A2**	**A3**	**A4**	**A5-A6**	**A7**	**A8**	**A9**	**A10**	**B1C**	**B2C**	**B1**	**B1C**	**B2**	**B2C**	**B3**	**B4**
III	H	C18:1	H	Fuc												X					
III	Me	C16:0	Cb	H						X											
III	Me	C18:0	Cb	Fuc						X							X		X X X		X X X
III	Me	C18:1	Cb	H					X X X												
III	**Me**	**C18:1**	**Cb**	**Fuc**						**X X X**	**X**		**X X X**			**X X X**					
IV	H	C18:1	H	H			X														
IV	Me	C16:0	H	H			X														
IV	Me	C18:0	Cb	H	X X X														X X X		X X X
IV	**Me**	**C18:1**	**H**	**H**			**X X X**		**X X X**	**X X X**	**X X X**					**X X X**	**X X X**			**X X X**	
IV	Me	C18:1	Cb	H	X X X																
IV	Me	C18:1	Cb	Fuc					X												
V	H	C18:1	H	H							X										
V	Me	C16:0	Cb	Fuc							X										
V	Me	C18:0	Cb	H					X												
V	Me	C18:1	Cb	Fuc								X X X									

Based on relative frequency of detection within a sample, LCOs are designated as major (XXX) or minor (X). The most abundant LCOs are **bolded**.

***Culture Medium**: MP is complete MP medium (carbon sources = 1 g L^{-1} casein peptone, 5 g L^{-1} malt extract, 5 g L^{-1} glucose) and MPM is modified MP medium (carbon source = 2.5 g L^{-1} glucose).

****Functional Groups**: Me = methylated, Cb = carbomoylated, Fuc = fucosylated

Supplemental Table 2 RNA interference constructs used for knocking down the expression of *CASTORa/b*, *POLLUXa/b*, and *CCaMKa/b*

Target Gene	Size	Sequence
CASTORa/b	175 bp	ATGCAGGAGCTTGATGATATTGGTTATGGTAGTGATAACGGGTTAAAGAATTTGGCTTTGATTGTTTCAGTTACGCTATTGTCTATTCCGGTTCTTGCTTTCAAGTACATTGATTTTGTATCGAAATCCAGATCATCGGATAGTGTTTCGGAAGAGGCGTTGTTGAATAAGCAGC
POLLUXa/b	153 bp	ATGCTGACAGCAGAACTGTTGCTTTGTATACTGTGATGTTCACACTCGCCATACCTTTTTTGTTGTATAAATATCTTGATTATCTTCCCCAAATAAAGACTCTCTCAAAAAGAACAATGAATAACAAGGAGGAGGCTCCCCTGAAGAAGAGAG
CCaMK a/b	200 bp	TGGAAGAACATTACTTCATCAGCAAAACAACTGATCACTGATCTCCTGCAAGTTGATCCCGAAAGGAGACCGAGTGCTCAAGATGTTTTAAATCATCCTTGGGTGATAGGGGATTCTGCAAAAGAGGAACAAATGGACCCCGAGATTGTCTCAAGGCTGCAGAGTTTCAATGCCCGTCGCAAATTCCGAGCTGCAGCAAT

Supplemental Table 3 Primers used for PCR and qRT-PCR in This Study.

Primer Set Use	Forward Primer Sequence	Reverse Primer Sequence
pK7GWIWG2(II) RNAi fragment insertion site 1	5'-CAGATAAACATAACTCAGCACACCAG-3'	5'-CCACTATCCTTCGCAAGACCCTTCC-3'
pK7GWIWG2(II) RNAi fragment insertion site 2	5'-GGTTTCTTATATGCTCAACACATGAGCG-3'	5'-ATTCATATACCAGTTAACGTGTCTCA-3'
CASTOR RNAi fragment amplification	5'-CACCATGCAGGAGCTTGATGATATTGG-3'	5'-GCTGCTTATTCAACAACGCCTCT-3'
POLLUX RNAi fragment amplification	5'-CACCATGCTGACAGCAGAACTGTTGCT-3'	5'-CTCTCTTCTTCAGGGGAGCCTCC-3'
CCaMK RNAi fragment amplification	5'-CACCTGGAAGAACATTACTTCATC-3'	5'-ATTGCTGCAGCTCGGAATTTGC-3'
CASTOR qRT-PCR expression	5'-GTGGAGCTAAGTGATCTTGAC-3'	5'-CGTAGGTAATGCTGCTGGAG-3'
POLLUX qRT-PCR expression	5'-GACGTGACATTGATGACATG-3'	5'-GCATTTCACGGATCCATGAGC-3'
CCaMK qRT-PCR expression	5'-TCACTGATCTCCTGCAAGTTG-3'	5'-CGACGGGCATTAAAACTCTG-3'
PT12 qRT-PCR expression	5'-GGAAACCATGTGGGAGTGC-3'	5'-CTGGCCAGCTAAAGTTCCAC-3'
PutativeProtein qRT-PCR reference gene expression	5'-GCTGCACTTGCATCAAAAGA-3'	5'-GCAACTTGGCATGACTCTCA-3'
Ubiquitin qRT-PCR reference gene expression	5'-GCAGGGAAACAGTGAGGAAGG-3'	5'-TGGACTCACGAGGACAG-3'

3.9 Supplemental Movie Legends

Supplemental Movie 1 Wild-type *Populus* transformed with nuclear-localized G-GECO and treated with germinating spore exudates from the arbuscular mycorrhizal fungus *Rhizophagus irregularis.*

Supplemental Movie 2 Wild-type *Populus* transformed with nuclear-localized G-GECO and treated with non-sulfated lipochitooligosaccharides (10^{-7} M).

Supplemental Movie 3 Wild-type *Populus* transformed with nuclear-localized G-GECO and treated with sulfated lipochitooligosaccharides (10^{-7} M).

Supplemental Movie 4 Wild-type *Populus* transformed with nuclear-localized G-GECO and treated with four-chain chitin oligomer (10^{-6} M).

Supplemental Movie 5 Wild-type *Populus* transformed with nuclear-localized G-GECO and mock treated with water containing 0.005% ethanol.

Supplemental Movie 6 Wild-type *Populus* transformed with nuclear-localized G-GECO and treated with germinating spore exudates from the arbuscular mycorrhizal fungus *Rhizophagus irregularis.*

Supplemental Movie 7 *CASTOR*/*POLLUX*-RNAi *Populus* transformed with nuclear-localized G-GECO and treated with germinating spore exudates from the arbuscular mycorrhizal fungus *Rhizophagus irregularis.*

Supplemental Movie 8 Wild-type *Populus* transformed with nuclear-localized G-GECO and treated with hyphae from the ectomycorrhizal fungus *Laccaria bicolor.*

Supplemental Movie 9 Wild-type *Populus* transformed with nuclear-localized G-GECO and treated with germinating spore exudates from the arbuscular mycorrhizal fungus *Rhizophagus irregularis.*

Supplemental Movie 10 Wild-type *Populus* transformed with nuclear-localized G-GECO and mock treated with water.

Supplemental Movie 11 Wild-type *Populus* transformed with nuclear-localized G-GECO and treated with hyphae from the ectomycorrhizal fungus *Laccaria bicolor.*

Supplemental Movie 12 *CASTOR*/*POLLUX*-RNAi *Populus* transformed with nuclear-localized G-GECO and treated with hyphae from the ectomycorrhizal fungus *Laccaria bicolor.*

3.10 Additional Data

Diverse ectomycorrhizal fungi produce lipochitooligosaccharides

Root hair branching assays with common vetch (*Vicia sativa*) and the barrel medic (*Medicago truncatula*) were performed as described for *Laccaria bicolor* using hyphal exudates from three additional ECM fungal species: *Paxillus ammoniavirescens*, *P. involutus*, and *Hebeloma cylindrosporum* (all basidiomycetes). Similar to *L. bicolor*, all three of these ECM fungal species induced root hair branching in both *V. sativa* and *M. truncatula* (**Figure I**), suggesting that they produce both non-sulfated and sulfated LCOs, respectively. To confirm this assay, mass spectrometry was used to detect the presence of LCOs in the culture medium of *P. ammoniavirescens*, *P. involutus*, and *H. cylindrosporum* as described for for *L. bicolor*. Mass spectrometry also allowed for further characterization of the structure of the LCOs produced by these ECM fungi. Similar to *L. bicolor*, LCOs with C16:0, C18:0 and C18:1 lipid chains were

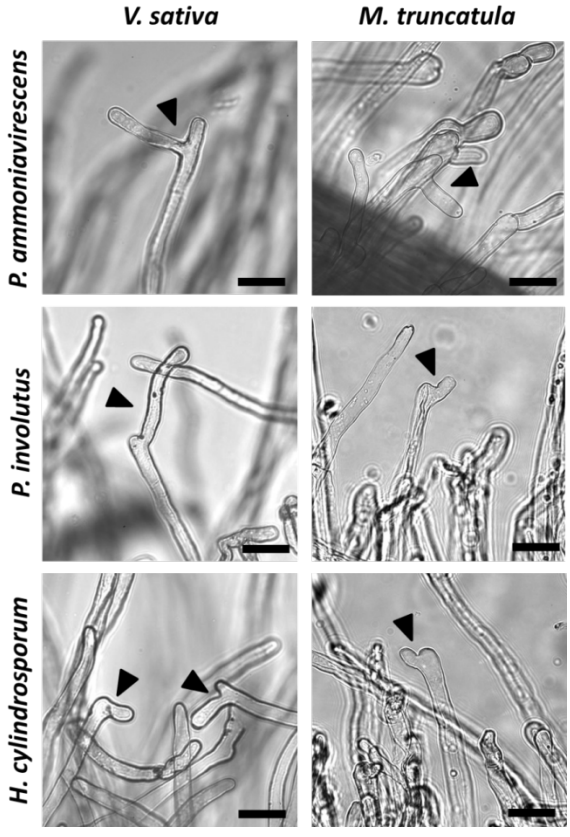

<u>Figure I</u> Root hair branching assays in two leguminous plant species in response to hyphal exudates from three ectomycorrhizal fungal species

Hyphal exudates from the ectomycorrhizal (ECM) fungi *Paxillus ammoniavirescens*, *P. involutus*, and *Hebeloma cylindrosporum* were applied onto root hairs from the primary roots of two leguminous plant species: *Vicia sativa* (***left***) and *Medicago truncatula* (***right***). Root hair branching was observed on both plant species in response to all three ECM hyphal exudates suggesting that all three fungal species produce non-sulfated and sulfated lipo-chitooligosaccharides. Black arrows indicate branched root hairs. Scale bars = 50 µm.

Table I Variation in lipid chain length and type on lipochitooligosaccharides produced by different fungi

		Lipid Chain*			
Fungal Species	**Type**	**C16:0**	**C18:0**	**C18:1**	**C20:1**
Hebeloma cylindrosporum	ECM	+	+	+	+
Laccaria bicolor	ECM	+	+	+	-
Paxillus ammoniavirescens	ECM	+	+	+	-
Paxillus involutus	ECM	+	+	+	-
Rhizophagus irregularis	AM	+	+	+	+

**The lipid chains found on the terminal end of these fungal LCOs were identified using MS/HPLC; (+) indicates the presence and (-) indicates the absence of specified lipid chains.*

detected in the culture medium of all three ECM fungal species; however, similar to the AM fungus *R. irregularis*, LCOs with C20:1 lipid chains were only detected in the culture medium of *H. cylindrosporum* (**Table I**). Regarding chemical substitutions on the LCOs produced by these ECM fungi, none were acetylated, two were fucosylated, one methyl fucosylated, two N-methylated, and all four both N-methyl carbamoylated and sulfated, or not (**Table II**).

Multiple species of ectomycorrhizal fungi can induce calcium spiking in Populus

Given that *L. bicolor* hyphae were able to induce Ca^{+2} spiking in *Populus*, it seemed possible that other fungal species that produce LCOs could trigger spiking as well. To test this

Table II Variation in chemical substitutions on lipochitooligosaccharides produced by different fungi

		Chemical Substitution*						
Fungal Species	**Type**	**Ace**	**Fuc**	**MeFuc**	**NMe**	**NMe-Cb**	**NS**	**S**
Hebeloma cylindrosporum	ECM	-	-	-	+	+	+	+
Laccaria bicolor	ECM	-	+	-	+	+	+	+
Paxillus ammoniavirescens	ECM	-	-	+	-	+	+	+
Paxillus involutus	ECM	-	+	-	-	+	+	+
Rhizophagus irregularis	AM	-	+	+	-	-	+	+
Saccharomyces cerevisiae	Yeast	-	-	-	-	-	-	-

**The chemical substitutions found on these fungal LCOs were identified using MS/HPLC; (+) indicates the presence and (-) indicates the absence of chemical substitutions. Acronyms are denoted as acetylated (Ac), fucosylated (Fuc), methyl fucosylated (MeFuc), N-methylated (NMe), N-methyl carbamoylated (NMe-Cb), non-sulfated (NS), and sulfated (S).*

hypothesis, fungal hyphae from *P. ammoniavirescens* and *H. cylindrosporum* were prepared as described in Chapter 3 for *L. bicolor*. The hyphae from both species were then applied onto lateral roots from wild-type *Populus* transformed with G-GECO and imaged under a confocal microscope as described in Chapter 3 for the Ca^{2+} spiking assays. *L. bicolor* was used as a positive control and mock treatment as a negative control. Both *P. ammoniavirescens* and *H. cylindrosporum* induced Ca^{2+} spiking (**Figure IIA**). The ratio of spiking nuclei and the average spiking frequency across all nuclei observed were calculated for both treatments. Compared to *L. bicolor*, the ratio of spiking nuclei was the same for *H. cylindrosporum* but less for *P. ammoniavirescens* (p-value < 0.05). However, spiking frequency was lower for both *H. cylindrosporum* and *P. ammoniavirescens* (p-value < 0.05; **Figure IIB**). These data show that *Populus* is more responsive to *L. bicolor* than to the other ECM fungi.

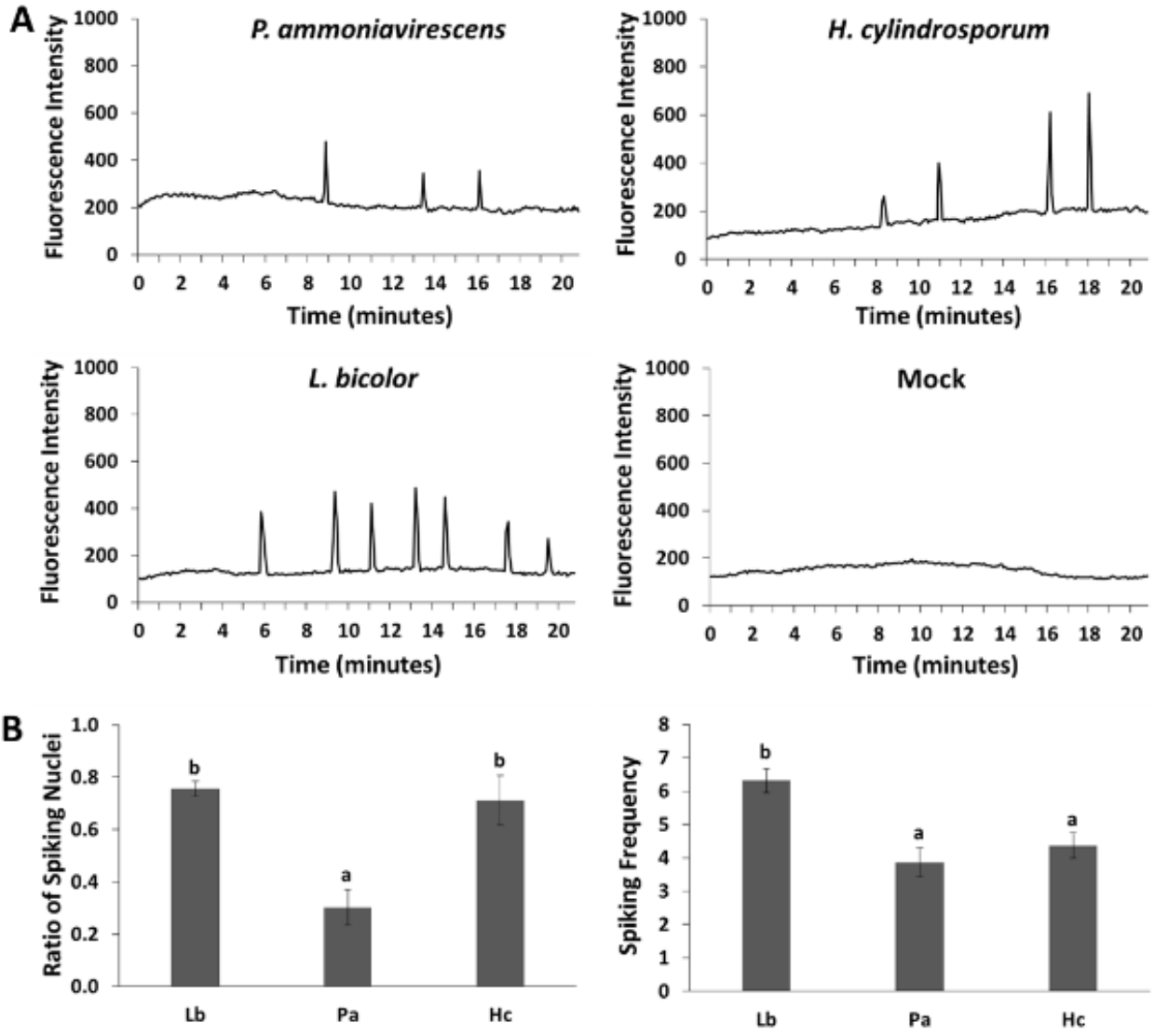

<u>Figure II</u> Ca^{2+} spiking data in *Populus* in response to ectomycorrhizal fungal hyphae
(A) Representative plots of Ca^{2+} spiking in response to ectomycorrhizal (ECM) fungal hyphae from *Paxillus ammoniavirescens* and *Hebeloma cylindrosporum*. Ca^{2+} spiking in response to *Laccaria bicolor* is shown as a positive control and the lack of Ca^{2+} spiking in response to mock treatment (water) is shown as a negative control. **(B)** Summary of Ca^{2+} spiking data. The ratio of spiking nuclei (***right***) in roots treated with *P. ammoniavirescens* (Pa, n=3) was lower than for roots treated with either *H. cylindrosporum* (Hc, n=3) or *L. bicolor* (Lb, n=4; p-value < 0.05). The average spiking frequency (***left***) across nuclei was lower in response to both Pa (n=21) and Hc (n=68) compared to Lb (n=90; p-value < 0.05). For both graphs, bars represent the mean of the data and error bars represent the standard error of the mean. The data were statistically analyzed by one-way ANOVA with Tukey pairwise comparison to assign significance groups (p-value < 0.05).

3.11 References

Akiyama, K. and Hayashi, H. (2006). Strigolactones: Chemical signals for fungal symbionts and parasitic weeds in plant roots. Handb. Environ. Chem. Vol. 5 Water Pollut. **97**: 925–931.

Akiyama, K., Matsuzaki, K., and Hayashi, H. (2005). Plant sesquiterpenes induce hyphal branching in arbuscular mycorrhizal fungi. Nature **435**: 824–827.

Ané, J.-M. et al. (2004). Medicago truncatula DMI1 required for bacterial and fungal symbioses in legumes. Science **303**: 1364–1367.

Ardourel, M., Lortet, G., Maillet, F., Roche, P., Truchet, G., Promé, J. -C, and Rosenberg, C. (1995). In Rhizobium meliloti, the operon associated with the nod box n5 comprises nodL, noeA and noeB, three host-range genes specifically required for the nodulation of particular Medicago species. Mol. Microbiol. **17**: 687–699.

Balestrini, R. and Bonfante, P. (2014). Cell wall remodeling in mycorrhizal symbiosis: a way towards biotrophism. Front. Plant Sci. **5**: 237.

Berbee, M.L. and Taylor, J.W. (1993). Dating the evolutionary radiations of the true fungi. Can. J. Bot. **71**: 1114–1127.

Besserer, A., Bécard, G., Jauneau, A., Roux, C., and Séjalon-Delmas, N. (2008). GR24, a synthetic analog of strigolactones, stimulates the mitosis and growth of the arbuscular mycorrhizal fungus Gigaspora rosea by boosting its energy metabolism. Plant Physiol. **148**: 402–413.

Besserer, A., Puech-Pagès, V., Kiefer, P., Gomez-Roldan, V., Jauneau, A., Roy, S., Portais, J.C., Roux, C., Bécard, G., and Séjalon-Delmas, N. (2006). Strigolactones stimulate arbuscular mycorrhizal fungi by activating mitochondria. PLoS Biol. **4**: 1239–1247.

Bhuvaneswari, T. V. and Solheim, B. (1985). Root hair deformation in the white clover/Rhizobium trifolii symbiosis. Physiol. Plant. **63**: 25–34.

Bonfante, P. and Genre, A. (2010). Mechanisms underlying beneficial plant-fungus interactions in mycorrhizal symbiosis. Nat. Commun. **1**: 48.

Bravo, A., York, T., Pumplin, N., Mueller, L.A., and Harrison, M.J. (2016). Genes conserved for arbuscular mycorrhizal symbiosis identified through phylogenomics. Nat. Plants **2**: 15208.

Brundrett, M.C. (2002). Coevolution of roots and mycorrhizas of land plants. New Phytol. **154**: 275–304.

Brundrett, M.C. and Tedersoo, L. (2018). Evolutionary history of mycorrhizal symbioses and global host plant diversity. New Phytol.

Capoen, W., Sun, J., Wysham, D., Otegui, M.S., Venkateshwaran, M., Hirsch, S., Miwa, H., Downie, J.A., Morris, R.J., Ané, J.-M., and Oldroyd, G.E.D. (2011). Nuclear membranes control symbiotic calcium signaling of legumes. Proc. Natl. Acad. Sci. U. S. A. **108**: 14348–14353.

Casieri, L. et al. (2013). Biotrophic transportome in mutualistic plant-fungal interactions. Mycorrhiza **23**: 597–625.

Charpentier, M., Bredemeier, R., Wanner, G., Takeda, N., Schleiff, E., and Parniske, M. (2008). Lotus japonicus CASTOR and POLLUX are ion channels essential for perinuclear calcium spiking in legume root endosymbiosis. Plant Cell **20**: 3467–3479.

Charpentier, M., Sun, J., Vaz Martins, T., Radhakrishnan, G. V, Findlay, K., Soumpourou, E., Thouin, J., Véry, A.-A., Sanders, D., Morris, R.J., and Oldroyd, G.E.D. (2016). Nuclear-localized cyclic nucleotide-gated channels mediate symbiotic calcium oscillations. Science **352**: 1102–5.

Chen, C., Fan, C., Gao, M., and Zhu, H. (2009). Antiquity and Function of CASTOR and POLLUX, the Twin Ion Channel-Encoding Genes Key to the Evolution of Root Symbioses in Plants. PLANT Physiol. **149**: 306–317.

Dauphin, a, Gérard, J., Lapeyrie, F., and Legué, V. (2007). Fungal hypaphorine reduces growth and induces cytosolic calcium increase in root hairs of Eucalyptus globulus. Protoplasma **231**: 83–8.

Delaux, P.M., Séjalon-Delmas, N., Bécard, G., and Ané, J.M. (2013). Evolution of the plant-microbe symbiotic "toolkit." Trends Plant Sci. **18**: 298–304.

Delaux, P.M., Varala, K., Edger, P.P., Coruzzi, G.M., Pires, J.C., and Ané, J.M. (2014). Comparative Phylogenomics Uncovers the Impact of Symbiotic Associations on Host Genome Evolution. PLoS Genet. **10**.

Ditengou, F. a, Béguiristain, T., and Lapeyrie, F. (2000). Root hair elongation is inhibited by hypaphorine, the indole alkaloid from the ectomycorrhizal fungus Pisolithus tinctorius, and restored by indole-3-acetic acid. Planta **211**: 722–728.

Ehrhardt, D.W., Wais, R., and Long, S.R. (1996). Calcium spiking in plant root hairs responding to rhizobium modulation signals. Cell **85**: 673–681.

FÅHRAEUS, G.G. (1957). The Infection of Clover Root Hairs by Nodule Bacteria Studied by a Simple Glass Slide Technique. Microbiology **16**: 374–381.

Feijen, F.A.A., Vos, R.A., Nuytinck, J., and Merckx, V.S.F.T. (2018). Evolutionary dynamics of mycorrhizal symbiosis in land plant diversification. Sci. Rep. **8**: 10698.

Felten, J., Kohler, A., Morin, E., Bhalerao, R.P., Palme, K., Martin, F., Ditengou, F.A., and Legue, V. (2009). The Ectomycorrhizal Fungus Laccaria bicolor Stimulates Lateral Root Formation in Poplar and Arabidopsis through Auxin Transport and Signaling. PLANT

Physiol. **151**: 1991–2005.

Felten, J., Legué, V., Anicet Ditengou, F., and Ditengou, F.A. (2010). Lateral root stimulation in the early interaction between Arabidopsis thaliana and the ectomycorrhizal fungus Laccaria bicolor: Is fungal auxin the trigger? Plant Signal. Behav. **5**: 864–867.

Filichkin, S.A., Meilan, R., Busov, V.B., Ma, C., Brunner, A.M., and Strauss, S.H. (2006). Alcohol-inducible gene expression in transgenic Populus. Plant Cell Rep. **25**: 660–667.

Fusconi, A. (2014). Regulation of root morphogenesis in arbuscular mycorrhizae: What role do fungal exudates, phosphate, sugars and hormones play in lateral root formation? Ann. Bot. **113**: 19–33.

Garcia, K., Chasman, D., Roy, S., and Ané, J.-M. (2017). Physiological Responses and Gene Co-Expression Network of Mycorrhizal Roots under K + Deprivation. Plant Physiol. **173**: 1811–1823.

Garcia, K., Delaux, P.M., Cope, K.R., An, J., and Ané, J.M. (2015). Molecular signals required for the establishment and maintenance of ectomycorrhizal symbioses. New Phytol. **208**: 79–87.

Garcia, K., Doidy, J., Zimmermann, S.D., Wipf, D., and Courty, P.E. (2016). Take a Trip Through the Plant and Fungal Transportome of Mycorrhiza. Trends Plant Sci. **21**: 937–950.

Garcia, K. and Zimmermann, S.D. (2014). The role of mycorrhizal associations in plant potassium nutrition. Front. Plant Sci. **5**: 1–9.

GAY, G., NORMAND, L., MARMEISSE, R., SOTTA, B., and DEBAUD, J.C. (1994). Auxin overproducer mutants of Hebeloma cylindrosporum Romagnesi have increased mycorrhizal activity. New Phytol. **128**: 645–657.

Genre, A., Chabaud, M., Balzergue, C., Puech-Pagès, V., Novero, M., Rey, T., Fournier, J., Rochange, S., Bécard, G., Bonfante, P., and Barker, D.G. (2013). Short-chain chitin oligomers from arbuscular mycorrhizal fungi trigger nuclear Ca2+ spiking in Medicago truncatula roots and their production is enhanced by strigolactone. New Phytol. **198**: 190–202.

Glassop, D., Smith, S.E., and Smith, F.W. (2005). Cereal phosphate transporters associated with the mycorrhizal pathway of phosphate uptake into roots. Planta **222**: 688–698.

Gomez-Roldan, V. et al. (2008). Strigolactone inhibition of shoot branching. Nature **455**: 189–194.

Groten, K., Pahari, N.T., Xu, S., Van Doorn, M.M., Baldwin, I.T., Miloradovic van Doorn, M., and Baldwin, I.T. (2015). Virus-Induced Gene Silencing Using Tobacco Rattle Virus as a Tool to Study the Interaction between Nicotiana attenuata and Rhizophagus irregularis. PLoS One **10**: e0136234.

Gutjahr, C., Casieri, L., and Paszkowski, U. (2009). Glomus intraradices induces changes in root system architecture of rice independently of common symbiosis signaling. New Phytol. **182**: 829–837.

Gutjahr, C. and Paszkowski, U. (2013). Multiple control levels of root system remodeling in arbuscular mycorrhizal symbiosis. Front. Plant Sci. **4**: 204.

Harrison, M.J., Dewbre, G.R., and Liu, J. (2002). A phosphate transporter from Medicago truncatula involved in the acquisition of phosphate released by arbuscular mycorrhizal fungi. Plant Cell **14**: 2413–29.

Heckman, D.S., Geiser, D.M., Eidell, B.R., Stauffer, R.L., Kardos, N.L., and Hedges, S.B. (2001). Molecular evidence for the early colonization of land by fungi and plants. Science (80-.). **293**: 1129–1133.

Heidstra, R., Geurts, R., Franssen, H., Spaink, H.P., van Kammen, a., and Bisseling, T. (1994). Root Hair Deformation Activity of Nodulation Factors and Their Fate on Vicia sativa. Plant Physiol. **105**: 787–797.

van der Heijden, M.G.A., Martin, F.M., Selosse, M.-A., and Sanders, I.R. (2015). Mycorrhizal ecology and evolution: the past, the present, and the future. New Phytol. **205**: 1406–1423.

Hibbett, D.S. and Matheny, P.B. (2009). The relative ages of ectomycorrhizal mushrooms and their plant hosts estimated using Bayesian relaxed molecular clock analyses. BMC Biol. **7**: 13.

Hoeksema, J.D. et al. (2018). Evolutionary history of plant hosts and fungal symbionts predicts the strength of mycorrhizal mutualism. Commun. Biol. **1**: 116.

Horváth, B. et al. (2011). Medicago truncatula IPD3 Is a Member of the Common Symbiotic Signaling Pathway Required for Rhizobial and Mycorrhizal Symbioses. **24**: 1345–1358.

Ivanchenko, M.G., Muday, G.K., and Dubrovsky, J.G. (2008). Ethylene-auxin interactions regulate lateral root initiation and emergence in Arabidopsis thaliana. Plant J. **55**: 335–347.

Jargeat, P., Chaumeton, J.P., Navaud, O., Vizzini, A., and Gryta, H. (2014). The Paxillus involutus (Boletales, Paxillaceae) complex in Europe: Genetic diversity and morphological description of the new species Paxillus cuprinus, typification of P. involutus s.s., and synthesis of species boundaries. Fungal Biol. **118**: 12–31.

Javot, H., Penmetsa, R.V., Terzaghi, N., Cook, D.R., and Harrison, M.J. (2007). A Medicago truncatula phosphate transporter indispensable for the arbuscular mycorrhizal symbiosis. Proc. Natl. Acad. Sci. **104**: 1720–1725.

Jeffries, P., Gianinazzi, S., Perotto, S., Turnau, K., and Barea, J.M. (2003). The contribution of arbuscular mycorrhizal fungi in sustainable maintenance of plant health and soil fertility. Biol. Fertil. Soils **37**: 1–16.

Kamel, L., Keller-Pearson, M., Roux, C., and Anï¿½, J.M. (2017). Biology and evolution of arbuscular mycorrhizal symbiosis in the light of genomics. New Phytol. **213**: 531–536.

Karabaghli-Degron, C., Sotta, B., Bonnet, M., and Gay, G. (1998). The auxin transport inhibitor 2,3,5-triiodobenzoic acid (TIBA) inhibits the stimulation of in vitro lateral root formation and the colonization of the tap-root cortex of Norway spruce (Picea abies) seedlings by the ectomycorrhizal fungus Laccaria bicolor. New Phytol. **140**: 723–733.

Karandashov, V., Nagy, R., Wegmüller, S., Amrhein, N., and Bucher, M. (2004). Evolutionary conservation of a phosphate transporter in the arbuscular mycorrhizal symbiosis. Proc. Natl. Acad. Sci. U. S. A. **101**: 6285–6290.

Kelner, A., Leitão, N., Chabaud, M., Charpentier, M., and de Carvalho-Niebel, F. (2018). Dual Color Sensors for Simultaneous Analysis of Calcium Signal Dynamics in the Nuclear and Cytoplasmic Compartments of Plant Cells. Front. Plant Sci. **9**: 245.

Kevei, Z. et al. (2007). 3-Hydroxy-3-Methylglutaryl Coenzyme A Reductase1 Interacts with NORK and Is Crucial for Nodulation in Medicago truncatula. PLANT CELL ONLINE **19**: 3974–3989.

Kohler, A. et al. (2015). Convergent losses of decay mechanisms and rapid turnover of symbiosis genes in mycorrhizal mutualists. Nat. Publ. Gr. **47**: 410–415.

Krebs, M., Held, K., Binder, A., Hashimoto, K., Den Herder, G., Parniske, M., Kudla, J., and Schumacher, K. (2012). FRET-based genetically encoded sensors allow high-resolution live cell imaging of Ca2+ dynamics. Plant J. **69**: 181–192.

Kretzschmar, T., Kohlen, W., Sasse, J., Borghi, L., Schlegel, M., Bachelier, J.B., Reinhardt, D., Bours, R., Bouwmeester, H.J., and Martinoia, E. (2012). A petunia ABC protein controls strigolactone-dependent symbiotic signalling and branching. Nature **483**: 341–344.

Lagrange, H., Jay-Allgmand, C., and Lapeyrie, F. (2001). Rutin, the phenolglycoside from eucalyptus root exudates, stimulates Pisolithus hyphal growth at picomolar concentrations. New Phytol. **149**: 349–355.

Lepage, B.A., Currah, R.S., Stockey, R.A., and Rothwell, G.W. (1997). Fossil ectomycorrhizae from the middle Eocene. Am. J. Bot. **84**: 410–412.

Lerouge, P., Roche, P., Faucher, C., Maillet, F., Truchet, G., Promé, J.C., and Dénarié, J. (1990). Symbiotic host-specificity of Rhizobium meliloti is determined by a sulphated and acylated glucosamine oligosaccharide signal. Nature **344**: 781–784.

Lévy, J. et al. (2004). A Putative Ca 2 and Calmodulin- Dependent Protein Kinase Required. Science **303**: 1361–4.

Loth-Pereda, V., Orsini, E., Courty, P.-E., Lota, F., Kohler, A., Diss, L., Blaudez, D., Chalot, M., Nehls, U., Bucher, M., and Martin, F. (2011). Structure and Expression Profile of the Phosphate Pht1 Transporter Gene Family in Mycorrhizal Populus trichocarpa.

Plant Physiol. **156**: 2141–2154.

Luginbuehl, L.H. and Oldroyd, G.E.D. (2017). Understanding the Arbuscule at the Heart of Endomycorrhizal Symbioses in Plants. Curr. Biol. **27**: R952–R963.

MacLean, A.M., Bravo, A., and Harrison, M.J. (2017). Plant signaling and metabolic pathways enabling arbuscular mycorrhizal symbiosis. Plant Cell: tpc.00555.2017.

Maeda, D., Ashida, K., Iguchi, K., Chechetka, S.A., Hijikata, A., Okusako, Y., Deguchi, Y., Izui, K., and Hata, S. (2006). Knockdown of an arbuscular mycorrhiza-inducible phosphate transporter gene of Lotus japonicus suppresses mutualistic symbiosis. Plant Cell Physiol. **47**: 807–817.

Maillet, F. et al. (2011). Fungal lipochitooligosaccharide symbiotic signals in arbuscular mycorrhiza. Nature **469**: 58–64.

Marschner, P. and Rengel, Z. (2011). Nutrient Availability in Soils (Elsevier Ltd).

Martin, F., Kohler, A., Murat, C., Veneault-Fourrey, C., and Hibbett, D.S. (2016). Unearthing the roots of ectomycorrhizal symbioses. Nat. Rev. Microbiol. **14**: 760–773.

Martin, F.M., Uroz, S., and Barker, D.G. (2017). Ancestral alliances: Plant mutualistic symbioses with fungi and bacteria. Science (80-.). **356**: eaad4501.

Messinese, E., Mun, J.-H., Yeun, L.H., Jayaraman, D., Rougé, P., Barre, A., Lougnon, G., Schornack, S., Bono, J.-J., Cook, D.R., and Ané, J.-M. (2007). A Novel Nuclear Protein Interacts With the Symbiotic DMI3 Calcium- and Calmodulin-Dependent Protein Kinase of Medicago truncatula. Mol. Plant-Microbe Interact. **20**: 912–921.

Miyata, K. et al. (2014). The Bifunctional Plant Receptor, OsCERK1, Regulates Both Chitin-Triggered Immunity and Arbuscular Mycorrhizal Symbiosis in Rice. Plant Cell Physiol. **55**: 1864–1872.

Morandi, D., Prado, E., Sagan, M., and Duc, G. (2005). Characterisation of new symbiotic Medicago truncatula (Gaertn.) mutants, and phenotypic or genotypic complementary information on previously described mutants. Mycorrhiza **15**: 283–289.

Mukherjee, A. and Ané, J.-M. (2011). Germinating spore exudates from arbuscular mycorrhizal fungi: molecular and developmental responses in plants and their regulation by ethylene. Mol. Plant. Microbe. Interact. **24**: 260–270.

Müller, A., Volmer, K., Mishra-Knyrim, M., and Polle, A. (2013). Growing poplars for research with and without mycorrhizas. Front. Plant Sci. **4**: 332.

Negi, S., Sukumar, P., Liu, X., Cohen, J.D., and Muday, G.K. (2010). Genetic dissection of the role of ethylene in regulating auxin-dependent lateral and adventitious root formation in tomato. Plant J. **61**: 3–15.

Oláh, B., Brière, C., Bécard, G., Dénarié, J., and Gough, C. (2005). Nod factors and a diffusible factor from arbuscular mycorrhizal fungi stimulate lateral root formation in Medicago truncatula via the DMI1/DMI2 signalling pathway. Plant J. **44**: 195–207.

Op den Camp, R., Streng, A., De Mita, S., Cao, Q., Polone, E., Liu, W., Ammiraju, J.S.S., Kudrna, D., Wing, R., Untergasser, A., Bisseling, T., and Geurts, R. (2011). LysM-type mycorrhizal receptor recruited for rhizobium symbiosis in nonlegume Parasponia. Science **331**: 909–912.

Paszkowski, U., Kroken, S., Roux, C., and Briggs, S.P. (2002). Rice phosphate transporters include an evolutionarily divergent gene specifically activated in arbuscular mycorrhizal symbiosis. Proc. Natl. Acad. Sci. **99**: 13324–13329.

Peiter, E. et al. (2007). The Medicago truncatula DMI1 protein modulates cytosolic calcium signaling. Plant Physiol. **145**: 192–203.

Pellegrin, C., Daguerre, Y., Ruytinx, J., Guinet, F., Kemppainen, M., Plourde, M.B., Hecker, A., Morin, E., Pardo, A.G., Germain, H., Martin, F.M., and Veneault-Fourrey, C. (2017). Laccaria bicolor MiSSP8 is a small-secreted protein decisive for the establishment of the ectomycorrhizal symbiosis. bioRxiv: 218131.

Plett, J.M. et al. (2017). Populus trichocarpa encodes small, effector-like secreted proteins that are highly induced during mutualistic symbiosis. Sci. Rep. **7**: 382.

Plett, J.M., Daguerre, Y., Wittulsky, S., Vayssières, A., Deveau, A., Melton, S.J., Kohler, A., Morrell-Falvey, J.L., Brun, A., Veneault-Fourrey, C., and Martin, F. (2014). Effector MiSSP7 of the mutualistic fungus Laccaria bicolor stabilizes the Populus JAZ6 protein and represses jasmonic acid (JA) responsive genes. Proc. Natl. Acad. Sci. U. S. A. **111**: 8299–304.

Plett, J.M., Kemppainen, M., Kale, S.D., Kohler, A., Legué, V., Brun, A., Tyler, B.M., Pardo, A.G., and Martin, F. (2011). A secreted effector protein of laccaria bicolor is required for symbiosis development. Curr. Biol. **21**: 1197–1203.

Plett, J.M. and Martin, F. (2012). Poplar Root Exudates Contain Compounds that Induce the Expression of MiSSP7 in Laccaria bicolor. Plant Signal. Behav. **7**: 12–15.

Plett, J.M., Tisserant, E., Brun, A., Morin, E., Grigoriev, I. V, Kuo, A., Martin, F., and Kohler, A. (2015). The Mutualist Laccaria bicolor Expresses a Core Gene Regulon During the Colonization of Diverse Host Plants and a Variable Regulon to Counteract Host-Specific Defenses. Mol. Plant-Microbe Interact. **28**: 261–273.

Poinsot, V., Crook, M.B., Erdn, S., Maillet, F., Bascaules, A., and Ané, J.M. (2016). New insights into Nod factor biosynthesis: Analyses of chitooligomers and lipo-chitooligomers of Rhizobium sp. IRBG74 mutants. Carbohydr. Res. **434**: 83–93.

Price, N.P.J., RelicA, B., Talmont, F., Lewin, A., Promé, D., Pueppke, S.G., Maillet, F., Dénarié, J., Promé, J. -C, and Broughton, W.J. (1992). Broad-host-range Rhizobium

species strain NGR234 secretes a family of carbamoylated, and fucosylated, nodulation signals that are O-acetylated or sulphated. Mol. Microbiol. **6**: 3575–3584.

Rausch, C., Daram, P., Brunner, S., Jansa, J., Laloi, M., Leggewie, G., Amrhein, N., and Bucher, M. (2001). A phosphate transporter expressed in arbuscule-containing cells in potato. Nature **414**: 462–466.

Redecker, D., Kodner, R., and Graham, L.E. (2000). Glomalean fungi from the Ordovician. Science **289**: 1920–1921.

Remy, W., Taylort, T.N., Hass, H., and Kerp, H. (1994). Four hundred-million-year-old vesicular arbuscular mycorrhizae (Endomycorrhiae/symbiosis/fossil ft /mut). Plant Biol. **91**: 11841–11843.

Rupp, L. a., Mudge, K.W., and Negm, F.B. (1989). Involvement of ethylene in ectomycorrhiza formation and dichotomous branching of roots of mugo pine seedlings. Can. J. Bot. **67**: 477–482.

Rupp, L.A. and Mudge, K.W. (1985). Ethephon and auxin induce mycorrhiza-like changes in the morphology of root organ cultures of Mugo pine. Physiol. Plant. **64**: 316–322.

Singh, S. and Parniske, M. (2012). Activation of calcium- and calmodulin-dependent protein kinase (CCaMK), the central regulator of plant root endosymbiosis. Curr. Opin. Plant Biol. **15**: 444–453.

Smith, S.E. and Read, D. (2008). Mycorrhizal Symbiosis. Mycorrhizal Symbiosis: 611–XVIII.

Son, S.H. and Hall, R.B. (1990). Multiple shoot regeneration from root organ cultures of Populus alba x P. grandidentata. Plant Cell. Tissue Organ Cult. **20**: 53–57.

Spatafora, J.W. et al. (2016). A phylum-level phylogenetic classification of zygomycete fungi based on genome-scale data. Mycologia **108**: 1028–1046.

Splivallo, R., Fischer, U., Gobel, C., Feussner, I., and Karlovsky, P. (2009). Truffles Regulate Plant Root Morphogenesis via the Production of Auxin and Ethylene. PLANT Physiol. **150**: 2018–2029.

Steinkellner, S., Lendzemo, V., Langer, I., Schweiger, P., Khaosaad, T., Toussaint, J.P., and Vierheilig, H. (2007). Flavonoids and strigolactones in root exudates as signals in symbiotic and pathogenic plant-fungus interactions. Molecules **12**: 1290–1306.

Stracke, S., Kistner, C., Yoshida, S., Mulder, L., Sato, S., Kaneko, T., Tabata, S., Sandal, N., Stougaard, J., Szczyglowski, K., and Parniske, M. (2002). A plant receptor-like kinase required for both bacterial and fungal symbiosis. Nature **417**: 959–962.

Strullu-Derrien, C., Selosse, M.A., Kenrick, P., and Martin, F.M. (2018). The origin and evolution of mycorrhizal symbioses: From palaeomycology to phylogenomics. New Phytol.

Sukumar, P., Legué, V., Vayssières, A., Martin, F., Tuskan, G.A., and Kalluri, U.C. (2013). Involvement of auxin pathways in modulating root architecture during beneficial plant-microorganism interactions. Plant, Cell Environ. **36**: 909–919.

Sun, J. et al. (2015). Activation of Symbiosis Signaling by Arbuscular Mycorrhizal Fungi in Legumes and Rice. Plant Cell Online: tpc.114.131326.

Tedersoo, L., May, T.W., and Smith, M.E. (2010). Ectomycorrhizal lifestyle in fungi: Global diversity, distribution, and evolution of phylogenetic lineages. Mycorrhiza **20**: 217–263.

Tedersoo, L. and Smith, M.E. (2013). Lineages of ectomycorrhizal fungi revisited: Foraging strategies and novel lineages revealed by sequences from belowground. Fungal Biol. Rev. **27**: 83–99.

Truchet, G., Roche, P., Lerouge, P., Vasse, J., Camut, S., De Billy, F., Promé, J.C., and Dénarié, J. (1991). Sulphated lipo-oligosaccharide signals of Rhizobium meliloti elicit root nodule organogenesis in alfalfa. Nature **351**: 670–673.

Tuskan, G. a et al. (2006). The genome of black cottonwood, Populus trichocarpa (Torr. & Gray). Science **313**: 1596–1604.

Umehara, M., Hanada, A., Yoshida, S., Akiyama, K., Arite, T., Takeda-Kamiya, N., Magome, H., Kamiya, Y., Shirasu, K., Yoneyama, K., Kyozuka, J., and Yamaguchi, S. (2008). Inhibition of shoot branching by new terpenoid plant hormones. Nature **455**: 195–200.

Vayssières, A., Pěnčík, A., Felten, J., Kohler, A., Ljung, K., Martin, F.M., and Legue, V. (2015). Development of the *Populus-Laccaria bicolor* ectomycorrhiza modifies root auxin metabolism, signalling and response. Plant Physiol.: pp.114.255620.

Venkateshwaran, M., Cosme, a., Han, L., Banba, M., Satyshur, K. a., Schleiff, E., Parniske, M., Imaizumi-Anraku, H., and Ane, J.-M. (2012). The Recent Evolution of a Symbiotic Ion Channel in the Legume Family Altered Ion Conductance and Improved Functionality in Calcium Signaling. Plant Cell **24**: 2528–2545.

Venkateshwaran, M., Jayaraman, D., Chabaud, M., Genre, A., Balloon, A.J., Maeda, J., Forshey, K., den Os, D., Kwiecien, N.W., Coon, J.J., Barker, D.G., and Ané, J.-M. (2015). A role for the mevalonate pathway in early plant symbiotic signaling. Proc. Natl. Acad. Sci. **112**: 9781–9786.

Venkateshwaran, M., Volkening, J.D., Sussman, M.R., and Ané, J.M. (2013). Symbiosis and the social network of higher plants. Curr. Opin. Plant Biol. **16**: 118–127.

Wang, B. and Qiu, Y.-L. (2006). Phylogenetic distribution and evolution of mycorrhizas in land plants. Mycorrhiza **16**: 299–363.

El Yahyaoui, F. (2004). Expression Profiling in Medicago truncatula Identifies More Than 750 Genes Differentially Expressed during Nodulation, Including Many Potential Regulators of

the Symbiotic Program. PLANT Physiol. **136**: 3159–3176.

Yano, K. et al. (2008). CYCLOPS, a mediator of symbiotic intracellular accommodation. Proc. Natl. Acad. Sci. U. S. A. **105**: 20540–20545.

Yoneyama, K., Yoneyama, K., Takeuchi, Y., and Sekimoto, H. (2007). Phosphorus deficiency in red clover promotes exudation of orobanchol, the signal for mycorrhizal symbionts and germination stimulant for root parasites. Planta **225**: 1031–1038.

Yoshida, K., Ma, D., and Constabel, C.P. (2015). The MYB182 Protein Down-Regulates Proanthocyanidin and Anthocyanin Biosynthesis in Poplar by Repressing Both Structural and Regulatory Flavonoid Genes. Plant Physiol. **167**: 693–710.

Zhang, X., Dong, W., Sun, J., Feng, F., Deng, Y., He, Z., Oldroyd, G.E.D., and Wang, E. (2015). The receptor kinase CERK1 has dual functions in symbiosis and immunity signalling. Plant J. **81**: 258–267.

Zhao, Y., Araki, S., Wu, J., Teramoto, T., Chang, Y.F., Nakano, M., Abdelfattah, A.S., Fujiwara, M., Ishihara, T., Nagai, T., and Campbell, R.E. (2011). An expanded palette of genetically encoded Ca2+ indicators. Science (80-.). **333**: 1888–1891.

Chapter 4: Conclusions and Future Directions

4.1 Summary

The work presented in this thesis contributes to our understanding of the molecular mechanisms regulating both arbuscular mycorrhizal (AM) and ectomycorrhizal (ECM) associations in woody plants. In Chapter 2, genomic data was presented that provided preliminary evidence that ECM fungi can produce lipochitooligosaccharides (LCOs). This claim was substantiated by additional genomic data in woody plants which showed that the genetic components of the common symbiosis pathway (CSP) are present in all angiosperms that associate with ECM fungi. Also, the known molecular mechanisms that regulate the establishment and maintenance of both AM and ECM associations were thoroughly reviewed.

In Chapter 3, concrete evidence was provided showing that the ECM fungus *Laccaria bicolor* produces LCOs and can trigger calcium (Ca^{2+}) spiking in *Populus* in a *CASTOR*/*POLLUX*-dependent manner. Non-sulfated LCOs were shown to enhance lateral root formation in *Populus* in a *CCaMK*-dependent manner while sulfated LCOs enhanced colonization of *Populus* by the ECM fungus *L. bicolor*. Finally, RNA interference-based knock-down of three CSP genes (*CASTOR*, *POLLUX*, and *CCaMK*) resulted in reduced colonization by *L. bicolor* and expression of the mycorrhiza-induced phosphate transporter PT12 was reduced in the *CCaMK*-RNAi line compared to wild-type.

At the end of Chapter 3, additional data was presented that was not included in the manuscript submitted for publication. This data indicated that additional species of ECM fungi produce LCOs and, similar to *L. bicolor*, they are also capable of activating Ca^{2+} spiking in *Populus*. In this chapter, the data are discussed in greater detail and future experiments are

proposed that will further expand our knowledge of molecular mechanisms regulating mycorrhizal associations in woody plants.

4.2 Discussion

Lipochitooligosaccharides produced by ectomycorrhizal fungi are diverse and the genetic basis for their biosynthesis is unknown

Based on the mass spectrometry data presented in Chapter 3, no two species of ECM fungi produced the same mixture of LCOs, not even the two species from the same genus (*P. ammoniavirescens* and *P. involutus*). This finding may suggest that each ECM fungal species produces a unique suite of LCOs that it can use to aid in the colonization of a range of host plants; however, this remains to be tested. Although *H. cylindrosporum* produces LCOs, it is unlikely that it uses them during the colonization of *Pinus*, one of its primary host plants, particularly since data presented in Supplemental Figures 14 and 15 in Chapter 3 indicate *Pinus*, unlike *Populus*, is nonresponsive to LCOs. This result is not surprising based on the genomic data shown in Figure 2 from Chapter 2 which shows that the CSP is absent from *Pinus*. Based on our current knowledge of plant perception of LCOs, the CSP is the only known pathway used for their detection. Therefore, it is plausible to assume that *Pinus*, and perhaps many other gymnosperms, cannot detect LCOs. Additional experimentation is likely needed to verify this claim.

As described in Table 1 from Chapter 2, the *nodA/B/C*-like genes identified in the genomes of two ECM fungal species—*L. bicolor* (a basidiomycete) and *Tuber melanosporum* (an ascomycete)—are the most likely candidate genes necessary for LCO biosynthesis in ECM fungi. However, the high copy number of each of these homologs precludes the experiments

necessary to determine which specific genes are needed for LCO biosynthesis. As such, with the influx of available genomes from ECM fungi (Kohler et al., 2015), the homologs of *nodA*/*B*/*C*-like genes should be identified in each of these species. Ideally, one or more species will contain a low copy number of candidate LCO biosynthesis genes thus allowing for genetic studies. The technology already exists for transforming various ECM fungi, including *L. bicolor, P. involutus* and *H. cylindrosporum,* using *Agrobacterium tumefaciens* (Pardo et al., 2002; Combier et al., 2003; Kemppainen et al., 2005). Furthermore, the genome-editing technique CRISPR/*Cas9* has been successfully implemented in filamentous fungi (Nødvig et al., 2015). By combining these two techniques, it would likely be possible to knock-out candidate LCO biosynthesis genes in one or more ECM fungi. Exudates for the transgenic fungi could then be screened using root hair branching assays, and the hyphae could be used to test for induction of Ca^{2+} spiking in *Populus*. Using the culture medium from the transgenic lines giving negative responses, altered LCO or precursor molecules could be identified by mass spectrometry to determine if or how LCO biosynthesis was interrupted. In this way, a picture of LCO biosynthesis in fungi could begin to unfold.

The production of lipochitooligosaccharides may be conserved across the fungal kingdom

Before this work was carried out, the only fungal species known to produce LCOs was the AM fungus *Rhizophagus irregularis* (Maillet et al., 2011). Based on the findings presented here, it appears that LCO production is more widespread within the fungal kingdom than previously thought. As discussed previously, AM fungi belong to the phylum Mucoromycota and ECM fungi belong to the phyla Ascomycota, Basidiomycota, and Mucoromycota (Spatafora et al., 2016). Although we identified LCOs in ECM fungi belonging to the phylum Basidiomycota,

we still do not know if ECM fungi belonging to the phylum Ascomycota produce LCOs as well. Given the presence of *nodA*/*B*/*C*-like genes in the genome of *T. melanosporum*, this seems likely but still needs to be tested. Furthermore, given the phylogenetic diversity of the fungi known to produce LCOs, it seems likely that LCOs may be produced in non-mycorrhizal fungi as well, mainly since saprotrophic fungi are often found in the same genus as ectomycorrhizal fungi (e.g., *Amanita*; Wolfe et al., 2012). As such, root hair branching could be used as a preliminary screen to detect LCOs produced by non-mycorrhizal fungi as well. Then, using mass spectrometry as described in Chapter 3 for *L. bicolor* and later applied to three additional ECM fungal species, LCO production could be confirmed and specific structures of LCOs produced by non-mycorrhizal fungi fully characterized. If non-mycorrhizal fungi produce LCOs, it would be interesting to see if their structure differs from LCOs produced by mycorrhizal fungi. If so, this will likely provide insight into what is necessary for LCOs to serve as symbiotic signals. Furthermore, it will open up a new field of research to determine why non-symbiotic fungi produce LCOs and the role that they play in other processes.

Induction of nuclear Ca^{2+} spiking in Populus by ectomycorrhizal fungi is not host specific

As discussed in Chapter 3, the activation of Ca^{2+} spiking in *Populus* by ECM fungi has never been observed previously. It is surprising that *H. cylindrosporum* was able to trigger Ca^{2+} spiking in *Populus* since neither is known to associate with one another in nature. However, *H. crustilinoforme*—a close relative of *H. cylindrosporum*—was shown to not only associate with but also support nitrogen nutrition of trembling aspen (*Populus tremuloides*) (Siemens et al., 2011). Therefore, it is possible that a *Populus–H. cylindrosporum* association has simply never been observed in nature or recapitulated in a laboratory setting.

Future experiments with Ca^{2+} spiking should focus on evaluating if it occurs in a known broad-host for ECM fungi that contains the CSP. For example, *Eucalyptus globulus* is a host of not only AM fungi but also ECM fungi from 25 genera, including both basidiomycetes and ascomycetes. In contrast, *Populus* only associates with ECM fungi from a few genera, and all of them are basidiomycetes (Hoeksema et al., 2018). Given that *E. globulus* can be transformed using *A. tumefaciens*, the fluorescent Ca^{2+} reporter G-GECO (Zhao et al., 2011) could be integrated into *E. globulus* thereby allowing for Ca^{2+} spiking assays to be performed with a broad range of ECM fungi with a compatible host species.

The dependence of ectomycorrhizal associations on the common symbiosis pathway remains unknown but can be determined using CRISPR/Cas9 technology

Due to limitations in technology at the time this project was initiated, RNAi was the only rapid method of gene disruption available in *Populus.* As such, this work was only able to demonstrate that reduced expression of *CASTOR*, *POLLUX*, and *CCaMK* resulted in reduced colonization of *Populus* by *L. bicolor.* Thus, the results do not conclusively show that the CSP is *required* for *L. bicolor* to colonize *Populus*; instead, they only show that *L. bicolor* uses the CSP to colonize *Populus fully.* Fortunately, with the advent of CRISPR/*Cas9*, the genomes of many plant species have been efficiently edited via gene knock-out (Ma et al., 2016). In particular, several studies have demonstrated the use of CRISPR/*Cas9* in *Populus* (Fan et al., 2015; Zhou et al., 2015). Future experiments should focus on utilizing CRISPR/*Cas9* to knock-out components of the CSP in *Populus* to determine if the CSP is genuinely *required* for colonization by *L. bicolor.*

Transformation is a critical technique for studying gene function, but it is often a rate-limiting step in molecular biology. Over four decades ago, the first procedure for transforming *Populus* with *Agrobacterium tumefaciens* was published (Parsons et al., 1986). It required that *Populus* tissue exposed to *A. tumefaciens* pass through callus, shoot induction, and root induction phases on selective medium with phytohormones in order to successfully generate a stable transgenic *Populus* line. Unfortunately, this original transformation procedure required about one year to complete. Furthermore, the method was not compatible with all species of *Populus*, even though most of them are highly hybridizable. As such, dozens of methods have been developed for transforming specific *Populus* species or hybrids using an accelerated approach. For example, in *P. tremuloides* and *P.trichocarpa*, it is now possible to skip the callus phase and immediately induce the generation of transgenic shoots from tissue inoculated with *A. tumefaciens* (Cseke et al., 2007; Li et al., 2017). This method reduces the length of the transformation procedure from more than one year to less than four months. Unfortunately, the methods described are not suitable for the *Populus* hybrid *P. tremula* x *P. alba*, which was used in Chapter 3 for the development of the RNAi lines used for the experiments described therein. In order to rapidly transform this hybrid with the Ca^{2+}-sensitive reporter G-GECO, a *P. tremula* x *P. alba*-specific, *A. rhizogenes*-mediated transformation method for the production of transgenic roots (Yoshida et al., 2015) was coupled with a method for shoot-induction from transgenic roots specific to a related *Populus* hybrid (Son and Hall, 1990). In this way, a unique four-month transformation method specific to *P. tremula* x *P. alba* was developed. In future studies, this transformation procedure could be used to efficiently transform CRISPR/*Cas9* binary vectors into *Populus* in order to generate CSP mutants promptly.

Golden Gate cloning is a technique for rapidly assembling multiple modules of expression cassettes within a binary vector for transformation into plant tissues. It is a technique that relies on type IIs restriction enzymes that cut outside of their recognition sequence. In one cloning step, fragments of DNA (e.g., promoter sequences, localization signals, coding DNA sequences, terminator sequences, etc.) can be cut with a type IIs restriction enzyme and immediately ligated together with other DNA fragments containing compatible four base pair overhangs in a predicted and directional pattern (Engler et al., 2009, 2014). The method has been standardized among plant scientists to ensure that specific four base pair overhangs exist at all junctions between specific DNA fragments (Patron and et al., 2015). This technology has allowed for the development of a variety of Golden Gate-based CRISPR/*Cas9* vector assembly methods. Early on, many guide (g)RNAs were assembled individually under the control of one promoter; although successful, this method resulted in variable expression of gRNAs within the same expression cassette leading to variability in gRNA efficiency (Fan et al., 2015). As such, superior multiplexing methods were developed which allowed for up to 12 gRNAs to be assembled under the control of one promoter, which, upon expression in the pant, are post-transcriptionally cleaved using either innate tRNA processing machinery or Csy4 ribonuclease to generate a stoichiometrically even copy number of each gRNA (Cermak et al., 2017).

This multiplexing method proved successful in many plant species, but unfortunately, due to limitations in vector assembly and availability of suitable transformation markers, was unsuccessful in editing *Populus* in our hands. As such, through collaboration with Dr. Ray Collier, Molecular Technologies lead at the Wisconsin Crop Innovation Center, a new and more versatile CRISPR/*Cas9* tRNA multiplex system (BLACKSMITH v2) is currently under development for use in *Populus* as well as additional plant species. In future experiments, this

system will allow for the rapid construction of CRISPR/*Cas9* vectors targeting CSP genes that are suitable for *A. rhizogenes*-mediated transformation into *Populus*.

The requirement for nutrient exchange in ectomycorrhizal associations remains unknown

Nutrient transporters in mycorrhizal associations are vital to the success of the symbiotic interaction between plant and fungus (Casieri et al., 2013; Garcia et al., 2016). In Chapter 3, it was shown that expression of the *Populus* mycorrhiza-induced phosphate transporter *PT12* is reduced in the *CCaMK*-RNAi *Populus* line. We argued that this reduction in expression is evidence that the CSP plays a role not only in establishing the *Populus–L. bicolor* association, but also in regulating the central purpose of the association—nutrient exchange. As discussed in Chapter 3, some AM-induced phosphate transporters, e.g., *MtPT4* (Javot et al., 2007) are required for the perpetuation of this symbiotic association. However, due in part to the limited ability to produce mutants in woody plant species, the necessity of nutrient transporters up-regulated during ECM associations, e.g., *PtPT12* (Loth-Pereda et al., 2011), has never been investigated. In future experiments, it will be important that in addition to knocking-out CSP genes in *Populus* using the CRISPR/*Cas9* method described above, nutrient transporters upregulated during *Populus*–ECM associations should also be knocked-out to determine if they are required for the symbiotic association to persist. If so, this will provide preliminary evidence that plants are capable of regulating the ability of ECM fungi to colonize their root system based on the fruitful exchange of mineral nutrients. Such a regulation has already been demonstrated in AM associations (Kiers et al., 2011; Fellbaum et al., 2012), and providing additional support for this finding with an additional class of mycorrhizal fungi would provide an exceptional contribution to the field as well as a platform for developing an independent research program.

4.3 References

Casieri, L. et al. (2013). Biotrophic transportome in mutualistic plant-fungal interactions. Mycorrhiza **23**: 597–625.

Cermak, T., Curtin, S.J., Gil-Humanes, J., Čegan, R., Kono, T.J.Y., Konečná, E., Belanto, J.J., Starker, C.G., Mathre, J.W., Greenstein, R.L., and Voytas, D.F. (2017). A multi-purpose toolkit to enable advanced genome engineering in plants. The Plant Cell **29**: tpc.00922.2016.

Combier, J.P., Melayah, D., Raffier, C., Gay, G., and Marmeisse, R. (2003). *Agrobacterium tumefaciens*-mediated transformation as a tool for insertional mutagenesis in the symbiotic ectomycorrhizal fungus Hebeloma cylindrosporum. FEMS Microbiol. Lett. **220**: 141–148.

Cseke, L.J., Cseke, S.B., and Podila, G.K. (2007). High efficiency poplar transformation. Plant Cell Rep. **26**: 1529–1538.

Engler, C., Gruetzner, R., Kandzia, R., and Marillonnet, S. (2009). Golden gate shuffling: A one-pot DNA shuffling method based on type ils restriction enzymes. PLoS One **4**: e5553

Engler, C., Youles, M., Gruetzner, R., Ehnert, T.M., Werner, S., Jones, J.D.G., Patron, N.J., and Marillonnet, S. (2014). A Golden Gate modular cloning toolbox for plants. ACS Synth. Biol. **3**: 839–843.

Fan, D., Liu, T., Li, C., Jiao, B., Li, S., Hou, Y., and Luo, K. (2015). Efficient CRISPR/Cas9-mediated targeted mutagenesis in *Populus* in the first generation. Sci. Rep. **5**: 12217.

Fellbaum, C.R., Gachomo, E.W., Beesetty, Y., Choudhari, S., Strahan, G.D., Pfeffer, P.E., Kiers, E.T., and Bucking, H. (2012). Carbon availability triggers fungal nitrogen uptake and transport in arbuscular mycorrhizal symbiosis. Proc. Natl. Acad. Sci. **109**: 2666–2671.

Garcia, K., Doidy, J., Zimmermann, S.D., Wipf, D., and Courty, P.E. (2016). Take a trip

through the plant and fungal transportome of mycorrhiza. Trends Plant Sci. **21**: 937–950.

Hoeksema, J.D. et al. (2018). Evolutionary history of plant hosts and fungal symbionts predicts the strength of mycorrhizal mutualism. Commun. Biol. **1**: 116.

Javot, H., Penmetsa, R.V., Terzaghi, N., Cook, D.R., and Harrison, M.J. (2007). A *Medicago truncatula* phosphate transporter indispensable for the arbuscular mycorrhizal symbiosis. Proc. Natl. Acad. Sci. **104**: 1720–1725.

Kemppainen, M., Circosta, A., Tagu, D., Martin, F., and Pardo, A.G. (2005). *Agrobacterium*-mediated transformation of the ectomycorrhizal symbiont *Laccaria bicolor* S238N. Mycorrhiza **16**: 19–22.

Kiers, E.T. et al. (2011). Reciprocal rewards stabilize cooperation in the mycorrhizal symbiosis. Science **333**: 880–882.

Kohler, A. et al. (2015). Convergent losses of decay mechanisms and rapid turnover of symbiosis genes in mycorrhizal mutualists. Nat. Gen. **47**: 410–415.

Li, S., Zhen, C., Xu, W., Wang, C., and Cheng, Y. (2017). Simple, rapid and efficient transformation of genotype Nisqually-1: a basic tool for the first sequenced model tree. Sci. Rep. **7**: 2638.

Loth-Pereda, V., Orsini, E., Courty, P.-E., Lota, F., Kohler, A., Diss, L., Blaudez, D., Chalot, M., Nehls, U., Bucher, M., and Martin, F. (2011). Structure and expression profile of the phosphate Pht1 transporter gene family in mycorrhizal *Populus trichocarpa*. Plant Physiol. **156**: 2141–2154.

Ma, X., Zhu, Q., Chen, Y., and Liu, Y.G. (2016). CRISPR/Cas9 platforms for genome editing in plants: Developments and applications. Mol. Plant **9**: 961–974.

Maillet, F. et al. (2011). Fungal lipochitooligosaccharide symbiotic signals in arbuscular

mycorrhiza. Nature **469**: 58–64.

Nødvig, C.S., Nielsen, J.B., Kogle, M.E., and Mortensen, U.H. (2015). A CRISPR-Cas9 system for genetic engineering of filamentous fungi. PLoS One **10**: e0133085.

Pardo, A.G., Hanif, M., Raudaskoski, M., and Gorfer, M. (2002). Genetic transformation of ectomycorrhizal fungi mediated by *Agrobacterium tumefaciens*. Mycol. Res. **106**: 132–137.

Parsons, T.J., Sinkar, V.P., Stettler, R.F., Nester, E.W., and Gordon, M.P. (1986). Transformation of poplar by *Agrobacterium tumefaciens*. Bio/Technology **4**: 533–536.

Patron, N. and et al (2015). Standards for plant synthetic biology: A common syntax for exchange of DNA parts. New Phytol. **208**: 13–19.

Siemens, J.A., Calvo-Polanco, M., Zwiazek, J.J., and Näsholm, T. (2011). *Hebeloma crustuliniforme* facilitates ammonium and nitrate assimilation in trembling aspen (*Populus tremuloides*) seedlings. Tree Physiol. **31**: 1238–1250.

Son, S.H. and Hall, R.B. (1990). Multiple shoot regeneration from root organ cultures of *Populus alba* x *P. grandidentata*. Plant Cell. Tissue Organ Cult. **20**: 53–57.

Spatafora, J.W. et al. (2016). A phylum-level phylogenetic classification of zygomycete fungi based on genome-scale data. Mycologia **108**: 1028–1046.

Wolfe, B.E., Tulloss, R.E., and Pringle, A. (2012). The irreversible loss of a decomposition pathway marks the single origin of an ectomycorrhizal symbiosis. PLoS One **7**: e39597.

Yoshida, K., Ma, D., and Constabel, C.P. (2015). The MYB182 protein down-regulates proanthocyanidin and anthocyanin biosynthesis in poplar by repressing both structural and regulatory flavonoid genes. Plant Physiol. **167**: 693–710.

Zhao, Y., Araki, S., Wu, J., Teramoto, T., Chang, Y.F., Nakano, M., Abdelfattah, A.S., Fujiwara, M., Ishihara, T., Nagai, T., and Campbell, R.E. (2011). An expanded palette

of genetically encoded Ca2+ indicators. Science (80). **333**: 1888–1891.

Zhou, X., Jacobs, T.B., Xue, L.J., Harding, S.A., and Tsai, C.J. (2015). Exploiting SNPs for biallelic CRISPR mutations in the outcrossing woody perennial Populus reveals 4-coumarate: CoA ligase specificity and redundancy. New Phytol. **208**: 298–301.